TRANSPORTATION RESEARCH

RECORD

No. 1437

Soils, Geology, and Foundations; Materials and Construction

Aggregates: Waste and Recycled Materials; New Rapid Evaluation Technology

A peer-reviewed publication of the Transportation Research Board

TRANSPORTATION RESEARCH BOARD
NATIONAL RESEARCH COUNCIL

NATIONAL ACADEMY PRESS
WASHINGTON, D.C. 1994

Transportation Research Record 1437
ISSN 0361-1981
ISBN 0-309-05515-6
Price: $21.00

Subscriber Categories
IIIA soils, geology, and foundations
IIIB materials and construction

Printed in the United States of America

Sponsorship of Transportation Research Record 1437

GROUP 2—DESIGN AND CONSTRUCTION OF TRANSPORTATION FACILITIES
Chairman: Charles T. Edson, Greenman, Pederson Inc.

Evaluations, Systems, and Procedures Section
Chairman: Earl C. Shirley, Auburn, California

Committee on Mineral Aggregates
Chairman: Vernon J. Marks, Iowa Department of Transportation
Bernard D. Alkire, Michael E. Ayers, John S. Baldwin, George M. Banino, James R. Carr, Robert J. Collins, Graham R. Ford, Stephen W. Forster, David W. Fowler, James G. Gehler, Richard H. Howe, Ian L. Jamieson, Rita B. Leahy, Kamyar Mahboub, Charles R. Marek, W. R. Meier, Jr., Richard C. Meininger, D. C. Pike, William O. Powell, Charles A. Pryor, Jr., Norman D. Pumphrey, Jr., Stuart L. Schwotzer, Larry Scofield, Barbara J. Smith, Mary Stroup-Gardiner, Kenneth R. Wardlaw, Lennard J. Wylde

Transportation Research Board Staff
Robert E. Spicher, Director, Technical Activities
G. P. Jayaprakash, Engineer of Soils, Geology, and Foundations
Nancy A. Ackerman, Director, Reports and Editorial Services
Naomi Kassabian, Associate Editor

The organizational units, officers, and members are as of December 31, 1993.

Transportation Research Record 1437

Contents

Foreword

Aggregates, which constitute 95 percent of all construction materials, have always been and will continue to be an important factor in the longevity and performance of transportation structures. With restricted transportation budgets, more emphasis is being given to longevity, so quality of aggregate is important. Improved aggregate tests that enable better evaluation of aggregate quality and consideration of waste or by-product materials as substitutes for natural aggregate are needed to build durable structures, as well as to protect the environment and conserve natural resources.

This volume contains eight papers arranged into two groups. In the first group, information from research related to waste and recycled materials is provided. These studies resulted in data on the use of shredded rubber tires as lightweight material for construction of roadway embankments, use of crushed glass as a partial replacement for natural aggregate, use of slag aggregate from phosphogypsum in portland cement concrete, and use of waste foundry sand as partial replacement of aggregate in asphalt concrete.

In the second group of papers, the development and use of aggregate tests based on new technologies are described. Information presented includes an automated method of determining fine aggregate gradations, a slightly modified National Aggregate Association flow test method for determining fine aggregate angularity, an image analyzer for automatic determination of the percentage of natural sand in an aggregate mixture, and a stoichiometric analysis for identifying the original mineral compositions of aggregate used in portland cement concrete.

Engineering Properties of Shredded Tires in Lightweight Fill Applications

DAVID E. NEWCOMB AND ANDREW DRESCHER

It is estimated that approximately 240 million automobile and truck tires are discarded annually in the United States. Until recently, these have typically been disposed of in landfills and in tire stockpile sites where they pose potential safety and health problems as well as being unsightly. The latest use of shredded tires as lightweight fill material is encouraging, however, and the number of applications may grow provided that their engineering properties become more understandable and the quantifying parameters are known. Exploratory field and laboratory tests for determining the basic properties of shredded tires are reported in this paper. In the field tests, where large-size shreds were used, the effort necessary for compacting layers of shredded tires with a bulldozer was measured. In the laboratory tests, the compressibility of small-size shreds was investigated by means of a one-dimensional compression test. In addition, for both the large- and small-size shreds, their gradation, bulk density, porosity, and void ratio were determined. For comparison, wood chips were tested. The results show that the bulk density of shredded tires is between that of traditional granular fills and wood chips. However, their compressibility and rebound are much higher than those of the latter material, which could lead to premature fatigue failure of hard surface pavements. The apparent anisotropy of a shredded tire mass may also cause errors in predicting pavement deflections by means of classical, elastic multilayer system analysis, which assumes material isotropy.

Lightweight fill materials are appropriate where dead-load induced settlements of embankments must be reduced or where high stresses on retaining or subsurface structures must be prevented. In the case of embankments, the fill should serve the purpose of reducing the overburden stresses on weak soils such that geometric requirements of the surface can be maintained. At the same time, the fill should be capable of providing enough load-bearing capacity to support any induced stresses transmitted through the pavement structure. The use of lightweight fill behind retaining walls is an effective means of reducing the stresses that the structure must resist. Therefore, a lighter, more economical cross section may be used in the wall.

Traditionally, materials such as wood chips from lumber manufacturing or specially produced aggregates such as expanded shale or clay have been used for lightweight fill construction. Waste wood chips have the advantage of low cost, and as long as they remain submerged in water, they provide a relatively long service life. However, wood is subject to decay when the water table fluctuates, and it is exposed to air periodically. Artificially produced lightweight aggregates have the advantages of strength and durability when compared with wood chips, but they are heavier and many times more expensive because of the energy and equipment required to produce them. An alternative to these sources of lightweight fill materials is shredded waste tires.

Department of Civil and Mineral Engineering, University of Minnesota, 500 Pillsbury Dr., S.E., Minneapolis, Minn. 55455.

It is estimated that more than 200 million automobile tires and 40 million truck tires are discarded annually in the United States. This is roughly equivalent to 4 million tons of waste (*1*). The safety and health problems created by this refuse have prompted engineers to seek innovative means for reusing the material. Waste tire rubber has been used in asphalt mixtures, as lightweight road fills, as artificial reefs and breakwaters, as erosion control, and as a source of energy (*1–4*). These applications range in the amount of tire-processing required. For instance, tire rubber used in asphalt mixtures must be ground to a relatively fine particle size of less than 2 mm, whereas whole tires can be used in erosion control. The cost of the processed material increases exponentially as the particle size is reduced. Thus, it is attractive to find applications that could benefit from the physical properties of the material while the required amount of size reduction would be minimized.

The use of shredded tires in lightweight fills has the advantage of allowing large quantities of waste tires to be consumed with minimal or moderate processing. Usually, either the tires are reduced to a particle size of about 30 to 50 mm or whole tires sliced only once are used. The use of finer particles is often preferred because it is much more difficult to work and compact the larger particles. The hydraulic systems of equipment such as dump trucks and loaders regularly suffer damage from large tire shreds that catch on the hoses.

The bulk density of the material is lower than that of granular fill and makes it attractive for minimizing settlement of weak, low-stiffness subgrades. The material is not subject to rapid degradation in the presence of air or water. If the load-bearing capacity is sufficient, a durable lightweight fill could be constructed providing long-term performance.

In some respects, largely because of the particle shape, bulk structure, and large voids, shredded tires are difficult to describe with normal geotechnical or pavement engineering parameters. The tire shreds are flat with the aspect ratio (length to width) being defined by the amount of processing used to reduce the particle size. A tire cut once or twice will have a much greater aspect ratio than one that has been passed through a shredder several times. The flatness of the tire particles as well as their possible elongated shape often lead to an anisotropic structure when the mass is compacted.

The elasticity of rubber is intuitive; however, the shredded tire mass is neither linearly elastic nor isotropic, and its stiffness is low even for moderate loads. An individual rubber particle may have a modulus of elasticity of approximately 7 MPa, a value that decreases considerably when voids are present in a mass of rubber particles. Typical modulus values for silty soils range from 35 to 150 MPa, so the rubber particle has a modulus of elasticity 5 to 20 times less than that of a typical subgrade soil (*5*). Although rubber lacks the stiffness of the soil, it has a greater capacity for rebound.

The implications of this elasticity for pavement structural behavior are not well understood, primarily because of lack of data on the mechanical behavior of the shredded tire mass. Projects involving shredded tire fill seldom report on deformability and strength. Local settlement or deflection measurements provide some information, but it is difficult if not impossible to backcalculate the primary parameters such as Young's modulus or internal friction angle. Except for some early work conducted by the California Department of Transportation (CalTrans) (*1,2*), no systematic studies on shredded tire properties have been reported in the literature.

The intent of this study was to identify and measure the basic engineering properties of shredded tires relevant in the design and performance of lightweight fill sections in roadways. In order to accomplish this, field observations and laboratory tests on shredded tires were performed. The nature of the tests was exploratory; nonetheless, the results may serve as reference for further studies aimed at developing engineering guidelines.

DESCRIPTION OF STUDY

Field Investigations

The main objective of the field tests was to determine the effort necessary for compacting layers of shredded tires with a bulldozer. The tests were conducted at a site located in Mora, Minnesota. An all-weather access road was being constructed with a layer of compacted shredded tires placed on a moderately stiff silty clay. The tires used in this project had been passed only once through a shredding machine, which resulted in rather large pieces of tire rubber. In addition to monitoring compaction, measurements were taken to determine the particle size, bulk density, and porosity. A detailed description of the site conditions and construction project may be found elsewhere (*6*).

Laboratory Tests

One-dimensional laboratory compression tests were used to determine the compressibility and rebound characteristics of waste tires shredded to small-size particles (approximately 50 mm mean size); for comparison, wood chips were also tested. The material parameters evaluated in the laboratory also included particle size, bulk density, and porosity.

SIZE, DENSITY, AND POROSITY CHARACTERISTICS OF MATERIALS

Particle Size

The methods used for determining particle size and aspect ratio differed between the field and the laboratory. Since the field project involved large pieces, a random sample of 144 particles was taken from the stockpiles and measured with a tape rule. In the laboratory, the shredded tire and wood chip particles were passed through sieves.

As stated earlier, the particle size of shredded tires is a function of the number of passes through the shredding device. Minimal processing (one pass) results in large, elongated pieces that, for the tested sample, are characterized by a dominant aspect ratio of about 2 to 4. Because the particle thickness is much less than the width or length, the size of the pieces is best represented by the largest surface area calculated as the product of width and length. The distribution curve of this area is shown in Figure 1; the mean area is about 0.093 m^2.

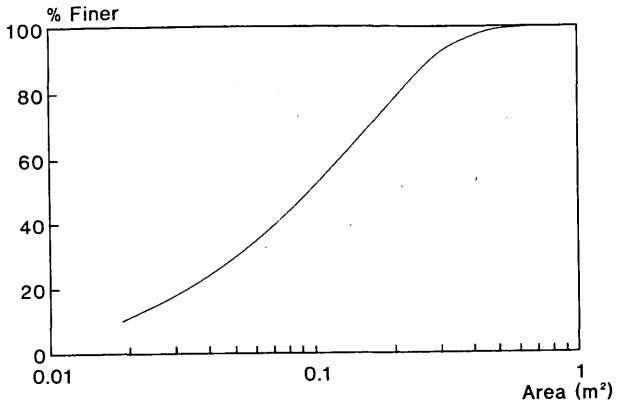

FIGURE 1 Particle area distribution curve of large-size shredded tires.

Two to four passes through a shredder result in much smaller pieces, whose size can be characterized by the opening size of a sieve. The gradation of the shredded tires used in the laboratory compressibility tests is shown in Figure 2, with a mean size of about 30 mm. A similar size was reported by CalTrans (*2*) and compares well with wood chip material used in the tests, whose gradation is shown in Figure 2, with a mean size of about 25 mm.

Bulk Density

The bulk density of the materials in this study was measured by filling a container of known volume and then weighing it. For the large-size tire particles used in the field, the bed of a dump truck was used. The uncompacted bulk density (ρ_o) was determined

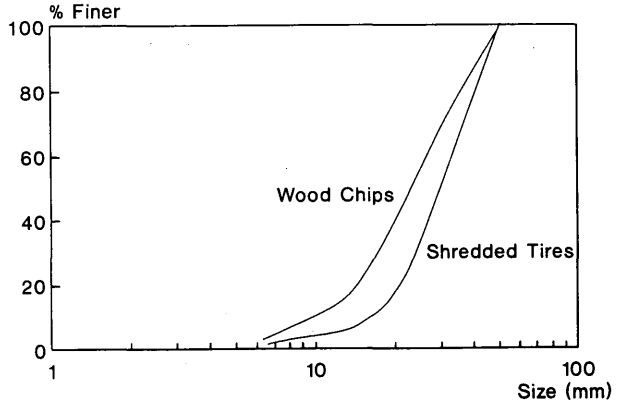

FIGURE 2 Particle size distribution curves of small-size shredded tires and wood chips.

from

$$\rho_o = \frac{m_{st}}{V} \tag{1}$$

where m_{st} is the mass of shredded tires filling a dump truck bed, and V is its volume; m_{st} was determined at a local truck weigh station. The compacted bulk density (ρ_c) was calculated from

$$\rho_c = \rho_o \frac{H_o}{H_o - \Delta H} \tag{2}$$

where H_o is the initial thickness of the shredded tire layer and ΔH is the vertical settlement induced by compaction. For the small-size particles used in the laboratory, a small container was filled and weighed using a laboratory scale.

The bulk density of the shredded tires is a function of the particle size. In general, large-size particles yield a lower bulk density (ρ_o = 230 kg/m^3, ρ_c = 350 kg/m^3) than smaller particles (ρ_o = 500 kg/m^3). Table 1 gives the bulk densities determined in the field and laboratory, including the results obtained by CalTrans (*2*); for comparison, average values of the bulk density of wood chips and granular fills are given also. The following approximate ratio of the average densities of soils (ρ_s), shredded tires (ρ_{st}), and wood-chips (ρ_{wc}) can be established:

$$\rho_s:\rho_{st}:\rho_{wc} = 12:2.5:1 \tag{3}$$

This ratio also applies to the bulk unit weight.

Porosity and Void Ratio

The porosity (n) of the large-sized shredded tires was determined indirectly by means of

$$n = \frac{G_s\rho_w - \rho_{st}}{G_s\rho_w} \tag{4}$$

where G_s is the specific gravity of the shredded tire particles, and ρ_w is the density of water; the specific gravity G_s = 1.08 was determined in the laboratory.

For the small-size shredded tires particles and wood chips, the porosity of the uncompacted mass was determined from

$$n = \frac{V_v}{V} \tag{5}$$

where V_v is the volume of voids, and V is the total volume. The volume of voids was measured directly in a mass filling a 0.138-m^3 container by measuring upon drainage the weight of water filling the voids.

Once the porosity was determined, the void ratio (e) was calculated from

$$e = \frac{n}{1 - n} \tag{6}$$

The results shown in Table 1 indicate that the porosity, and thus void ratio, depends on the particle size. Large shredded tire pieces yield a porosity of about 80 percent, whereas smaller particles have a value of about 60 percent; for wood chips the porosity is about 70 percent. In comparison with soils, the porosity of shred-

TABLE 1 Fill Material Properties

Material	Mean Area (m^2)	Mean Size (mm)	Density (kg/m^3)	Porosity (%)	Void Ratio (-)	Compress. Index (-)	Swell Index (-)	Young's Modulus (MPa)	Poisson's Ratio (-)
Shredded Tires	0.093	_	230-350	79	3.76	n.a.	n.a.	n.a.	n.a.
Shredded Tires	_	30	500	57	1.32	0.50	0.27	0.78	0.45
Shredded Tires (4)	_	20-46	500-565	55-60	1.22-1.50	n.a.	n.a.	n.a.	n.a.
Wood Chips	_	25	160	67	2.03	0.35	0.034	70	0.26
Granular Fill	_	~2	1850-2250	12-46	0.14-0.85	0-0.19	_	75-300	~0.40

ded tires and wood chips is not much different. What is significantly different, however, is the size of voids; the latter materials have much greater voids, and this can be evaluated indirectly by measuring the permeability coefficient. As reported by CalTrans (*2*), the permeability coefficient of a small-size shredded tire mass (50 mm size) is about 2.1 m/min, which is 20 to 30 times higher than the permeability coefficient of a typical granular base. The high permeability of shredded tires is one of the main advantages in using them as fill, because water can drain out of the pavement easily.

FIELD COMPACTION OF LARGE-SIZE TIRE SHREDS

The shredded tires were placed in the excavated road bed in two 1- to 2-m lifts. The elevation of the excavation was measured at three transverse points in nine evenly spaced lines throughout a section 45 m long. These points provided the reference datum for subsequent elevation measurements at the same points after the placement and compaction of the shredded tires. Dump trucks were used to deposit the tires, and the compaction was achieved using a 27-ton Caterpillar D7F bulldozer. The compaction effort was quantified as the number of bulldozer passes over the whole width of the road; 22 total passes were performed for the first lift and 12 passes for the second lift.

Figure 3 shows the initial and final lift thicknesses of the shredded tire layer. It can be seen that the initial thickness of the first lift was about 1 m, and the final thickness was about 0.6 m. The initial thickness of the second lift varied from 1.3 to 2 m, and its final thickness was 0.9 to 1.2 m after compaction. The average relationship between the settlement of the shredded tires and the number of bulldozer passes for the first and second lifts is shown in Figure 4. It can be seen that there was little additional compaction of the material beyond 15 passes of the bulldozer for the first lift. A similar number of passes can be anticipated for the second lift.

ONE-DIMENSIONAL COMPRESSION TEST

Test Procedure

A schematic of the test device used in the laboratory is shown in Figure 5. A cylindrical steel container 97 cm high by 74 cm in diameter was filled with the material to be tested (shredded tires or wood chips) and subjected to a vertical load applied by a closed-loop testing system through steel plates. The load was applied to the samples using a constant rate of displacement of 5 mm/min, and the vertical load was measured by load cells with a capacity of 111.2 kN (shredded tires) or 2668.8 kN (wood chips); loading and unloading cycles were performed to determine the magnitude of rebound. In order to reduce the side friction between the cylinder and the sample, the inner wall was coated with silicon grease.

The vertical stresses (σ_v) were calculated as

$$\sigma_v = \frac{P}{A} \tag{7}$$

where P is the vertical force, and A is the cross-sectional area of the container. The vertical strains (ϵ_v) were computed as

$$\epsilon_v = \frac{\Delta H}{H_o} \tag{8}$$

where H_o is the initial height of the material in the container, and ΔH is the change in height.

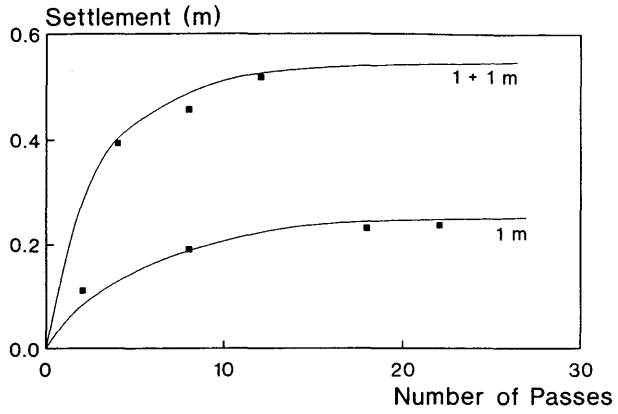

FIGURE 4 Settlement of shredded tires as function of number of bulldozer passes.

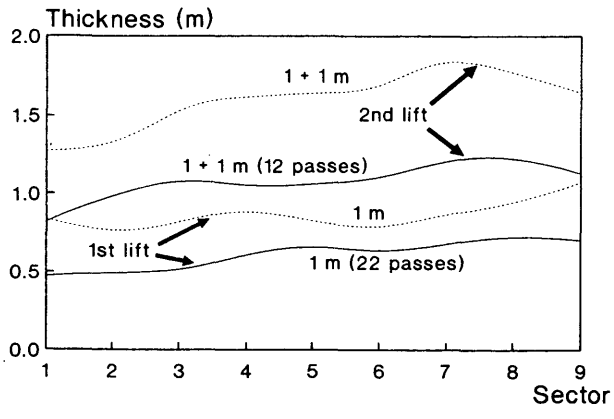

FIGURE 3 Thickness of shredded tire layer.

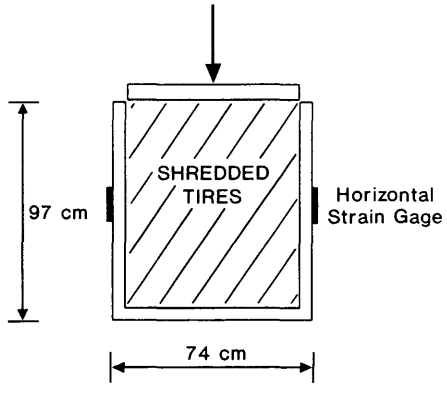

FIGURE 5 Schematic of one-dimensional compression test.

To determine the magnitude of the horizontal (radial) stress (σ_h), the container was instrumented around its circumference with four strain gauges at 90 degrees to one another 30 cm above the base of the container. These measurements allowed for the computation of σ_h using the following relationship:

$$\sigma_h = \epsilon_\theta E \frac{t}{r} \tag{9}$$

where

ϵ_θ = average circumferential strain,
E = modulus of elasticity of container,
t = thickness of container, and
r = radius of container.

Test Results

Figure 6 shows the typical relationship between vertical stress and vertical strain of shredded tires during multiple loading cycles. The material easily deforms at very low levels of vertical stress and becomes significantly stiffer at about 5 kPa, which corresponds to about 25 percent strain. The maximum stress applied, limited by the ram travel, was about 0.4 MPa with corresponding strains of about 40 percent. Upon unloading and reloading, the stress-strain relationship follows a path parallel to the steeper portion of the initial loading path. This latter behavior would seem to more accurately reflect the characteristics of shredded tires in the field after compaction and placement of overburden. Still, the strain ranges about 10 percent over a range of 0.05 to 0.38 MPa vertical stress.

The typical result for wood chips shown in Figure 7 shows a similarity to the result for shredded tires; the end of the soft response is again at about 20 percent vertical strain although the corresponding stress of about 1 MPa is much higher. At larger strains the material rapidly stiffens, with stresses of about 4 MPa at a strain of 27 percent. The unloading path is very steep and is no longer parallel to the loading path.

The relationship between the horizontal and vertical stress for shredded tires and wood chips is shown in Figures 8 and 9, respectively. Clearly, this relationship is bilinear for shredded tires and linear for wood chips; also, for the same vertical stress, the horizontal stress is higher in shredded tires.

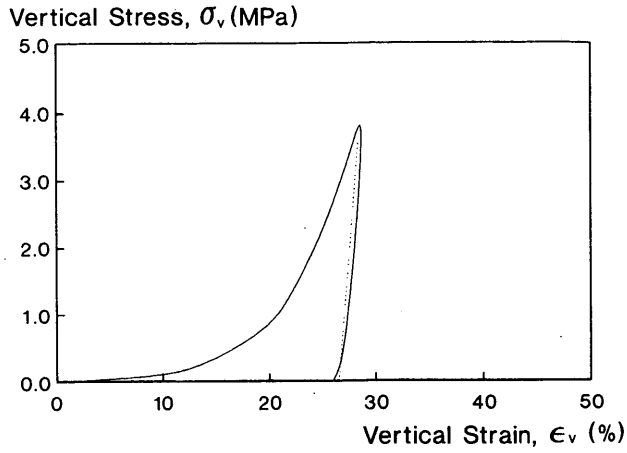

FIGURE 7 Vertical stress versus vertical strain for wood chips.

Analysis of Results

The analysis of compressibility test results was performed within the framework of (*a*) the settlement analysis used in geotechnical engineering and (*b*) deflection analysis applicable to pavement systems.

In the first approach, the compressibility and rebound of a material are characterized by the compressibility index (C_c) and the swell index (C_s) (*5*). These indexes are defined as slopes of a void ratio (e) versus the decimal logarithm of vertical stress (log σ_v) plot obtained directly from the one-dimensional compression test. This implies that the nonlinearity of the stress-strain response and the difference in loading and unloading behavior are accounted for. Because only a one-dimensional response is considered, no assumption as to material isotropy or anisotropy is made.

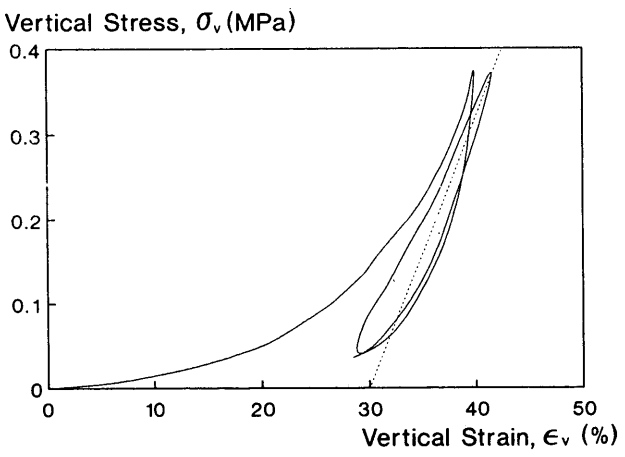

FIGURE 6 Vertical stress versus vertical strain for shredded tires.

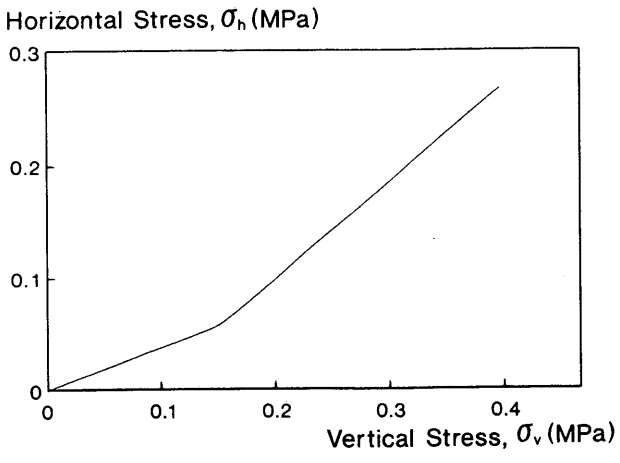

FIGURE 8 Horizontal stress versus vertical stress for shredded tires.

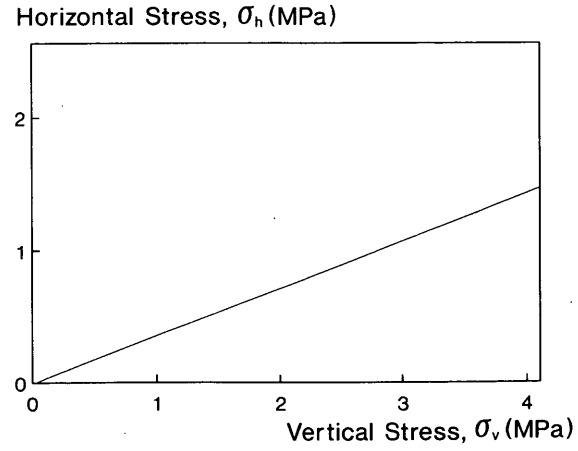

FIGURE 9 Horizontal stress versus vertical stress for wood chips.

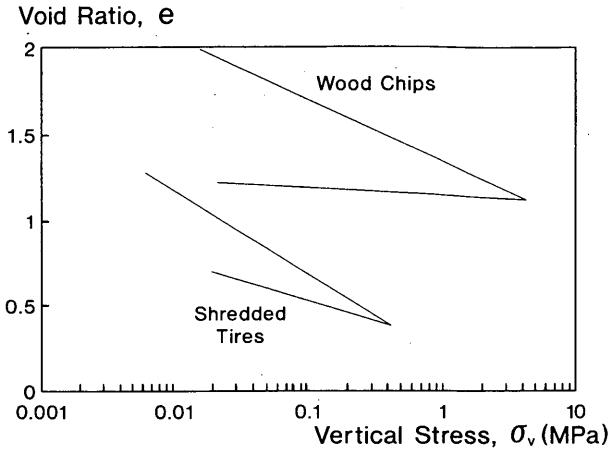

FIGURE 10 Void ratio versus vertical stress for shredded tires and wood chips.

Figure 10 shows the corresponding plots for shredded tires and wood chips. The resulting indexes for shredded tires are $C_c = 0.50$ and $C_s = 0.27$; for wood chips, $C_c = 0.35$ and $C_s = 0.034$ (see Table 1). These results indicate that the compression index for wood chips is comparable to a moderate value for soils, whereas for shredded tires it would be considered high for a typical geotechnical material (*5*). Upon unloading, the swell index for shredded tires is almost eight times that of wood chips.

In the layered system approach, each layer is regarded as linearly elastic and isotropic, with two material parameters: the Young's modulus (E) and Poisson's ratio (ν). As Figures 6 and 7 indicate, the first assumption does not hold true for the shredded tires and wood chips when they are loaded and unloaded from the initial, uncompacted state; the relationship between σ_v and ϵ_v is nonlinear. However, when loading and unloading cycles are applied, which can be regarded as simulation of field compaction, the response is much closer to linear elastic. With this approximation, which is shown in Figures 6 and 7 as dashed lines, parameters E and ν can be determined from the one-dimensional compression test in which the horizontal stress is measured.

In view of symmetry about the vertical axis, and $\epsilon_h = 0$, the three generalized Hooke's law equations for normal strains reduce to two (*7*):

$$\epsilon_v = \frac{1}{E}(\sigma_v - 2\nu\sigma_h) \tag{10}$$

$$0 = \frac{1}{E}[\sigma_h(1 - \nu) - \nu\sigma_v] \tag{11}$$

The proportionality between the vertical stress and strain, and between the horizontal and vertical stress, can be written as

$$\sigma_v = m\epsilon_v \tag{12}$$

$$\sigma_h = K\sigma_v \tag{13}$$

which, when substituted into Equations 10 and 11, gives

$$E = \left(1 - 2\frac{K^2}{1 + K}\right)m \tag{14}$$

$$\nu = \frac{K}{1 + K} \tag{15}$$

It was found that the values of m and K for shredded tires are about $m = 3$ MPa, and $K = 0.82$. For wood chips these are about $m = 150$ MPa, and $K = 0.36$. When these values are substituted in Equations 14 and 15, the Young's modulus and Poisson's ratio for shredded tires are $E = 0.78$ MPa, $\nu = 0.45$, and for wood chips $E = 70$ MPa, $\nu = 0.26$ (see Table 1). It is seen that Young's modulus for shredded tires is about 1/100 that for wood chips, and the Poisson's ratio is about two times higher.

The above calculation of Young's modulus and Poisson's ratio is based on the assumption that the material is isotropic. Because the shredded tires particles are flat, they tend to arrange themselves mutually parallel when compacted or loaded. This creates a structure that is no longer isotropic; a honeycomb-type structure with horizontally elongated cells would be a good approximation. Accordingly, the stiffness in the vertical direction may be higher than in the horizontal plane, and the material can be termed anisotropic-transversely isotropic. This type of elastic material is described by five material constants rather than two (*7*): two Young's moduli, two Poisson's ratios, and one shear modulus (in an isotropic material the shear modulus can be expressed as a function of E and ν). A direct evaluation of these constants requires tests other than one-dimensional compression, and these can be difficult to perform. In particular, evaluating the shear modulus would require a very complex torsion-type experiment. An alternative would be to evaluate some constants from an inverse analysis, in which actual layered-system deflections are measured and the constants are backcalculated. This methodology has found application in evaluating Young's modulus for isotropic materials (*8*); an adequate methodology would have to be developed for anisotropic materials.

CONCLUSIONS

An attempt has been made to address the characterization of shredded tires in terms of standard geotechnical engineering properties. Ranges of values have been identified for properties such as size, bulk density, porosity, and permeability. However, questions remain regarding the mechanical behavior of shredded tire deposits and their effect on the performance of pavements and

other geotechnical structures such as retaining walls and foundations. More field and laboratory tests are required to assess the deformability parameters over a wider range of stress levels. From the work presented here, the following conclusions may be drawn:

1. The lightweight nature, durability, and high permeability of shredded tires makes this an attractive material for use in embankments over weak soils. However, such use must be tempered by considerations of its mechanical behavior as discussed below.
2. The bulk density of shredded tires is approximately 2.5 times greater than that of wood chips; yet it is still almost 4 times lower than that of conventional geotechnical materials.
3. Large-size shredded tires (those sliced only once) are difficult to work with during construction. Field observations revealed excessive damage to placement and compaction equipment. Adequate compaction of this material was normally achieved after 15 passes of a 27-ton bulldozer on a 1-m lift.
4. The results of compressibility tests clearly illustrate that shredded tires are far more compressible than wood chips, the Young's modulus of small-size particles is about 100 times lower, and this material possesses much more capability for rebound. The implication for a roadway pavement is that the pavement system would be subject to much higher deflections under loads and that the materials would experience a higher degree of strain reversal. This, if not accounted for, may lead to premature fatigue failure of hard surface pavement materials such as asphalt or portland cement concrete.
5. Classical multilayer elastic analysis for pavement systems may be inadequate for representing the stresses and strains in systems containing shredded tire fill because the structure of the shredded tire mass is anisotropic, with a stiffer response in the vertical direction. It seems imperative to undertake studies on the influence of material anisotropy on layered system response. The difficulty in performing such studies lies not in theoretical solutions but in experimental determination of the material parameters. The simplest transversely isotropic elastic material is characterized by five constants, whose direct determination may be very difficult if not impossible. An inverse analysis (backcalculation) of measured deflections may offer a way for determining some constants.

ACKNOWLEDGMENTS

The authors gratefully acknowledge financial support provided by the Minnesota Department of Transportation. The involvement of M. Bouhaja in conducting the tests is also appreciated.

REFERENCES

1. Williams, J., and D. Weaver. *Guidelines for Using Recycled Tire Carcasses in Highway Maintenance*. California Department of Transportation, Sacramento, May 1987.
2. Brassette, T. *Used Tire Material as An Alternate Permeable Aggregate*. California Department of Transportation, Sacramento, June 1984.
3. Giesler, E., W. K. Cody, and M. K. Nieme. Tires for Subgrade Support. Presented at Annual Conference on Forest Engineering, Coeur D'Alene, Aug. 1989.
4. Rudd, C. J., and B. Loney. The Use of Shredded Tires as a Lightweight Subgrade. Presented at 38th Geotechnical Engineering Conference, University of Minnesota, Feb. 1991.
5. Sowers, G. B., and G. F. Sowers. *Introductory Soil Mechanics and Foundations*. Macmillan, New York, 1951.
6. Drescher, A., D. Newcomb, and M. Bouhaja. *Development of Design Guidelines for Shredded Tire Fill in Road Subgrades and in Retaining Walls*. Draft Final Report. Minnesota Department of Transportation, St. Paul, June 1992.
7. Sokolnikoff, I. S. *Mathematical Theory of Elasticity*, 2nd ed. McGraw-Hill, New York, 1956.
8. Mahoney, J. P., D. E. Newcomb, N. C. Jackson, and L. M. Pierce. *Pavement Moduli Backcalculation Shortcourse*. FHWA, U.S. Department of Transportation, Sept. 1991.

Using Recovered Glass as Construction Aggregate Feedstock

C. J. SHIN AND VICTORIA SONNTAG

The success of recycling collection programs has resulted in an oversupply of broken glass, or cullet, in many parts of the country. To open the construction aggregate market, a multistate and industry evaluation of glass as construction aggregate was conducted. The study defines the suitability of cullet as a construction aggregate in terms of its engineering performance, environmental impact, cost comparability with natural aggregates, and safety in handling. The analysis concludes that glass, as an aggregate, is strong, clean, safe, and economical. From an engineering standpoint, cullet appears to be an excellent supplement or replacement for natural aggregates in many construction applications. Comprehensive tests were performed for specific gravity, gradation, workability, durability, compaction, permeability, thermal conductivity, and shear strength. The effects of debris level, cullet content as a percentage of aggregate, and cullet size were also investigated. When cullet is compacted to a dense state, the material is rigid and strong. The test data indicate that under normal working stresses, the moduli and shear strength of the cullet samples are similar to those of natural aggregate. In the case of $^1/_4$-in. minus cullet, adding cullet to the natural aggregate can even increase the rigidity and strength. Compaction curves tend to become flatter as cullet content increases, implying that the maximum dry density is relatively insensitive with respect to moisture. From a construction standpoint, this means that the material can be compacted even in wet weather.

Construction aggregates promise to be a viable market option for glass recycling. The size of the construction aggregate market dwarfs the potentially available supply of recovered glass, and in most cases, the cost to recover and market glass as a construction aggregate is less than the cost to use it as landfill. As a unique material, glass can contribute to performance in many engineered applications.

To open this market for glass, a multistate and industry study (*1*), with participation and support from three state departments of transportation, undertook to demonstrate the technical and economic feasibility of using glass as construction aggregate feedstock. The purpose of the Glass Feedstock Evaluation Project was to provide the necessary information on cullet properties and processing so that engineers can specify the use of cullet as a construction aggregate with confidence and suppliers of recycled glass aggregate can invest in market development with minimal risk. The study defines the suitability of cullet as a construction aggregate in terms of its engineering performance, environmental impact, cost comparability with natural aggregates, and safety in handling. The analysis concludes that recovered glass used as aggregate is strong, clean, safe, and economical.

C. J. Shin, Dames & Moore, 2025 First Avenue, Seattle, Wash. 98121. V. Sonntag, Clean Washington Center, Washington Department of Trade and Economic Development, 2001 6th Avenue, Suite 2700, Seattle, Wash. 98121.

GLASS RECYCLING IN 1993

The one well-established market for recovered glass, the glass container industry, is characterized by oversupply. The advent of community recycling programs in the late 1980s and early 1990s resulted in a tremendous surge in the supply of recovered glass. This growth in supply continues unabated as more communities join the ranks of recyclers and more people are drawn into existing recycling programs. For a community of 10,000, the supply can be roughly estimated at 250 tons per year, assuming 50 percent recovery at an annual consumption level of 80 lb of glass per person. Many communities recover upward of 70 percent of the available glass.

On the demand side, many glass plants are limited to a low percentage of cullet (crushed glass) in their batch for technical and economic reasons. This market also suffers supply-and-demand dislocations because of geographic concentration of glass plants, and transportation costs often outweigh the market price of cullet. Also, although cullet processed to furnace-ready standards brings up to $60 per ton, the costs to color-sort and remove such contaminants as ceramics and metals can exceed the cullet's present market value.

Because there is no need to color-sort glass for aggregate use and because the contaminant specifications are less stringent, the cost to supply to the construction aggregates market is far less than that of beneficiating glass to be remade into bottles. As a materials source for either the container or the construction aggregate markets, unprocessed cullet exhibits varying quality in terms of its nonglass content depending on how the glass is collected and sorted for recycling. A principal aim of the Glass Feedstock Evaluation Project was to assess the engineering performance and environmental suitability of glass in aggregate applications over the range of debris content levels that would reasonably be associated with the different collection and sorting techniques.

TECHNICAL APPROACH

For the study, glass sources were selected from around the country to represent the spectrum of glass collection and sorting systems—drop boxes, deposit collection, curbside commingled collection, and blue bag programs, among others. (In a commingled collection program, one or more recyclables are collected together and then later sorted; in a blue bag program, all recyclables are collected together.) Sample material was composited from stockpiles and ranged in size from whole bottles to fines. A laboratory jaw crusher was used to prepare the glass for environmental testing and debris-level classification. All debris was passed through

with the glass. Debris was defined as any deleterious material that could affect the performance of engineered fill, generally, nonceramic materials. Types of debris observed in cullet samples included paper, foil, and plastic labels; plastic and metal caps; cork; paper bags; wood debris; food residue; and grass.

Twenty-nine sources were categorized for debris content level, and representative high and low debris-level sources were selected for engineering performance testing. In addition to debris content level, the study investigated two other key independent variables to determine their effect on engineering performance. These were the cullet content in the aggregate mix (15, 50, or 100 percent by weight) and the aggregate mix gradation ($^1/_4$ or $^3/_4$-in. minus). Affordable techniques are available to control both these variables: aggregate mixing equipment for cullet content and glass crushers for gradation. Two types of natural aggregate—a crushed rock and a gravelly sand—were selected for the mixed samples.

The applications of interest were all unbound aggregate applications. It was beyond the scope of the study to look at glass in composites such as glassphalt and glasscrete. A statistical analysis was conducted on the environmental data and on key engineering data to ensure that any variability in results was within the expected range at a high confidence level.

ENVIRONMENTAL SUITABILITY

No appreciable environmental impact could be detected. The testing program contained three components: organic and inorganic chemical characterization, including evaluation of the potential for bacterial growth; an assessment of contaminant leachability over time; and a determination of the incidence of lead and leachable lead.

Limited organic compounds were found, not at harmful levels, including plastic debris, low concentrations of food residues, and organics that occur naturally in the environment. One atypical blue bag collection source contained elevated levels of polycyclic aromatic hydrocarbons (PAHs), attributed to the inclusion in the collection program of recyclable plastic bottles that once contained oil products.

The incidence of lead contamination was found to be within acceptable limits. Lead foil wrappers used on wine bottles do cause highly localized peaks of lead concentration, but these concentrations statistically average to levels typical of many natural soils. All sources were examined to determine lead incidence, and for 10 of those indicating the presence of lead, multiple samples were analyzed (6 discrete samples from composited sources).

SAFETY ANALYSIS

Bulk samples showed crystalline silica concentrations of less than 1 percent, placing glass dust in the nuisance category according to federal regulations (20 CFR 1910.1000), and air samples taken during compaction testing showed total dust concentrations below 0.5 mg/m^3 compared with the permissible exposure limit of 10.0 mg/m^3. There is evidence for the carcinogenicity of crystalline silica, and dusts from materials containing greater than 1 percent crystalline silica are classified as toxic, as is silica sand. Silica in glass is in the amorphous form.

Cullet is an abrasive material, causing irritation when the skin comes in contact with very fine fragments. Bottle cullet crushed to $^3/_4$-in. minus does not normally present the skin cut or penetration hazards associated with larger glass bottle fragments, drinking glasses, and plate glass. Although there are no standard methods for recording the skin penetration hazard, it is noted that laboratory personnel experienced no lacerations while handling this material. The $^1/_4$-in. minus material was particularly benign from this standpoint. Recycling and glass industry personnel working with crushed cullet report no undue skin penetration hazards either. Routine handling precautions are recommended.

ENGINEERING SUITABILITY

From an engineering standpoint, cullet appears to be an excellent supplement or replacement for natural aggregates in many construction applications. Comprehensive tests were performed for specific gravity, gradation, workability, durability, compaction, permeability, thermal conductivity, and shear strength. The effects of debris level in the cullet (high and low debris), cullet content by weight (15, 50, and 100 percent), and size of cullet ($^1/_4$- and $^3/_4$-in. minus) were investigated.

Debris levels were determined using a visual method adapted from the American Geological Institute (AGI) (2). Accuracy of visual classification, which is easily employed in the field, was confirmed through quantifying the debris by weight and volume in six samples. Because of the platy nature of the debris, visual classification produces a greater quantitative difference between high and low debris levels than do volume- and weight-testing methods. Relatively high-debris and low-debris sources, with 5 percent and 1 percent debris levels, respectively, by visual classification, were selected for testing.

Principal findings of the engineering performance evaluation include the following:

- The data show that both $^1/_4$- and $^3/_4$-in. minus cullet are durable and mechanically sound. Cullet resistance to degradation is lower than that of natural aggregate. However, when cullet is mixed with natural aggregate, the resulting material will most likely have acceptable Los Angeles (L.A.) abrasion, *R*-value, and resilient modulus properties for use as roadway aggregate.
- Cullet compacted to a dense state is rigid and strong. These characteristics are attributed to the compactness of the bulk material, high shear strength of individual particles, and high interparticle frictional resistance. Under normal working stresses, the moduli and shear strength of the cullet samples are similar to those of natural aggregate. In the case of $^1/_4$-in. minus cullet, adding cullet to the natural aggregate can even increase the rigidity and strength.
- Cullet experiences very little gradation change under normal compaction and loading conditions. This gradation stability is due to the strength of the individual particles. The stable gradation translates to constant engineering properties, making it possible to base engineering designs on properties derived from laboratory tests.
- The cullet and cullet-aggregate mixtures have favorable compaction characteristics, which provide good workability of the material. In general, density of the compacted cullet samples is not sensitive to moisture content, an advantage in wet weather. Choosing the appropriate laboratory compaction method could be important, as is evident from the sensitivity of test data such as

California bearing ratio (CBR) values (presented below) to the compaction methods.

- Debris level does affect some engineering properties of the cullet, but on the basis of the test data, good engineering performance can be expected for cullet containing up to 5 percent (by visual classification) debris.

Individual test results and their significance are summarized in the following sections.

Specific Gravity

Fourteen specific gravity tests (ASTM D854) were conducted on the fraction of the samples finer than the standard U.S. No. 4 sieve. Fourteen bulk specific gravity tests (ASTM C127) were conducted on the fraction of the samples coarser than $^1/_4$ in. Specific gravities of coarse cullet samples ranged from 1.96 to 2.41 and of fine cullet samples from 2.49 to 2.52. Differences in the test procedures and in the debris levels of the samples contribute to the differences in range. The lowest specific gravity of 1.96 measured for the high-debris, $^3/_4$-in. minus cullet reflects its higher debris level.

Specific gravities of the natural aggregates used in the testing program—crushed rock and gravelly sand—ranged from 2.60 to 2.83. These values are typical and are higher than those of cullet. Specific gravities of the mixed samples were found between those of 100 percent cullet and 100 percent natural aggregate. The difference in the specific gravities between cullet and natural aggregate and between high-debris and low-debris cullet are believed to affect the relative density and unit weight of compacted samples.

Maximum and Minimum Index Densities

Thirteen maximum index density tests were conducted using the ASTM D4253 test procedure. Maximum index densities ranged from 1.46 to 1.75 g/cm^3 (90.9 to 109.3 pcf) for the 100 percent cullet samples, 1.96 to 2.08 g/cm^3 (122.6 to 130.0 pcf) for the 50 percent cullet samples, and 2.18 to 2.25 g/cm^3 (135.9 to 140.3 pcf) for the 15 percent cullet samples. Fourteen minimum index density tests were conducted using the ASTM D4254 test procedure. The test results indicate that the minimum index densities range from 1.23 to 1.43 g/cm^3 (76.8 to 89.5 pcf) for the 100 percent cullet samples, 1.64 to 1.70 g/cm^3 (102.3 to 105.9 pcf) for the 50 percent cullet samples, and 1.83 to 1.87 g/cm^3 (114.2 to 116.6 pcf) for the 15 percent cullet samples.

The data indicate that maximum index density is affected largely by the cullet content. The trend of increasing density with decreasing cullet content is also true for the minimum index density. The 100 percent, $^3/_4$-in. minus, high-debris cullet sample also had the lowest density. Size has a minor effect on density. The reasons for the slightly higher density of the $^3/_4$-in. minus cullet samples is unclear. One possible explanation is that the presence of larger particles provides a lubrication effect that facilitates particle movement, resulting in a higher density.

Gradation

A total of 55 sieve analyses were conducted to investigate the degree of gradation change before and after the compaction, hydrostatic compression, and triaxial shear tests. Significant gradation change occurred only when 100 percent, $^3/_4$-in. minus cullet samples were subjected to heavy impact compaction, that is, the Modified Proctor test procedure, as exemplified in Figure 1. Note that the material has less than 5 percent fines (particle size less than No. 200 sieve) before and after compaction. (The before-compaction test curve is typical of the $^3/_4$-in. minus samples.) All other test conditions produced little or no gradation change.

The gradation test results indicate the feasibility of using both impact and vibratory compaction methods for field control of fill materials composed of cullet. Since these compaction methods mimic the compactive effort of field equipment, minimal gradation change implies minimal difference in the properties of laboratory-compacted samples as compared with field-compacted cullet. The exception to this is 100 percent cullet subjected to heavy impact compaction, which would normally be used for fill materials subjected to dynamic or heavy stationary loads, conditions precluding the use of 100 percent cullet.

The gradation change caused by the hydrostatic compression and triaxial shear tests was small, implying minimal breakage of the cullet under normal working loads. In other words, the cullet, like crushed rock, has adequate strength to behave like an elastic rigid body that deforms under hydrostatic loads and displaces or rotates near shear planes.

Particle Shape

Particle shapes were visually examined using the ASTM D2488 test procedure. All cullet particles tested were angular. About 20 to 30 percent of the $^3/_4$-in. minus cullet, but only 1 percent of the $^1/_4$-in. minus cullet, had a flat or platy shape. Both sizes had a low percentage of flat and elongated particles. This suggests that $^3/_4$-in. minus cullet has a potential to cut, puncture, or wedge into the moving parts of construction equipment, but similar problems are unlikely for $^1/_4$-in. minus cullet because of the low percentage of flat and elongated particles.

Durability

Durability was investigated by conducting the L.A. abrasion test on four samples. These included the 100 percent cullet content, $^1/_4$-in. minus, low-debris sample; 100 percent, $^3/_4$-in. minus, low-debris cullet sample; 100 percent, $^1/_4$-in. minus, high-debris cullet sample; and 100 percent crushed rock. The results were 29.9, 41.7, 30.9 and 13.6 percent, respectively. The percent loss of the 100 percent cullet samples represents the worse condition. It is reasonable to assume that the percent loss of mixed samples would lie somewhere between the percent loss of the two components.

These results indicate that cullet is not as sound mechanically as the crushed rock used in the program. The percent loss for $^1/_4$-in. minus cullet is about 30 percent and for $^3/_4$-in. minus cullet about 42 percent, losses at least two times that of the crushed rock. However, the values for 100 percent cullet are relatively close to the normal limiting values for roadway aggregate. For instance, the Washington State Department of Transportation (WSDOT) specifies a limiting value of 35 percent for a crushed surface course and 40 percent for ballast.

Compactability

Tests for compactability included 15 Standard Proctor compaction tests, 16 Modified Proctor compaction tests, and 15 WSDOT 606 vibratory compaction tests. Typical compaction curves are shown in Figures 2 to 4. In general, the Proctor compaction curves of the cullet samples are relatively flat. From a construction standpoint, this relative insensitivity to moisture content means that cullet can likely be placed during inclement weather.

Maximum density values obtained from the impact Modified Proctor and the vibratory WSDOT 606 tests are about equivalent. Both methods simulate the compaction efforts of heavy compaction field equipment. Since these methods produce little or no gradation change, the similarity in density values implies the feasibility of using either method for the field control of fill materials with cullet content. Again, this statement is not true for 100 percent cullet materials because of the gradation change induced by the Modified Proctor compaction method. For this reason, if 100 percent cullet is to be compacted by heavy field compaction equipment, a vibratory compaction method should be used.

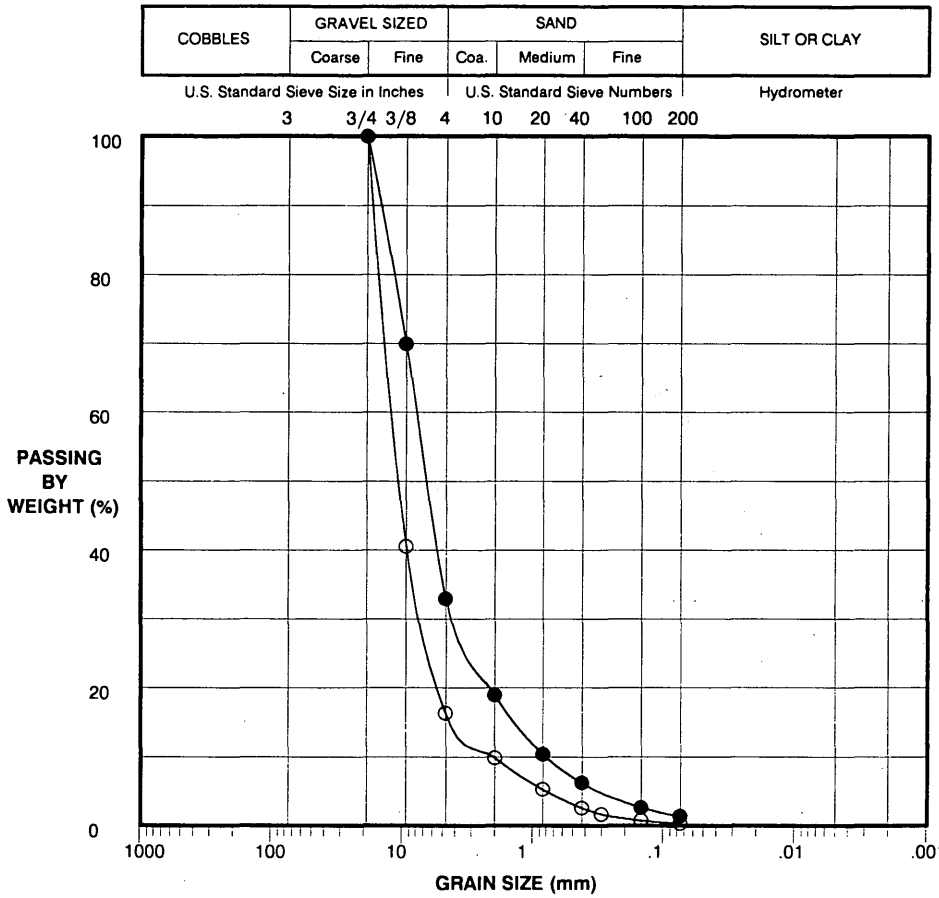

GRAIN SIZE DISTRIBUTION

SYMBOL	DESCRIPTION	% GRAVEL	% SAND	% FINES
○	Before Compaction	83.5	16.1	0.4
●	After Compaction	66.8	31.8	1.4

REMARKS: Sample composed of 100% cullet (high-debris,3/4 inch minus).
Curves depict sample gradation before and after compaction using the ASTM D1557 test procedure.

FIGURE 1 Grain size distribution, 100 percent, high-debris, $^{3}/_{4}$-in. minus cullet.

Feasibility of Nuclear Density Gauge Testing

The feasibility of using a nuclear density gauge was evaluated. Gauge measurements, taken in the backscatter mode, were compared with known density and moisture content. A total of 24 tests were conducted on 100 percent glass and glass-aggregate blends. Test results were inconclusive, because the results showed a wide variation between the gauge and true measurements.

The data appear to indicate that moisture measurements are affected by the debris level of the cullet. The reason for this effect is unclear. The reasons for the wide variation in the density measurements is also unclear. However, two possible sources of errors were identified during the test—the nonuniform density of the test specimens and the laboratory wall effects.

Permeability

A total of 28 constant head permeability tests were conducted. In general, 100 percent cullet samples exhibited high permeabilities (>0.1 cm/sec), and 50 percent and 15 percent cullet content samples exhibited medium permeabilities (0.001 to 0.1 cm/sec). These permeabilities correspond to those of a gravel and medium sand, which are commonly used as filter materials. Permeability increases with increasing cullet content, cullet size, and debris level but decreases with increasing degree of compaction. This trend is consistent with permeabilities of the 100 percent gravelly sand compacted to the 90 and 95 percent compaction levels.

Thermal Conductivity

Four thermal conductivity tests were performed using the ASTM C518 test procedure. Results ranged from 0.260 to 0.638 W/(m · K), results close to values for natural aggregate. Conductivity decreased with increasing cullet content.

Shear Strength

The shear strength of the cullet samples was investigated by conducting seven sets of direct shear for 100 percent cullet and cullet-

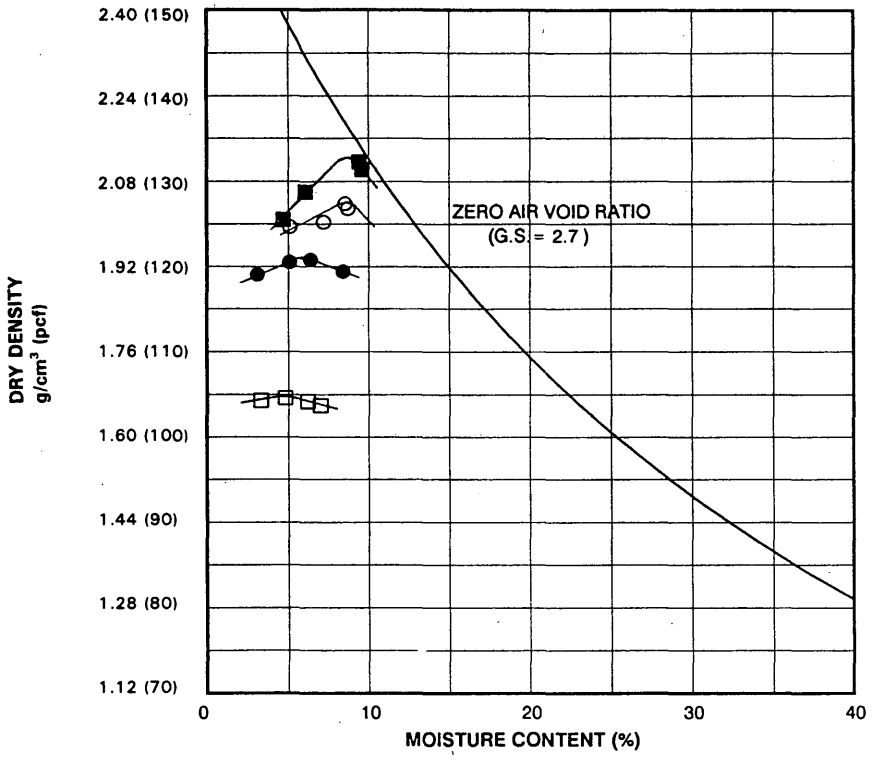

SYMBOL	DESCRIPTION	TEST METHOD	OPTIMUM MOISTURE(%)	MAX. DRY DENSITY g/cm³ (pcf)
○	15% cullet & 85% gravelly sand	ASTM D698	8.6	2.03 (127.0)
●	50% cullet & 50% gravelly sand	ASTM D698	6.0	1.95 (121.4)
□	100% cullet	ASTM D698	5.0	1.68 (104.9)
■	100% gravelly sand	ASTM D698	8.8	2.12 (132.5)

REMARKS: Sample composed of cullet (low-debris, 1/4 inch minus) and gravelly sand.

FIGURE 2 Standard Proctor compaction test, low-debris, $^1/_4$-in. minus cullet.

aggregate blends and five sets of triaxial shear tests on blends. In the direct shear tests the friction angles ranged from 49.4 to 53 degrees for cullet, where the friction angle of the gravelly sand sample was 51 degrees. The triaxial shear test results, presented in Table 1, gave friction angles from 42 to 46 degrees for cullet and a friction angle of 44 degrees for crushed rock. Cullet content and debris level do not appear to have an appreciable effect on the strength within the ranges tested.

In the triaxial shear results, the bulk modulus of $^1/_4$-in. minus cullet is slightly higher than that of the $^3/_4$-in. minus cullet, and the bulk modulus of the crushed rock lies between these. From the mechanics point of view, the $^1/_4$-in. minus samples are stiffer than the $^3/_4$-in. minus and 100 percent crushed rock samples. The better mechanical behavior can be explained by the better gradation of the $^1/_4$-in. minus cullet, which is indirectly validated by comparing the gradations of 100 percent crushed rock and $^1/_4$-in. minus and $^3/_4$-in. minus cullet. The $^1/_4$-in. minus cullet samples contained mostly sand-sized or "filler" particles, and the $^3/_4$-in. minus cullet and crushed rock samples contained mostly gravel-sized particles.

Resistance *R*-Value

Five *R*-value tests were performed using the WSDOT 611 test procedure, which is a modification of the AASHTO T-190 test method. The modification involves using 15 and 25 blows of kneading compaction at pressures of 690 and 1724 kPa (100 and 250 psi), respectively. These pressures are lower than those specified in the AASHTO T-190 method. The exudation pressure used in both test procedures is 2069 kPa (300 psi). Different exudation pressures may be used in other states; however, because of the granular nature of the test materials, it is believed that exudation pressure will not have a substantial effect on test results. No *R*-value tests were conducted on high-debris samples.

As seen from the results in Table 2, adding cullet to crushed rock reduces the *R*-value slightly, and this reduction increases slightly with increasing cullet content. *R*-value is commonly used to specify base or subbase aggregate. For instance, WSDOT specifies a minimum *R*-value of 72 for gravel base, Minnesota Department of Transportation specifies a minimum *R*-value of 65 for base materials, and the California Department of Transportation

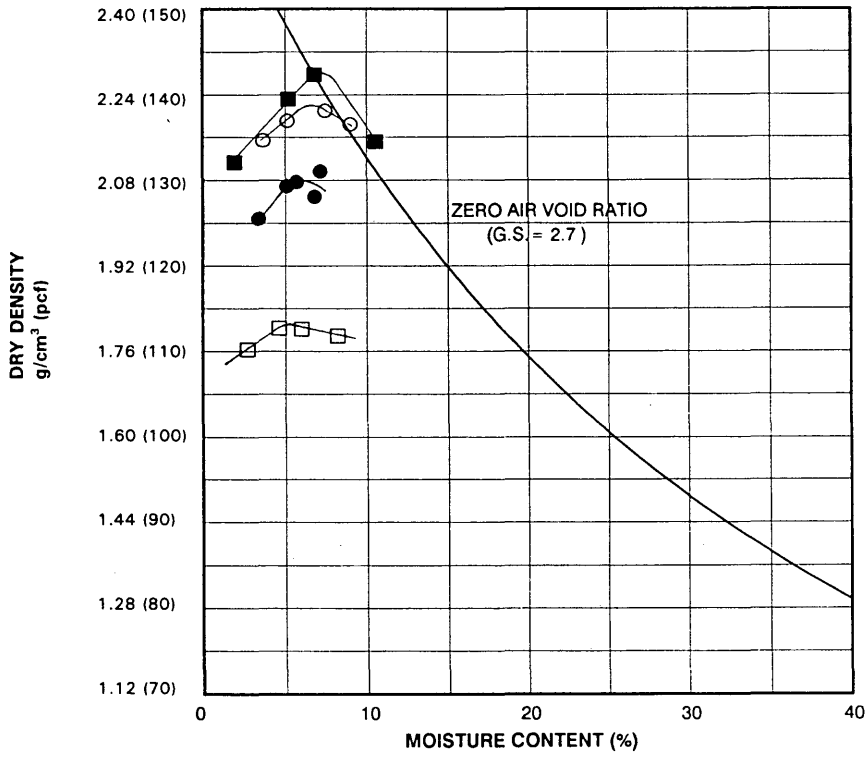

SYMBOL	DESCRIPTION	TEST METHOD	OPTIMUM MOISTURE(%)	MAX. DRY DENSITY g/cm³ (pcf)
○	15% cullet & 85% crushed rock	ASTM D1557	6.7	2.22 (138.5)
●	50% cullet & 50% crushed rock	ASTM D1557	6.5	2.08 (130.0)
□	100% cullet	ASTM D1557	5.2	1.81 (113.0)
■	100% crushed rock	ASTM D1557	7.2	2.23 (142.0)

REMARKS: Sample composed of cullet (low-debris, 1/4 inch minus) and crushed rock.

FIGURE 3 Modified Proctor compaction test, low-debris, $^1/_4$-in. minus cullet.

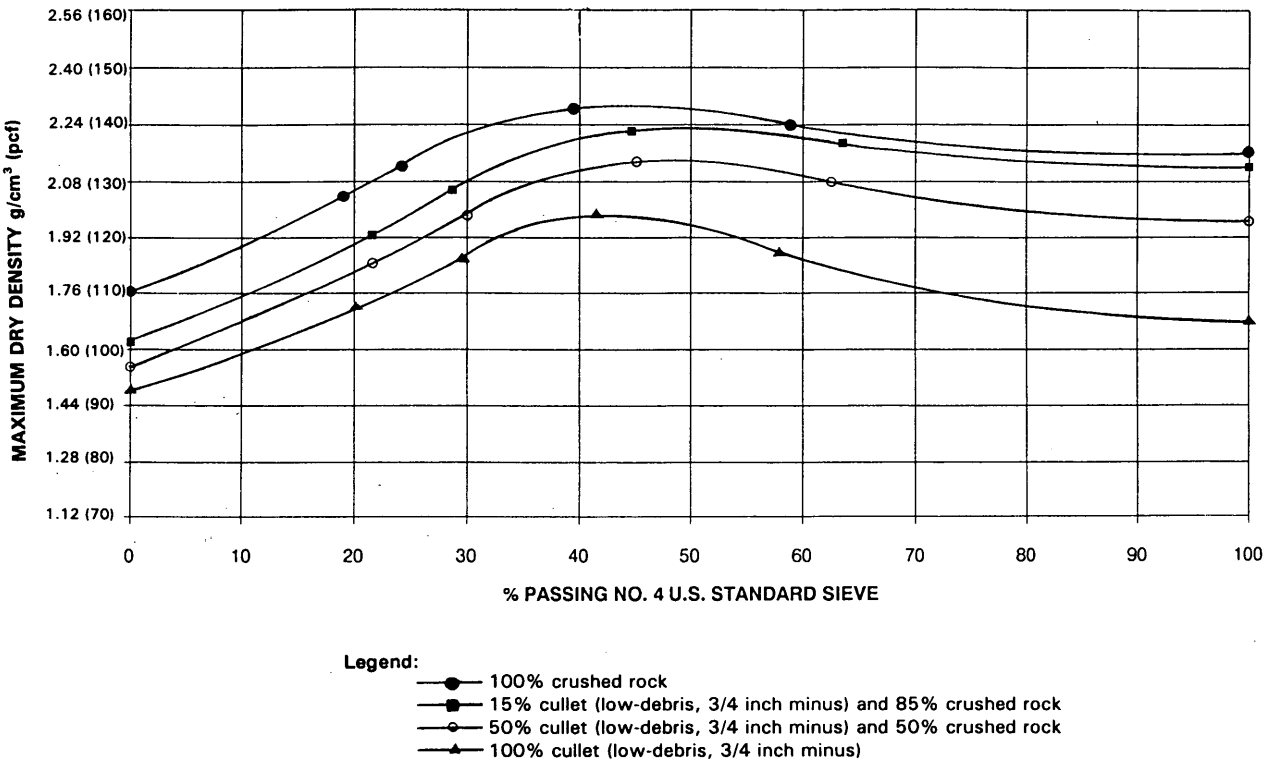

FIGURE 4 WSDOT 606 compaction test, low-debris, $^3/_4$-in. minus cullet.

TABLE 1 Triaxial Shear Test Results[a]

Sample Type	Cullet Content (%)	Cullet Gradation	Confining Pressure kPa (psi)	Bulk Modulus MPa (ksi)	Initial Tangent Modulus MPa (ksi)	Friction Angle (Degrees)
Low-debris sample	50	¼" minus	34.5 (5)	34.5 (5.0)	76.6 (11.1)	
Low-debris sample	50	¼" minus	68.9 (10)	31.7 (4.6)	125.5 (18.2)	43
Low-debris sample	50	¼" minus	103.4 (15)	35.1 (5.1)	109.0 (15.8)	
Low-debris sample	15	¼" minus	34.5 (5)	33.8 (4.9)	82.1 (11.9)	
Low-debris sample	15	¼" minus	68.9 (10)	31.7 (4.6)	91.1 (13.2)	46
Low-debris sample	15	¼" minus	137.8 (20)	35.1 (5.1)	81.4 (11.8)	
Low-debris sample	50	¾" minus	34.5 (5)	15.2 (2.2)	109.0 (15.8)	
Low-debris sample	50	¾" minus	68.9 (10)	23.4 (3.4)	81.4 (11.8)	42
Low-debris sample	50	¾" minus	137.8 (20)	26.9 (3.9)	148.4 (21.5)	
Low-debris sample	15	¾" minus	34.5 (5)	15.2 (2.2)	78.0 (11.3)	
Low-debris sample	15	¾" minus	68.9 (10)	23.4 (3.4)	109.0 (15.8)	44
Low-debris sample	15	¾" minus	137.8 (20)	24.8 (3.6)	163.5 (23.7)	
crushed rock	0	N/A[b]	34.5 (5)	28.9 (4.2)	65.6 (9.5)	
crushed rock	0	N/A[b]	68.9 (10)	28.9 (4.2)	161.5 (23.4)	44
crushed rock	0	N/A[b]	137.8 (20)	23.4 (3.4)	109.0 (15.8)	

Notes: a. All tests performed under consolidated and drained conditions. Samples were prepared closed to about 95% of the maximum dry density as determined by ASTM D 1557 test procedure.
b. Not Applicable.

TABLE 2 Resistance *R*-Value Test Results

Sample Type	Type of Natural Aggregate	Cullet Content (%)	Cullet Gradation	Resistance R Value
Low-debris sample	crushed rock	50	¼" minus	73
Low-debris sample	crushed rock	50	¾" minus	76
Low-debris sample	crushed rock	15	¼" minus	75
Low-debris sample	crushed rock	15	¾" minus	77
N/A	crushed rock	0	N/A	78

NOTES: All tests performed using the WSDOT 611 test procedure.

specifies a minimum *R*-value of 60 for Class 1 subbase and 78 for Class 2 aggregate base. Generally, the required *R*-value is higher for the base than for the subbase materials. From the test results it is clear that the cullet-added crushed rock, with a cullet content up to 50 percent, possesses adequate strength for both base and subbase aggregate.

California Bearing Ratio

CBR values of specimens prepared using the impact compaction method are higher than those of specimens prepared using vibratory compaction, as seen from the Table 3 test results. The discrepancy increases as cullet content increases; values for 15 percent cullet content samples are about the same as those for crushed rock, regardless of the compaction method used.

Typical CBR values of a compacted granular material range from 40 to 80 (New York State Department of Transportation). All values of the cullet-added samples lie within this typical range. Also, adding 15 percent cullet to the crushed rock does not produce a noticeable difference in the CBR value. However, as the cullet content increases to 50 percent, an obvious reduction occurs. For those samples prepared using the impact compactor, the reduction was about 25 percent when the cullet content increased from 15 to 50 percent. A much higher reduction, about 50 percent, was noted for samples prepared using the vibratory compactor. These results underscore the importance of choosing the correct specimen preparation method for materials with cullet content over 15 percent.

Resilient Modulus (Cyclic Triaxial)

Five resilient modulus tests were performed using a modified AASHTO T294 test procedure. In the modified procedure, an internal load cell was used instead of an external load cell as specified in the AASHTO standard.

Resilient modulus is a measure of a material's stiffness and can be used for pavement design. The resilient modulus of natural aggregate is typically about 206.7 MPa (30 ksi) at a bulk stress of 172 kPa (25 psi). For a granular natural aggregate, the typical value is 206.7 MPa (30 ksi) at a bulk stress of 172 kPa (5 psi). From Table 2, it can be seen that even the 50 percent cullet sample would have a resilient modulus value appropriate for use in a typical pavement design. Adding cullet to crushed rock will reduce the resilient modulus, and the reduction increases with increasing cullet content. Note that the low modulus value in Table 4 for the 15 percent, $^3/_4$-in. minus cullet sample is likely caused by the puncturing of the membrane during the test.

One concern regarding the use of cullet mixes in roadway construction is the ability of cullet to withstand repeated traffic loads without breakdown. To help address this concern, the change in resilient modulus of the cullet samples over the first 1,000 cycles may be compared with that of the crushed rock. This comparison is shown in Figure 5. The cullet samples, like crushed rock, do not show appreciable changes in the modulus value. Note that the samples were subjected to a confining pressure of 4 psi and deviator stress of 8 psi in the first 1,000 cycles. This stress level is typical of a subbase material under medium to heavy traffic loads and is much lower than the level at which crushing or breaking of the crushed rock particles would occur. In effect, cyclical load-

TABLE 3 California Bearing Ratio Test Results[a]

Sample Type	Type of Natural Aggregate	Cullet Content (%)	Cullet Gradation	Dry Density g/cm³ (pcf)	CBR VALUE [b]
Low-debris sample	crushed rock	50	¼" minus	1.98 (123.7)	70
Low-debris sample	crushed rock	50	¾" minus	2.01 (125.2)	95
Low-debris sample	crushed rock	15	¼" minus	2.13 (133.2)	110
Low-debris sample	crushed rock	15	¾" minus	2.12 (132.3)	115
Low-debris sample	crushed rock	50	¼" minus	1.93 (120.3)	42
Low-debris sample	crushed rock	50	¾" minus	1.99 (124.5)	44
Low-debris sample	crushed rock	15	¼" minus	2.13 (133.1)	109
Low-debris sample	crushed rock	15	¾" minus	2.12 (132.3)	90
N/A [d]	crushed rock	0	N/A [c]	12.24 (139.6)	105

Notes: a. All tests performed using the ASTM D 1883 test procedure.
b. Values correspond to 0.1 inches penetration.
c. Not Applicable

TABLE 4 Resilient Modulus (Cyclic Triaxial) Test Results[a]

Sample Type	Type of Natural Aggregate	Cullet Content (%)	Cullet Size	Dry Density g/cm³ (pcf)	Resilient Modulus MPa (ksi)[b]
Low-debris sample	crushed rock	50	¼" minus	1.91 (119.2)	212.2 (30.8)
Low-debris sample	crushed rock	50	¾" minus	1.95 (121.8)	217.0 (31.5)
Low-debris sample	crushed rock	15	¼" minus	2.19 (137.1)	238.4 (34.6)
Low-debris sample	crushed rock	15	¾" minus	2.06 (128.5)	136.4 (19.8)[c]
N/A	crushed rock	0	N/A	2.10 (131.1)	277.0 (40.2)

Notes: a. All tests performed using modified AASHTO T 292-91 I test procedure.
b. At bulk stress of 25 psi.
c. Membrane likely punctured during test.

ing of cullet, like crushed rock, did not result in any appreciable crushing.

APPLICATIONS AND MODEL SPECIFICATIONS

Model specifications for using cullet in aggregate applications were developed. Every effort was made to provide specifications that are conservative in light of the study findings. Maximum cullet content, maximum debris levels, minimum compaction levels, and gradation are presented in Table 5 for specific applications.

Debris is defined as any deleterious material that affects the performance of the engineered fill. The percentage of debris is quantified using the AGI comparison charts for estimating percentage composition (*2*).

Cullet should be placed in level loose lifts not exceeding 8 in. and compacted to the specified minimum dry density. The maximum dry density of cullet-aggregate mixtures should be determined by using the Modified Proctor test as described by ASTM D1557. The maximum dry density of 100 percent cullet fills should be determined by using the Standard Proctor test as described by ASTM D698. A minimum of one density test per 1,000 ft^2 of fill but not less than one test per lift should be performed. The nuclear gauge method should be field-verified by the engineer before its use.

EQUIPMENT EVALUATION

Crushing systems are currently available that appear well suited for production of construction-quality cullet. This phase of the study consisted of first surveying mill manufacturers and then monitoring performance tests of six promising candidates. Equipment feature recommendations were developed to help potential processors make purchasing decisions, highlights of which follow.

Because cullet gradation and debris level are important factors with regard to engineering performance, the crushing system

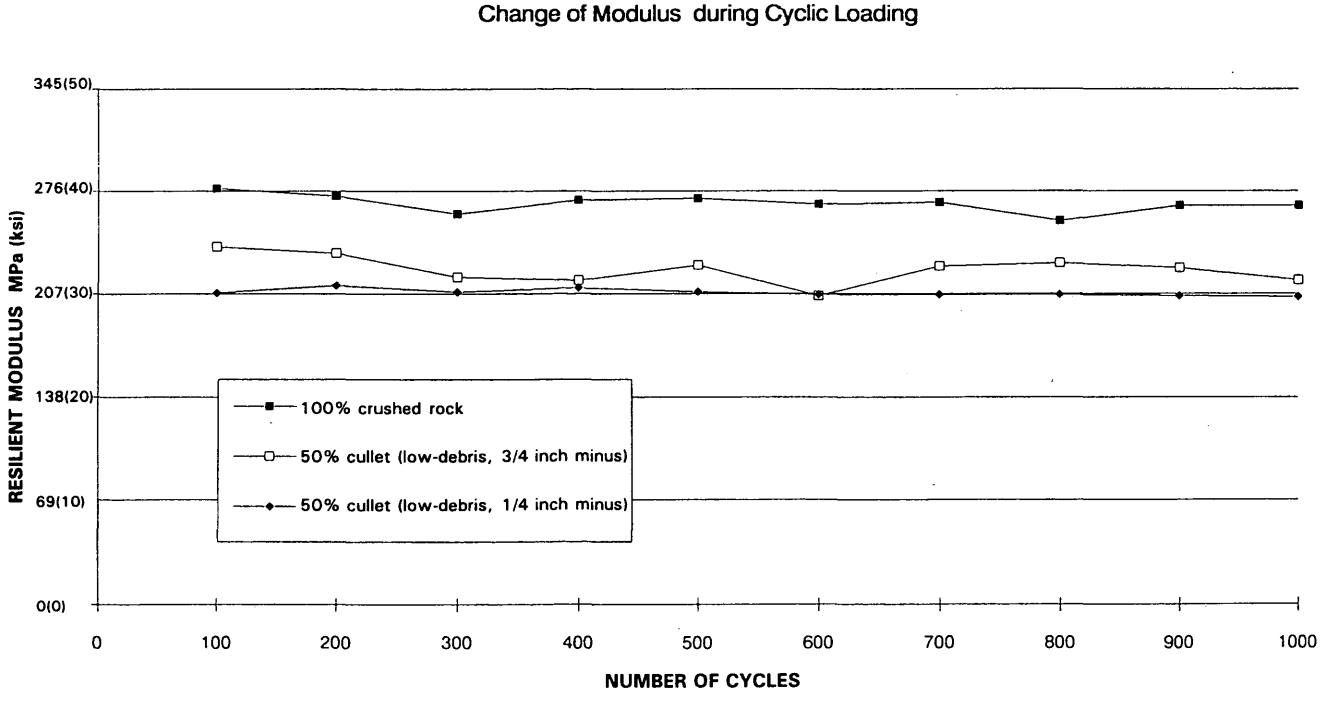

FIGURE 5 Resilient modulus test.

should have a screening system to control particle size and debris level. Ability to adjust the gradation is also a desirable feature option. By controlling gradation, a cullet supplier might target the glass product to specific applications. Cullet is also very abrasive, so wearing surfaces, particularly those of the crushing mechanism, should be constructed of abrasion-resistant material or, alternatively, wearing surfaces should be designed so that they may easily be replaced or resurfaced by depositional welding.

ECONOMICS OF CULLET AS AGGREGATE FEEDSTOCK

An economic model developed during the project identifies essential criteria and parameters for glass aggregate production and points to substantial economic incentives for cullet suppliers, aggregate suppliers, and aggregate buyers alike.

Although cullet used as aggregate feedstock does not command the high prices of the glass bottle market, neither does it require such high processing costs. Processing glass for aggregate feedstock costs from $5 to $9 per ton on the basis of the amortized equipment costs of the equipment evaluated and labor estimates. Sorting glass for the bottle market can run four to five times as much and processing color-sorted cullet to furnace-ready standards adds another $20 per ton. Because construction aggregate markets are primarily local, many recyclers will realize a substantial savings on transportation. Also, recycling costs less than landfilling—the savings of this avoided cost allows recyclers to supply cullet to aggregate processors or contractors at prices near the cost of transporting it, that is, in the $2 to $3 range as collection and processing costs are covered by recycling collection fees. For aggregate processors and purchasers, using cullet can therefore result in a significant cost savings on both a per-ton and per-project basis.

MARKET CONSIDERATIONS

The principal aim of the Glass Feedstock Evaluation Project was to open the way for glass cullet to be used in the construction aggregate market. The evaluation points to the technical and economic viability of using cullet as construction aggregate feedstock. From an engineering standpoint, cullet appears to be an excellent supplement or replacement for natural aggregates in many construction applications. Cullet was tested for harmful contaminants and their potential to leach over time. No appreciable environmental impact could be detected. Cullet can be safely used in construction using routine handling precautions. In many cases, depending on local conditions, glass can be competitive in price or less expensive than utilizing conventional aggregate. In summary, cullet is strong, clean, safe, and economical.

Although technical information is invaluable to opening markets, it is important to remember that there are other important market factors to consider in establishing a local market. Successful local markets are built on networks of suppliers, end users, and processors. Also important is targeting cullet at those applications that make the most sense locally. Factors such as what natural aggregates are locally available, how cullet might supplement or complement the natural aggregate supply, how much cullet might be supplied, what local specifications and environmental regulations apply, and the size of the demand for a given application should be reviewed. Transaction costs should be minimized.

Many jurisdictions around the country have specifications in place that prohibit the use of cullet. These specifications can now be updated on the basis of the information provided from this project. Finally, demonstration projects are also necessary to create local demand for glass cullet as aggregate. Demonstration projects provide local engineers with a chance to gain familiarity with glass and the way it behaves. Well-documented projects will add to the base of knowledge of using glass as a construction aggregate.

ACKNOWLEDGMENTS

This study was conducted under the management of the Clean Washington Center, a division of the Washington State Depart-

TABLE 5 Application Specifications

Structural Fill Gradation					
Sieve Size	Percent Passing By Weight	Use	Max. Cullet Content (%)	Max. Debris Level (%)	Min. Compaction Level (%)
3/4"	100	Base Course	15	5	95
1/4"	10-100	Subbase	30	5	95
No. 10	0-50	Embankments	30	5	90
No. 40	0-25	Static Structural Loads	30	5	95
No. 200	0-5	Fluctuating Loads	15	5	95
		Nonstructural Fill	100	10	85
		Utility Bedding & Backfill	100	5	90

Drainage Fill Gradation					
Sieve Size	Percent Passing By Weight	Use	Max. Cullet Content (%)	Max. Debris Level (%)	Min. Compaction Level (%)
3/4"	100	Retaining Walls	100	5	95
1/4"	10-100	Foundation Drainage	100	5	95
No. 10	0-100	Drainage Blankets	100	5	90
No. 40	0-50	French Drains	100	5	90
No. 200	0-5				

ment of Trade and Economic Development. The Clean Washington Center is the state's lead agency for the market development of recyclable materials. The study was cosponsored by the states of Arizona, California, Minnesota, New York, and Oregon, and by Browning-Ferris Industries and Waste Management of North America. The California, Oregon, and Washington departments of transportation participated in report reviews, and the Washington Department of Transportation Materials Lab performed portions of the engineering performance testing. Research was conducted by the Seattle office of Dames & Moore.

To order the Glass Feedstock Evaluation Project reports, please contact the Clean Washington Center at (206) 587-5520.

REFERENCES

1. Dames and Moore. *Glass Feedstock Evaluation Project: Reports for Tasks 1 through 5.* Clean Washington Center, Washington State Department of Trade and Economic Development, Seattle, 1993.
2. *AGI Data Sheets 15.1 and 15.2: Comparison Chart for Estimating Percentage Composition.* American Geological Institute, Alexandria, Va., 1982.

Utilization of Phosphogypsum-Based Slag Aggregate in Portland Cement Concrete Mixtures

PAUL T. FOXWORTHY, ELFRIEDE OTT, AND ROGER K. SEALS

Phosphogypsum is a by-product of the fertilizer industry, specifically the production of phosphoric acid from phosphate rock. It is produced in large quantities and generally disposed of by stockpiling in large stacks. An alternative to disposal is reuse as a construction material in some form. One such process to convert phosphogypsum to a usable product is the Davy McKee-Florida Institute of Phosphate Research thermal conversion sulfur recovery process, in which sulfur contained in the phosphogypsum is recovered and a slag aggregate by-product is produced. This study centers around the possible utilization of phosphogypsum-based slag aggregate as a substitute for coarse aggregate in portland cement concrete for highway construction. The physical properties of the slag aggregate, such as specific gravity, unit weight, gradation, and absorption, were determined for use in concrete mix design. The durability behavior of the slag aggregate was also explored, exclusive of cold weather performance, which would require further research if the aggregate were exported to northern climates. On the basis of the physical characteristics of the aggregate, a concrete mixture was developed and tested in both the fresh and hardened states. The specific properties evaluated were workability, unit weight, air content, and yield of the fresh concrete along with strength and deformation characteristics of the hardened concrete. The compressive strength, flexural strength, splitting tensile strength, modulus of elasticity, and Poisson's ratio results indicated that the slag aggregate performed well as a coarse aggregate in portland cement concrete and should perform satisfactorily in a highway pavement system.

Phosphogypsum (PG) is a by-product of the production of phosphoric acid, which is a major component in many agricultural fertilizers. It is a light tan, crystalline calcium sulfate powder in the dihydrate form ($CaSO_4 \cdot 2H_2O$) and is more soluble in water than natural gypsum. It is generated at a rate of approximately 4 to 5 Mg/Mg (4.5 to 5.5 tons/ton) of phosphoric acid produced. In the United States, about 31.7 million Mg (35 million tons) of PG is generated each year. There is about 86.2 million Mg (95 million tons) of PG stockpiled in Louisiana and 22.7 million Mg (25 million tons) in Texas, and by the year 2000, about 900 million Mg (1 billion tons) is expected to be stockpiled in Florida. PG is regulated by the Environmental Protection Agency because it contains radioactive Radium-226, which decays to radon gas and is vented into the atmosphere. Environmental concerns and the problems associated with stockpiling have prompted research in Louisiana, Florida, and Texas, as well as in other countries besides the United States, to investigate the utilization of PG (*1*).

There are basically two processes for producing PG-based slag aggregate. The two-stage fluidized bed process uses a fluidized bed reactor with raw PG as the feedstock to produce sulfur dioxide gas (SO_2) and quick lime (CaO). This process is referred to as the flash sulfur cycle process and is copyrighted under the name FLASC (*2*). The circular grate process, developed by the Davy McKee Corporation and the Florida Institute of Phosphate Research (FIPR), mixes predried PG with pulverized coal and silica-bearing minerals for spraying into the flame of the circular grate. Since PG quality varies depending on the source of the phosphate-bearing rock, this mixture can be adjusted to accommodate quality differences and to produce a slag aggregate with consistent quality. Sulfur dioxide gas is released at this point, and the minerals fuse together and drain from the reactor as a molten slag, which is quickly quenched to form the slag aggregate. The sulfur dioxide gas is converted to sulfuric acid and recycled to phosphoric acid production (*1*).

Research programs were initiated in 1982 at FIPR to study the process of thermal decomposition of PG to recover sulfur dioxide and produce a slag aggregate. Since that time, Freeport-McMoRan, Incorporated (FMI), a major producer of phosphoric acid, has constructed a pilot facility at their Uncle Sam Plant in Donaldsonville, Louisiana, in a cooperative venture with the Davy McKee Corporation. The purpose of this joint venture was to investigate the technical feasibility and economic viability of the process as well as the properties of the slag aggregate. Different experimental burns were conducted in an attempt to optimize the production parameters. Eventually, aggregates were produced in five distinct campaigns. Several problems arose during Campaigns 1 through 4 that caused variations in the quality of the slag aggregate produced, but Campaign 5 was judged to have produced successful results.

OBJECTIVE AND SCOPE

The objective of this study was to determine the technical feasibility of using PG-based slag aggregate, specifically slag aggregate produced from Campaign 5 at the Uncle Sam pilot plant facility, as a coarse aggregate in portland cement concrete (PCC) mixtures. In Phase One of the study, previous research on the properties and characteristics of the slag aggregates, primarily from Campaigns 1 through 4, was reviewed to gain an understanding of the nature and behavior of these materials. The physical properties of the aggregates, such as specific gravity, gradation, absorption, and porosity, were summarized, and comparisons were made with conventional aggregates to provide insight concerning their suitability for concrete production. The durability aspects of the slag aggregate were also critically reviewed in this phase to

P. T. Foxworthy and E. Ott, Department of Civil Engineering, College of Engineering, Louisiana State University, Baton Rouge, La. 70803. R. K. Seals, Institute for Recyclable Materials, College of Engineering, Louisiana State University, Baton Rouge, La. 70803.

assess its potential performance in PCC exposed to moderate climates. Additional research would be required to assess cold weather performance, however, if the aggregates were employed in northern climates. Finally, previous work regarding the environmental concerns of PG-based slag aggregates was reviewed in Phase One to assess the possibility of any unaccountable radiation emanation and leachate that might result from the embedment of the slag aggregate in a cement matrix.

Phase Two of the study supplemented the physical characterization studies of Campaign 5 material reported by Taha and Seals (*3*) and investigated the durability characteristics of the aggregate to determine its suitability for use as a coarse aggregate in PCC. Various physical tests, such as specific gravity and unit weight, absorption, porosity, and gradation, were performed on the slag aggregate to provide a basis for the design of PCC mixes. This test series was followed by soundness and freeze-thaw tests to assess the long-term durability potential of the aggregate. Phase Three of the project investigated the performance of the slag aggregate-based concrete using a variety of tests on the fresh and hardened states of the mixture. Comprehensive workability, strength, and elasticity measurements were performed and compared with typical representative properties of concrete made using conventional aggregates.

In this study the physical aspects of PG slag aggregate-based concrete were explored; the environmental and economic aspects of the use of this new material is the subject of companion studies currently under way. These studies will address such concerns as alkali-aggregate and sulfate reactions, chemical compatibility with portland cement, radiation emanations, and energy costs associated with the production of the aggregate. It must be emphasized, however, that this aggregate is a by-product of a process whose primary purpose is to recover the sulfur content of raw PG for the production of sulfuric acid. Thus, the market value of the aggregate represents a credit against the cost of sulfuric acid production, and the economic feasibility of the process is primarily dependent on the comparative cost of sulfuric acid produced using virgin sulfur versus the cost of production using the Davy McKee/FIPR process. At current virgin sulfur prices, the Davy McKee/FIPR process is not economical in the United States. According to tentative capital and production cost estimates, only when sulfur prices approach $125/Mg ($125/long ton) is the sulfur recovery process economical.

CHARACTERIZATION OF CAMPAIGN 5 SLAG AGGREGATE

Morphology

The Campaign 5 aggregate appears dark grey to black in color with a morphology that can best be described from two viewpoints. At the microtexture level, the basic particle is polished and well rounded. At the macrotexture level, however, these basic particles are fused together to form a very rough, angular shape that has a honeycomb appearance. Particle sizes vary from larger than 38 mm ($1^1/_2$ in.) to smaller than 0.075 mm (No. 200 sieve), but only the coarse fraction above 4.75 mm (No. 4 sieve) was characterized.

Specific Gravity and Absorption

The tests to determine the specific gravity and absorption of the slag aggregate were conducted in accordance with ASTM C 127-81 or AASHTO T 85-85 specifications. Table 1 provides the specific gravity and absorption values found for Campaign 5 slag aggregate and compares these values with those for the well-rounded, extremely hard river and pit-run gravels typically used in Louisiana. Apparent and saturated surface dry specific gravities, as well as absorption, were higher for Campaign 5 slag aggregate than for typical river and pit-run gravels. Although the specific gravity information reveals little about the quality of the slag aggregate when used in PCC, it does provide some insight into the expected unit weight of slag aggregate concrete. If the slag aggregate makes up 65 percent of the total volume of concrete and has a saturated surface dry specific gravity approximately 14 percent higher than that of conventional aggregates, the density of slag aggregate concrete should be about 9 percent greater than that of normal concrete. The absorption capacity for the slag aggregate was higher as well, denoting a higher water requirement when used in PCC for the same water-cement ratio.

Unit Weight

Unit weight and void content were determined according to the standard procedures outlined in ASTM C 29-78 or AASHTO T 19-80. Unit weight by compaction through rodding is applicable for the slag aggregate since the maximum size of particles is 25 mm (1 in.). Table 1 shows the results of these tests and a comparison with typical aggregates. Unit weight and void content in aggregates are seldom specification requirements, but ASTM and AASHTO recommend a minimum dry rodded unit weight of 972 to 1134 kg/m^3 (60 to 70 lb/ft^3) for normal weight concrete. The Campaign 5 slag aggregate meets this requirement but is relatively light compared with conventional aggregates. The void content of the aggregate is relatively high at 62.9 percent, reflecting the honeycomb texture of the aggregate particles.

Gradation

Sieve analysis results were used to develop an aggregate blend that conforms with ASTM C 33 and Louisiana Department of Transportation and Development (LDOTD) TR 1003 specifications for coarse aggregate in concrete. Freeport-McMoRan provided approximately 1072 kg (2,400 lb) of randomly sampled Campaign 5 slag aggregate for the research study. The grain size distribution was determined by sieving the entire batch into sep-

TABLE 1 Physical Test Results

	Slag Aggregate	Louisiana Aggregates
Apparent Specific Gravity	3.16	2.62 - 2.65
Saturated Surface Dry Specific Gravity	2.84	2.51 - 2.59
Absorption (%)	7.2	1.0 - 5.0
Rodded Unit Weight (kg/m^3)	1,183	1,540 - 1,702
Void Content (%)	62.9	30-45

1.0 lb/ft^3 = 16.21 kg/m^3

arate sieve fractions and weighing each fraction. The gradation analysis shown in Figure 1 indicates that the slag aggregate does not fall within the range specified by ASTM C 33 and LDOTD TR 1003 for coarse aggregate used in PCC. This does not restrict the material from being used, but merely means that it has to be regraded to meet the specifications.

Durability Analysis

Since the durability of an aggregate has such a profound effect on the performance of PCC, Campaign 5 slag aggregate was subjected to a series of tests in an attempt to identify any potential problems that might arise from its use.

Five-Cycle Sodium Sulfate Soundness

The soundness of aggregates is usually determined by the sodium or magnesium sulfate soundness test procedures given in ASTM C 88-76 or AASHTO T 104-86. The low precision of this test dictates that the results be interpreted carefully. Five test cycles were conducted in which the aggregate was immersed in saturated sodium sulfate solution for 17 hr, drained for 15 min, and then oven dried to reach a constant weight. Test data are shown in Table 2. Upon completion of the test, some disintegration of the aggregate, and in a very few cases splitting of entire aggregate particles, was observed. The results show an average weight loss of about 6 percent on each of the sieve fractions investigated, which is comparable with the degradation experienced by conventional Louisiana aggregates and well below the 15 percent maximum stipulated in the LDOTD specifications. Thus, satisfactory behavior of the slag aggregate with regard to long-term durability is indicated.

Aggregate Freeze-Thaw

A freeze-thaw test is not required for conventional aggregates used in Louisiana, since concrete is not generally subjected to such climatic conditions anywhere in the state. However, such a test is another way to assess the general durability of the slag aggregate. To estimate its behavior, a typical gradation of the slag aggregate used in concrete production was subjected to 50 freezing and thawing cycles using a test procedure developed by the state of Indiana. The aggregate was evaluated using the AASHTO T 103-83, Procedure A, in which the aggregate is totally immersed in water. Results of the test are reported in Table 2. The degradation weight loss after 50 cycles ranged from a high of 19.7 percent for the 2.36-mm (No. 8) sieve to only 1.6 percent for the 25-mm (1 in.) sieve. The weighted average degradation loss due to freezing and thawing for the composite gradation is 4.2 percent and compares favorably with the sodium sulfate soundness results. It should be noted that a hydrogen sulfide odor was evident immediately after the samples were removed from the freezer from the 20th to the 30th cycle. This phenomenon is being studied to determine the underlying cause, but it most likely stems from a residual sulfur impurity from the production process.

Los Angeles Abrasion

LDOTD TR111 and AASHTO T96 test methods describe the procedures for testing different gradations and sizes of coarse aggre-

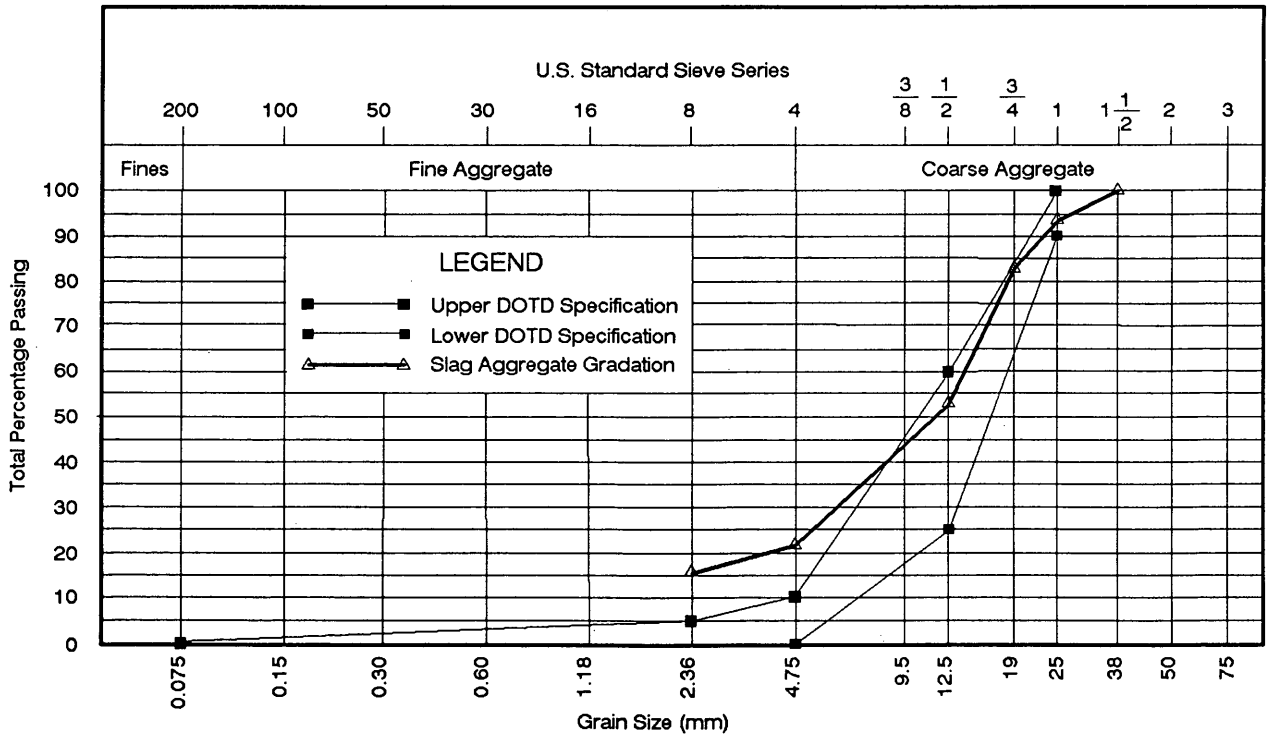

FIGURE 1 Natural gradation for Campaign 5 slag aggregate.

TABLE 2 Durability Test Results

	Sieve Size (mm)					
	2.36	4.75	9.5	12.5	19.1	25.4
Sodium Sulfate Soundness Loss (%)	12.7	4.6	6.3	6.6	8.0	8.0
Freeze-Thaw Soundness Loss (%)	1.6	3.2	4.3	10.6	15.1	19.7

25.4 mm = 1.0 in

gate for resistance to abrasion using the Los Angeles (LA) testing machine. Abrasion losses of selected samples from Campaign 5 ranged between 34.0 and 36.4 percent, values that approach the upper limit of 40 percent established by LDOTD. Additional samples of Campaign 5 slag were also subjected to LA abrasion testing after 4 weeks of immersion in 150°F tap water, and no significant differences in abrasion loss were observed as a result of the soaking.

PG SLAG AGGREGATE-BASED CONCRETE

Background

This portion of the research investigated the use of PG-based slag aggregate as a substitute for conventional aggregates in concrete production. After a mix design for this new material was developed, the study evaluated the engineering properties of fresh concrete, including slump, unit weight, air content, and yield. Attributes of the hardened concrete, such as compressive strength, splitting tensile strength, and flexural strength, were then examined, and an assessment was made of the feasibility of using the slag aggregate in concrete mixes.

Mixture Design

Coarse and Fine Aggregate Proportioning

The gradation of the PG slag coarse aggregate was chosen to meet the ASTM C 33 and LDOTD TR 1003 recommendations and can be seen in Figure 2. Masonry sand was selected for use as the fine aggregate, with 88 percent passing the 1.18-mm (No. 16) sieve and 8 percent passing the 0.075-mm (No. 200) sieve. The

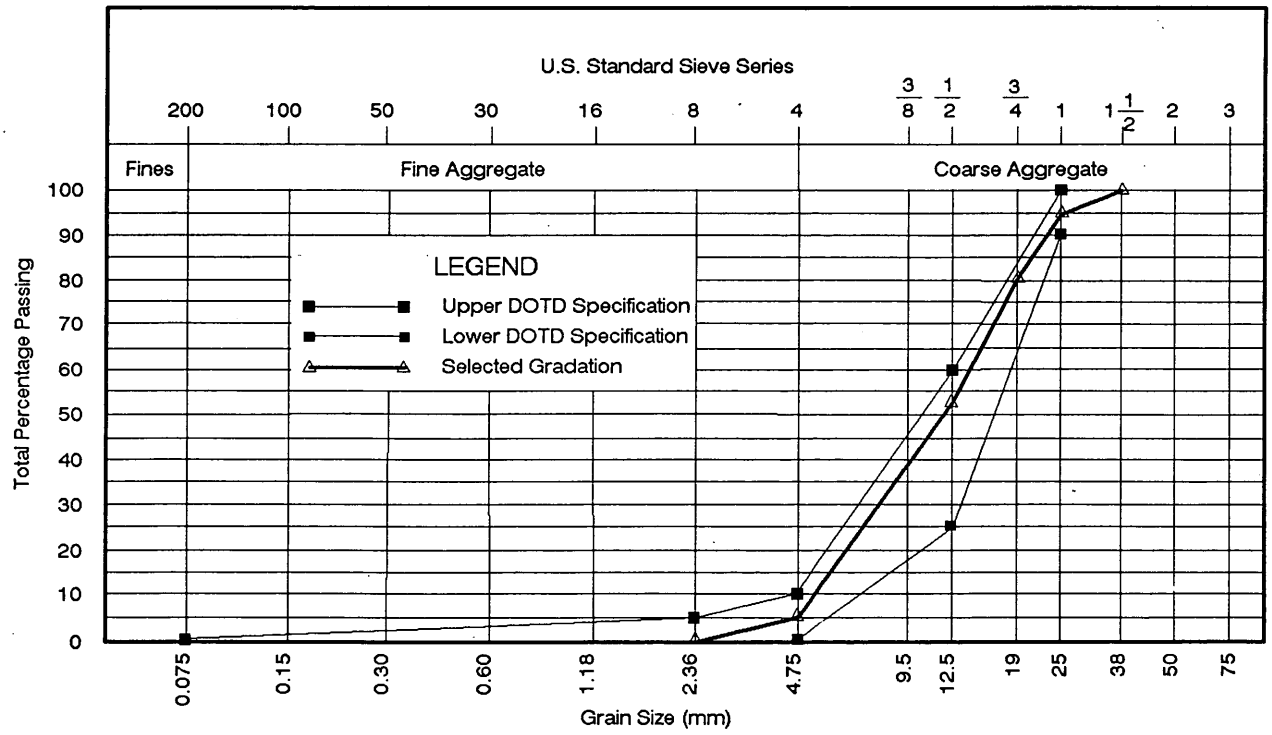

FIGURE 2 Selected gradation for Campaign 5 slag aggregate.

workability of a mixture depends on the volume of the coarse aggregate and the maximum size and fineness of the fine aggregate. Proportions of coarse to fine aggregates that give a workable mix have been developed by experience and are given in the American Concrete Institute (ACI) 211.1 Standard. For coarse aggregate with a maximum size of 25 mm and fine aggregate with a typical fineness modulus of 3.0, the recommended proportion of coarse to fine aggregate is 65 percent. Because of the lack of experience with the slag aggregate, however, four different coarse to fine aggregate proportions were subjectively evaluated for optimal workability, keeping the water content, cement content, and thus the water-cement ratio, constant at typical values for highway construction. The results of the subjective evaluation of the workability, appearance, and finishability of the fresh concrete indicated that a coarse to fine aggregate proportion of 65 to 35 percent was optimum, confirming the recommendations of the ACI and coinciding very well with common experience.

Water and Cement Content Determination

Workability is generally indicated by the slump of a mixture, which is specified for different types of applications. For highway construction, the ACI recommends a slump of 25 to 75 mm (1 to 3 in.) and water content of 193 kg/m^3 (325 lb/yd^3) of concrete. Since the water-cement ratio is a key parameter in determining the quality of concrete, however, four different water-cement ratios were evaluated using 28-day, moist-cured compressive strengths of cylinders 152 mm (6 in.) in diameter by 305 mm (12 in.) high and a 65/35 percent coarse to fine aggregate proportion. The water content was reduced, however, from the ACI recommended level of 193 kg/m^3 (325 lb/yd^3) to 178 kg/m^3 (300 lb/yd^3) to reduce the cement content of the mixes to 396 kg/m^3 (667 lb/yd^3), approximately a seven-bag mix and 0.45 water-cement ratio, and to provide a more economical mix. The mixture proportions used in the water-cement ratio determination and the results of the 28-day compressive strength tests are given in Table 3. Five specimens were cast, cured in water, and then tested in compression for each water-cement ratio.

On the basis of the results shown in Table 3, a mixture with a water-cement ratio of 0.45 was chosen for all further testing. This water-cement ratio provides good, workable concrete and 28-day compressive strengths well in excess of the 27,560 kPa (4,000 psi) minimum required by LDOTD for paving applications. Thus, a 1-m^3 (1.31-yd^3) batch of slag aggregate-based concrete for the study contains 178 kg (300 lb) of water, 396 kg (667 lb) of cement, 1424 kg (2,401 lb) of slag aggregate, and 658 kg (1,109 lb) of fine aggregate.

Characteristics of Fresh Concrete

Production Considerations

The PG-based slag aggregate used in this research effort as coarse aggregate in the production of PCC was blended according to the selected gradation shown in Figure 2, immersed in water for 24 hr, and then air dried to reach a saturated surface dry condition. Masonry sand was used as the fine aggregate in the concrete. The free moisture content of the sand was determined to be 1.5 percent and was taken into account in the calculation of the water added to the mixture. Type I portland cement was used for all batches produced. The properties of fresh concrete were determined primarily to control the quality of the mixture produced. The slump test was used to evaluate the workability of the mix, and unit weight, air content, and yield were measured to determine expected production quantities.

Workability

The slump test was performed in accordance with ASTM C 143 for each batch of the selected design mixture. The slump was found to be 1 in. for each batch, somewhat lower than expected but remarkably consistent, demonstrating that workable, consistent-quality concrete can be produced using PG-based slag aggregates.

Unit Weight

Unit weight or density of concrete depends on the amount and relative density of the aggregates, the amount of entrapped or purposely entrained air, and the water and cement contents. Determination of the unit weight for slag aggregate concrete followed ASTM C 138 procedures, using a 0.014-m^3 (0.5-ft^3) container, and was found to be approximately 2513 kg/m^3 (155 lb/ft^3).

TABLE 3 Compressive Strengths After 28 Days for Different Water-Cement Ratios

	Water - Cement Ratio			
	0.40	0.45	0.50	0.55
Water (kg/m^3)	178	178	178	178
Cement (kg/m^3)	445	445	445	445
Coarse aggregate (kg/m^3)	1,392	1,424	1,450	1,471
Fine Aggregate (kg/m^3)	642	658	669	679
Slump (mm)	25	25	38	38
28-Day Strength (kPa)	38,100	37,570	28,330	28,640

1.0 lb/yd^3 = 0.593 kg/m^3, 1.0 in = 25.4 mm, 1.0 psi = 6.89 kPa

Air Content

The non-air-entrained air content of the mix was determined using the pressure method specified in ASTM C 231. The pressure method is the most common method for measuring air content of fresh concrete and measures the changes in volume of the concrete when subjected to a given pressure. The air content of the slag aggregate concrete measured with a Press-Ur-Meter was 3.0 percent, a relatively high air content compared with the 1 to 2 percent for typical mixtures and probably is due to the honeycomb nature of the slag aggregate and the difficulty of filling those voids with fine aggregate and cement paste.

Yield

The yield of concrete is the amount of fresh concrete produced per sack of cement and is usually expressed in cubic meters per sack. On the basis of the batch proportions used, the specific gravities of the materials used, and the air content from above, approximately 0.110 m^3 (3.95 ft^3) of concrete can be produced for each sack of cement used, somewhat lower than the 0.112 to 0.126 m^3 (4.0 to 4.5 ft^3) per sack for typical aggregates.

Characteristics of Hardened Concrete

The characteristics of the PG slag aggregate and fresh concrete discussed to this point are certainly critical to the production and placement of quality concrete, but clearly the characteristics of the hardened mass must be thoroughly examined to assess the performance of slag aggregate-based concrete. In the next several paragraphs, the preparation, curing, and testing of the concrete specimens used in the study are briefly described.

Preparation and Curing of Test Specimens

Different sizes and shapes of test specimens were used for the various tests performed on the hardened concrete. For compressive strength, splitting tensile strength, and elastic modulus tests, cylindrical specimens with a diameter of 152 mm (6 in.) and a height of 305 mm (12 in.) were used. Beams 152 mm by 152 mm in cross section by 508 mm (20 in.) in length were used for flexural strength tests. For the compressive and splitting tensile strength tests, five cylinders were produced for each test series. For the flexural strength test, seven beams were cast. All test specimens were left in the molds for approximately 24 hr, unmolded, and then placed in a curing tank filled with water and kept at a temperature of 73.4 ± 3°F for the required duration of curing. The cylindrical specimens were removed from the curing tank at the proper time and capped for compressive strength, modulus of elasticity, and Poisson's ratio tests.

Compressive Strength

Tests after 1, 3, 7, 28, and 90 days were conducted to determine the strength increase of the concrete mixture with time. Specimens were tested according to ASTM C 39 or AASHTO T 22 while still in a moist condition. Five cylinders were produced and tested for compressive strength for each of the five curing periods. Table 4 presents a statistical summary of the load and deformation data collected in this phase of the study. Most of the cylinder breaks exhibited the classic conical shape indicative of uniaxial loading, and in general, the breaks occurred through the aggregate particles, indicating that the cement paste was controlling the strength of the hardened mass rather than the coarse aggregate, even at early stages of curing. However, the desired minimum compressive strength of 27,560 kPa (4,000 psi) specified by LDOTD for paving concrete was easily achieved at 28 days.

Figure 3 shows the strength increase with age for the PG slag aggregate-based concrete and for conventional concrete with approximately the same 28-day compressive strength. The curve for PG slag aggregate-based concrete generally follows the typical strength gain pattern for concrete produced with conventional aggregate. Strength at 28 days is considered to be 100 percent strength for most practical purposes and is the value used for structural design. The increase in compressive strength between 28 and 90 days for the slag aggregate concrete was 4000 kPa (583 psi) or about an additional 11.6 percent strength gain. Typical concretes will gain an additional 20 percent compressive strength between 28 and 90 days of moist curing.

Flexural Strength

Two test methods have been well established to assess the tensile strength of concrete. These are the splitting tensile strength test

TABLE 4 Compressive Strength Test Results

Curing Period (days)	Average Peak Load (kN)	Average Peak Strain ($\mu\varepsilon$)	Average Compressive Strength (kPa)	Standard Deviation of Strength (kPa)
1	214	4,390	11,713	703
3	349	5,620	19,085	2,204
7	473	3,204	25,906	4,665
28	645	7,610	35,277	8,406
90	716	7,750	39,273	9,908

1.0 lbf = 0.00445 kN, 1.0 psi = 6.89 kPa

and the flexure test. The flexural strength test is the most common method to estimate the resistance of concrete against tension and is widely used as a design criterion in many states for road construction. Seven beam specimens were tested according to ASTM C 78-84 or AASHTO T 97-86 after they had been cured for 28 days. The standard third-point loading method was used, and loads were applied at a rate of 556 N/sec (125 lbf/sec). Seven specimens were tested as compared with five for compressive strength because the results of tests for modulus of rupture of concrete beams typically have a higher standard deviation. The results of the flexural strength tests are shown in Table 5. The results of the flexural strength tests range from a low of 3730 kPa (541 psi) to a high of 5860 kPa (850 psi), giving a mean of 4940 kPa (717 psi) and a standard deviation of 2030 kPa (295 psi). The modulus of rupture for slag aggregate-based concrete is about 14 percent of the 28-day compressive strength, which compares very favorably with the typical flexural strength-compressive strength ratios for conventional aggregates of 13.5 percent found in the literature (*4*).

TABLE 5 Flexural Strength Test Results

Beam No.	Load at Failure (kN)	Modulus of Rupture (kPa)
1	36.0	4,650
2	44.9	5,795
3	36.5	4,706
4	28.9	3,727
5	45.4	5,857
6	32.9	4,244
7	43.6	5,622
Average	38.3	4,940

1.0 lbf = 0.00445 kN, 1.0 psi = 6.89 kPa

Splitting Tensile Strength

For splitting tensile strength tests, the cylindrical specimens were loaded on their side in diametral compression according to ASTM C 78-84 or AASHTO T 97-76. Five specimens were loaded to failure with a loading rate of 75.6 kN/min (17,000 lbf/min). The results are shown in Table 6. The splitting tensile strength of the slag aggregate-based concrete specimens varied between 2520 kPa (567 psi) and 3500 kPa (786 psi), with a mean of 2960 kPa (665 psi) and a standard deviation of 716 kPa (161 psi). Therefore, the splitting tensile strength of the concrete is 13.0 percent of its 28-day compressive strength. This value is slightly higher than the range of typical values between 7 and 11 percent reported in the literature (*4*).

Modulus of Elasticity and Poisson's Ratio

The tests to determine the static modulus of elasticity and Poisson's ratio were conducted according to ASTM C 469-87a using extensiometer and compressiometer measurements. Cylinders were moist cured for 90 days, capped, and then tested in axial compression. Table 7 gives the results of these tests. The average value for the modulus of elasticity was found to be 23.4 $\times$ 10^6

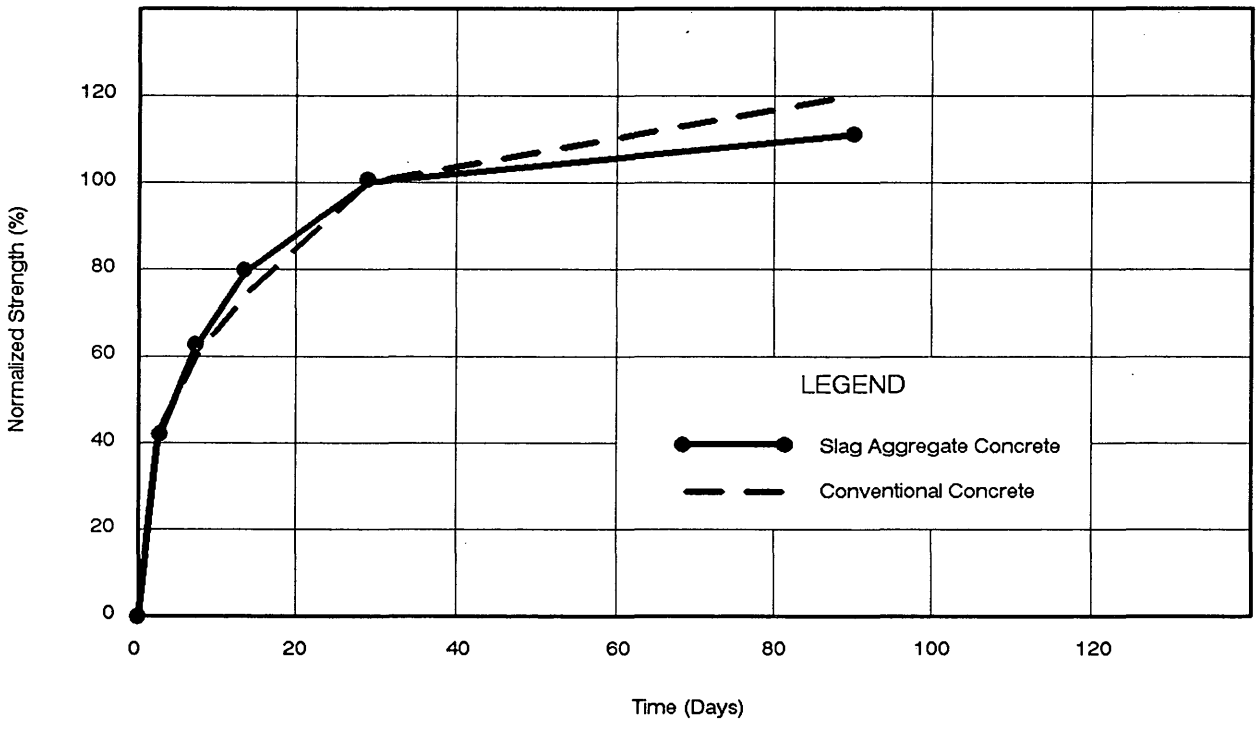

FIGURE 3 Compressive strength gain for slag aggregate-based concrete.

TABLE 6 Splitting Tensile Strength Test Results

Cylinder No.	Load at Failure (kN)	Splitting Tensile Strength (kPa)
1	45,867	637
2	49,620	689
3	55,343	786
4	40,864	567
5	46,587	647
Average	47,656	665

1.0 lbf = 0.00445 kN, 1.0 psi = 6.89 kPa

TABLE 7 Static Modulus and Poisson's Ratio Test Results

Cylinder No.	Modulus of Elasticity (kPa)	Poisson's Ratio
1	23.4×10^6	0.14
2	26.2×10^6	0.12
3	22.7×10^6	0.18
4	22.0×10^6	0.20
Average	23.4×10^6	0.16

1.0 psi = 6.89 kPa

kPa (3.4×10^6 psi), slightly below the typical values reported in the literature that ranged between 24.8×10^6 kPa (3.6×10^6 psi) and 30.3×10^6 kPa (4.4×10^6 psi) for concrete with compressive strengths between 27 560 kPa (4,000 psi) and 41 340 kPa (6,000 psi). The effect of this slightly low modulus value, however, should be minimal in highway applications.

Poisson's ratio is the ratio of lateral strain to axial strain within the elastic range of a material when subjected to axial loading. In Table 7, the average result for Poisson's ratio was 0.16, near the lower boundary of values found in the literature of 0.15 to 0.20 (*4*).

CONCLUSIONS

This investigation has shown that the PG-based slag aggregate possesses physical and durability properties comparable with those of conventional aggregates. The small dissimilarities do not appear to present any significant problems in the production and performance of concrete. It was clearly demonstrated that a concrete mixture using the PG-based slag aggregate as a substitute for conventional coarse aggregate could be developed to meet or exceed the ASTM and LDOTD specifications for concrete used in highway applications.

ACKNOWLEDGMENT

This research was sponsored under the auspices of the Institute for Recyclable Materials, Louisiana State University, with funds from Freeport-McMoRan, Inc., New Orleans, Louisiana.

REFERENCES

1. Taha, R., and R. K. Seals. *Phosphogypsum Literature Review.* Report I-90-4. Institute for Recyclable Materials, Baton Rouge, La., March 1991.
2. Collins, R. J., and S. K. Ciesielski. Highway Construction Use of Wastes and By-Products. In *Proceedings*, Materials Engineering Division Sessions, ASCE National Convention, New York, N.Y., 1992.
3. Taha, R., and R. K. Seals. Engineering Properties of Phosphogypsum-Based Slag Aggregate. In *Transportation Research Record 1345*, TRB, National Research Council, Washington, D.C., 1992.
4. Metha, P. K. *Concrete—Structure, Properties and Materials*. Prentice-Hall, Inc., New York, 1986.

Waste Foundry Sand in Asphalt Concrete

SAYEED JAVED, C. W. LOVELL, AND LEONARD E. WOOD

Sands, binders, and additives are used to form molds and cores of metal castings. The sands are reused a number of times but ultimately are sufficiently altered to require being discarded. A laboratory study of a variety of waste sands from Indiana foundries is reported. Most of the wastes were generated from a green sand molding of gray iron products. Other sands were from chemically bonded and shell molding processes. The suitability of waste sands for use as a fine aggregate in asphalt concrete has been examined by replacing some portions of conventional aggregates with a particular waste foundry sand. A replacement level of 15 percent was found to be suitable for this case.

Waste foundry sand (WFS) is a by-product of the casting industry that results from the molding and core-making processes. The mold forms the outside of the castings, and the core forms the internal shape. When the part to be made has deep recesses or hollow portions, sand cores must be provided in the mold.

The annual generation of WFS in Indiana is about 1.78 MN (200,000 tons) (*1*). The bulk of this WFS is nonhazardous and is currently deposited in landfills. The scarcity of landfill space and increase in tipping fees have stimulated the pursuit of disposal other than in landfill or beneficial reuse. A project was undertaken with the cooperation of Indiana Cast Metals Association (INCMA) to evaluate different beneficial reuses of WFS in highway construction. The different applications of WFS, which include geotechnical fill material, fine aggregate supplement in asphalt concrete, and fine aggregate in controlled low strength material (CLSM), are being evaluated. Previous work in geotechnical fill has shown that these materials have good shear strength properties and slightly higher compressibilities and are of low permeability as compared with conventional materials (*2*). The suitability of using WFS as a fine aggregate supplement in asphalt concrete is discussed.

Three types of WFS were tested. Seven were from green sand processes, which means that the metal is poured into the molds when the sand is damp, as it is when the mold is made (*3*). Two types were from chemically bonded processes and one was from the shell-molding process. Samples from green sand are designated G; chemically bonded, C; and shell molding, S. In the green sand process, bentonite is typically added as a binding agent with other additives like seacoal. Chemically bonded sands are those that use furan, phenolic urethane, and acid-cured no-bake systems (*4*). Shell molding uses a mixture of sand and thermosetting resin (usually phenol-formaldehyde) to form the mold. When it touches a heated pattern, the sand-resin mixture forms a thin shell due to the polymerization of the resin, which binds the sand particles (*5*).

Initially, characterization tests were performed to determine if the materials would meet basic requirements for mineral aggregates intended for use in asphalt concrete mixtures. On the basis of the characterization tests, G1 (the first sample of the green sand process) was then selected to compare physical and mechanical properties of a control asphalt mixture with a mixture containing different proportions of G1.

School of Civil Engineering, 1284 Civil Building, Purdue University, West Lafayette, Ind. 47907.

MATERIAL CHARACTERISTICS OF WFS

The suitability of aggregates for use in asphalt concrete was determined by evaluating the following material characteristics:

1. Gradation,
2. Cleanliness and deleterious materials,
3. Clay lumps and friable particles,
4. Durability and soundness,
5. Particle shape and surface texture, and
6. Affinity for asphalt.

Gradation

Aggregate gradation is the distribution of particle sizes expressed as a percent of the total weight. Gradation is one of the most important characteristics of an aggregate. It affects almost all the important properties of an asphaltic mixture, including stiffness, stability, durability, permeability, workability, fatigue resistance, skid resistance, and resistance to moisture damage (*6*). The particle size distributions of the 10 samples are shown in Figure 1. The foundry sands were found to be uniformly graded.

Deleterious Materials

Deleterious substances may include vegetation, clay coating on aggregate particles, iron oxides, gypsum, water-soluble salts, and other particles that affect proper bonding with asphalt. Deleterious materials may also increase the moisture susceptibility of an asphalt mixture. Aggregates with deleterious substances are undesirable and should not be used unless the amount of foreign matter is reduced by washing or other means. The plasticity index (PI) is used to identify and measure the quantity of deleterious materials. ASTM D1073 limits the PI to a value of 4 or less. Most of the WFSs tested were found to be nonplastic. Only G3 and G5 were found to be have a PI greater than 4.

Clay Lumps and Friable Particles

Clay lumps are composed of clay and silt that remains cohesive during processing. Friable particles are characterized by a poor bond between the grains; hence they break down easily into many smaller pieces. These lumps and friable particles in the finished hot-mix asphalt mixture can break down from freezing and thaw-

ing or wetting and drying and cause stripping or ravelling or otherwise affect the durability of the asphalt mixture. Specifications normally limit the amount of clay lumps and friable particles to a maximum of 1 percent. The quantities of clay lumps and friable particles for the 10 WFSs are summarized in Table 1. Since eight of them exceeded the recommended value of 1 percent, it appears that processing of these materials is required before their use.

Durability and Soundness

The soundness test, ASTM C 88, is an empirical screening test that is intended to provide an indication of durability. According to Indiana specifications for fine aggregates, weighted percent loss should not exceed 10 percent by weight after being subjected to five cycles of the sodium sulfate soundness test (*7*). Soundness values for the 10 samples are reported in Table 1. Six of the samples failed this requirement. The high soundness loss may be due to the agglomeration of fine particles during the mulling process of sand with binder and additives in the foundry operation. These agglomerates then tend to break down during the severe action of sodium and magnesium sulfate.

The soundness test has been widely criticized for its inability to accurately predict field performance for specific aggregates. Since in hot mixes there is low moisture in the aggregate, it is expected that freezing and thawing should not be a significant problem. Moreover, the aggregates are coated with a film of asphalt binder that would prevent the aggregates from absorbing a significant amount of moisture during the life of the mixture (*6*).

Particle Shape and Surface Texture

For mixes containing fine and coarse aggregates, the angularity of the fine aggregate is more important to mixture stability than is the angularity of the coarse aggregate (*8*). Angular aggregates are

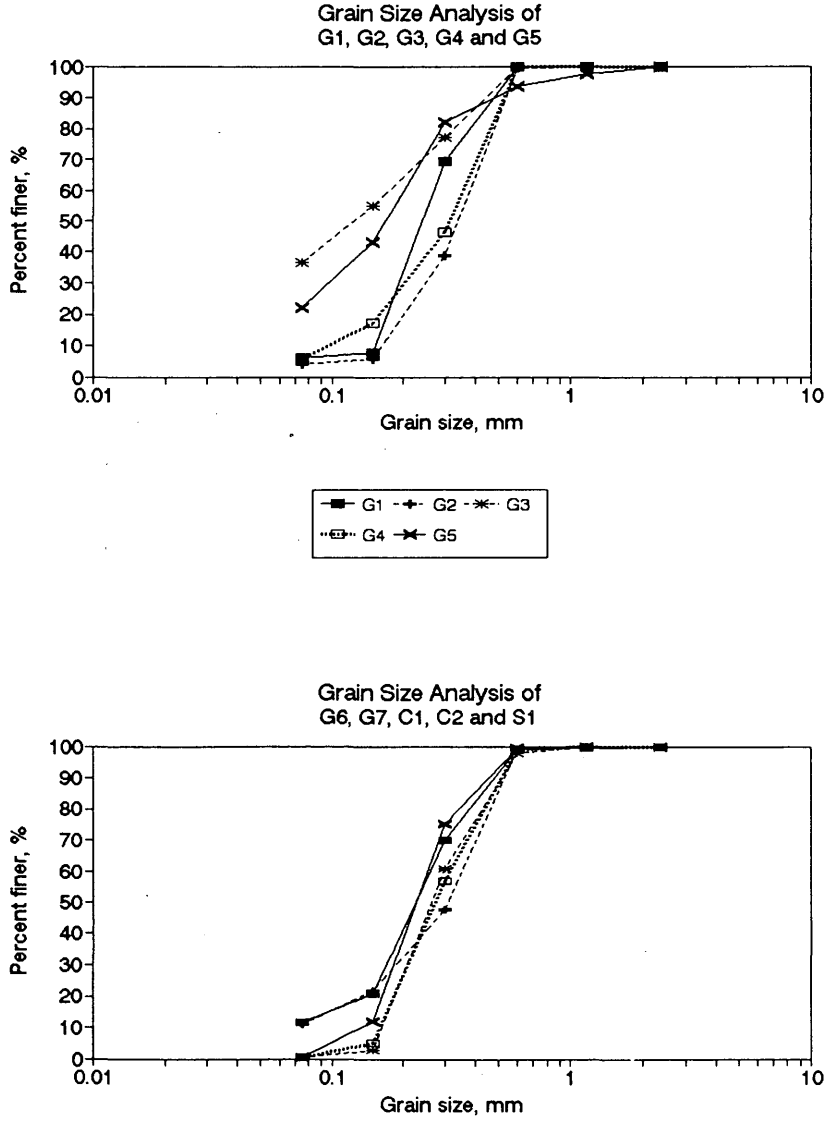

FIGURE 1 Grain size analysis of 10 samples tested.

desirable, as opposed to mixtures containing rounded particles, because they result in better workability and require less compactive effort to obtain the required density. This ease of compaction is not necessarily an advantage, however, since mixtures that are easy to compact during construction may continue to densify under traffic, ultimately leading to rutting due to low voids and plastic flow (*6*).

Smooth-textured aggregate is easy to coat with an asphalt film but offers little adhesion to hold the film in place. Thus the rougher the surface texture, generally the higher the stability and durability of the bituminous mixture.

The combined effect of particle shape and texture was determined from the National Aggregates Association uncompacted voids test (*9*) with the following exceptions: apparent specific gravity values according to ASTM D 854 were used to calculate the void content, and the right cylinder to be filled with fine aggregate was 7.6 cm (3 in.) in diameter and 8.9 cm (3.5 in.) high. The results are summarized in Table 1. An increase in void content indicates greater angularity or rougher texture or both. Lower void content results are associated with more rounded, smooth-surfaced fine aggregate. The uncompacted void content for a virgin foundry sand was found to be 43.7 percent. This suggests that WFSs were a little rougher. This roughness may be due to agglomeration of sand with binder and additives.

Affinity for Asphalt

It is known that WFS contains a large portion of silica. Silicates are acidic in nature and generally have a greater affinity for water than for bituminous material, and bituminous films may be more or less easily displaced from them by water. However, affinity for asphalt of the combined aggregates in an asphalt concrete mixture is more significant than for this fraction alone.

PHYSICAL AND MECHANICAL PROPERTIES OF CONTROL AND BLENDED MIXTURES

On the basis of the characterization test results, G1 was selected for detailed testing. The physical and mechanical tests included in this category were bulk specific gravity and theoretical maximum specific gravity as physical tests and Marshall stability and flow as mechanical tests.

The experimental mixture of conventional aggregates and WFS was blended to produce final products with 15, 20, and 30 percent WFS by weight of total aggregates. The total weight of aggregates for a typical mix was 1200 g (2.65 lb). Thus 15 percent blending means 156.5 g (0.35 lb) of WFS and 1043.5 g (2.30 lb) of conventional aggregates and so on for increased percentages of blending. The gradations of the control (aggregates with no WFS) and the samples prepared by blending 15, 20, and 30 percent of WFS with respect to control are shown in Figure 2. The upper and lower limits of No. 12 mix according to Indiana specifications are also included. Instead of the fines being scalped from the normal fine aggregate, blending was carried out as a partial replacement keeping in mind that a scalping procedure would be expensive and nonproductive.

The control contained crushed angular limestone aggregates down to the No. 16 sieve. The balance consisted of natural sands. These aggregates were combined with asphalt in accordance with procedures outlined by the Marshall method of mixture design (*10*), using 75 blows per side of each specimen. Tests of bulk specific gravity and Marshall stability and flow were carried out

TABLE 1 Characterization of Test Results on 10 Samples Tested

Sample #	Soundness %	Clay Lumps & Friable Particles, %	Uncompacted Voids, %
G1	9	1.35	48.6
G2	6	1.72	45.1
G3	25	44.33	58.3
G4	45	2.59	47.8
G5	9	0.62	49.9
G6	17	2.26	51.3
G7	47	23.22	51.1
C1	12	100.00	45.2
C2	21	0.00	47.0
S1	10	10.64	47.2

on the compacted mixtures in accordance with ASTM D2726 and D1559. Results of this work produced mixtures with the properties shown in Figure 3. The design criteria according to the Asphalt Institute (*10*) are shown in Table 2.

Figure 3 when compared with design criteria indicates that control specimens prepared at 5.75 percent asphalt were at or near optimum. WFS was then blended in different proportions at 5.75 percent asphalt and the above properties were again determined. Figure 4 shows these properties when WFS was blended at 15, 20, and 30 percent of the total aggregates. However, it would be more interesting to compare these properties at optimum asphalt content for each percentage of blending.

MOISTURE SUSCEPTIBILITY

The control and mixtures containing 15 percent WFS and 30 percent WFS were then evaluated to determine their indirect tensile strength under normal conditions and soaked conditions to determine the effect of moisture susceptibility. Six specimens at 5.75 percent asphalt content using 75 blows at each side were prepared for each type of three mixtures, including two WFS mixes (15 percent WFS and 30 percent WFS) and one control mix. Thus a total of 18 specimens were prepared. Each mixture of six specimens was then sorted into two groups so that both the groups yielded similar average bulk specific gravity. The first group of three samples was then tested after an air bath of 5 hr at 25°C temperature. The second group of another three samples was tested after first immersing the samples in water at 60°C for 24 hr and then later submerging them at 25°C for 2 hr. The results are shown in Table 3.

DISCUSSION OF TEST RESULTS

The uncompacted void content (UVC) for the sand used in the control mix was found to be 43.3, and that of the virgin sand for WFS was 43.7. Thus, in terms of particle shape and texture, both sands were similar. However, the UVC for all the WFSs was higher than 43.6. The G1 sand used in this study had a UVC of

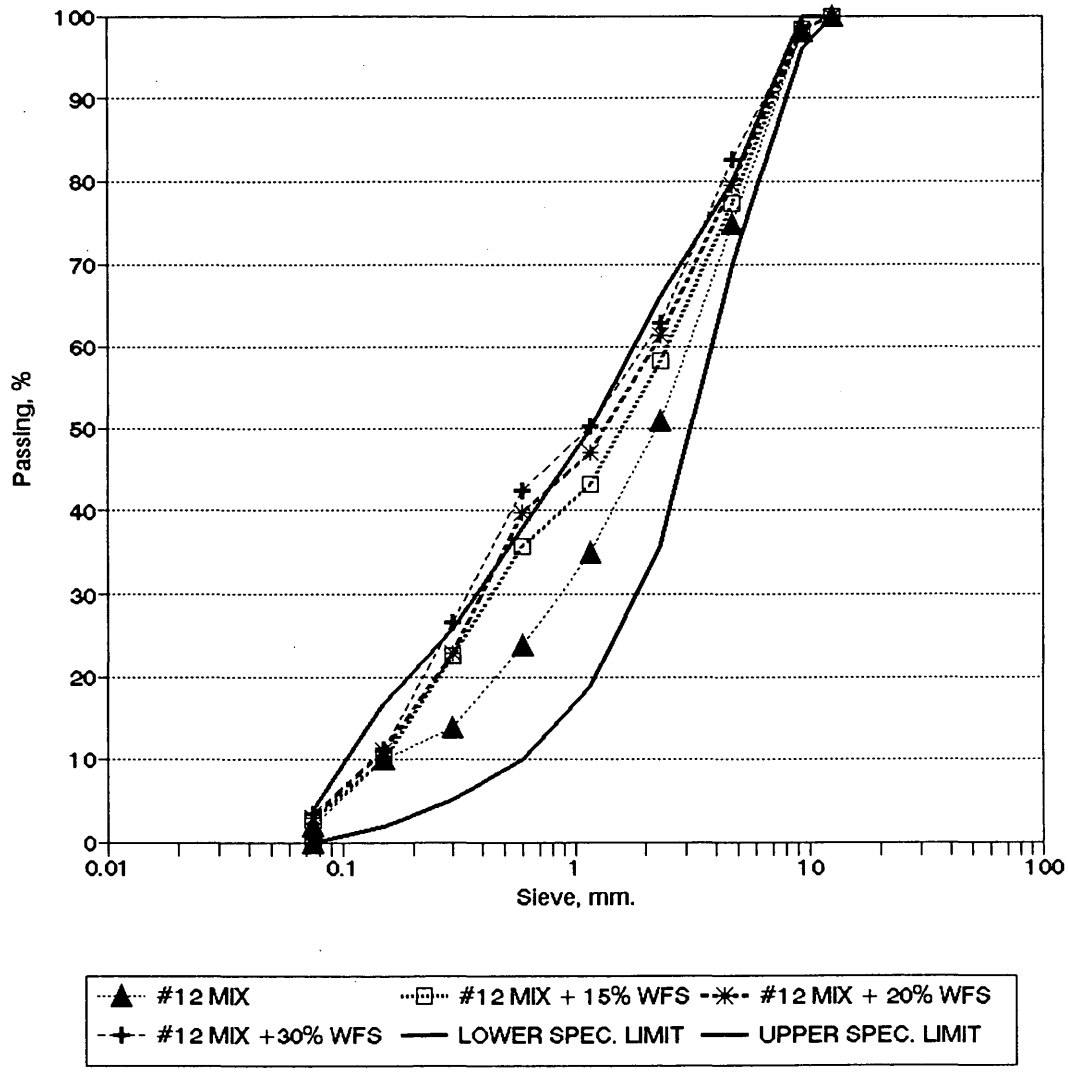

FIGURE 2 Gradation of control, specimens blended with WFS, and boundary limits of No. 12 mix.

48.6 (Table 1). The UVC for the portion of limestone aggregates passing the No. 8 sieve and being retained on the No. 16 sieve was found to be 50.1. The UVC for limestone aggregates above the No. 8 sieve could not be determined because of the limitation of the 1.27-cm (0.5-in.) funnel opening. If the UVC for the aggregates coarser than No. 8 is assumed to be the same as that for limestone aggregates passing the No. 8 and being retained on the No. 16 sieve, the resulting weighted UVC with increased blending of WFS would be calculated as shown in Table 4, which shows that the angularity or roughness, or both, with increased blending of WFS was very insignificant and was almost the same as that of the control mix.

Increasing amounts of WFS in the control mix resulted in a decrease of the unit weight. This was expected because increasing amounts of WFS were replacing the heavier conventional materials. The bulk specific gravity of G1 was 2.50, whereas that of the control mix was 2.66. Moreover, uniformly graded and relatively more rough-textured WFS tends to increase voids, which results in a decrease of unit weight.

Percentage of air voids and voids in the mineral aggregate (VMA) were found to increase with blending of increased quantities of WFS. This was due to deviation from dense gradation. VMA has two components: the volume of the voids that is filled with asphalt and the volume of voids remaining after compaction. The volume of asphalt was same for different replacement levels. However, it was the percentage of air voids that was increasing VMA. A certain percentage of air voids is always desirable to ensure that space will remain for expansion of the bitumen if

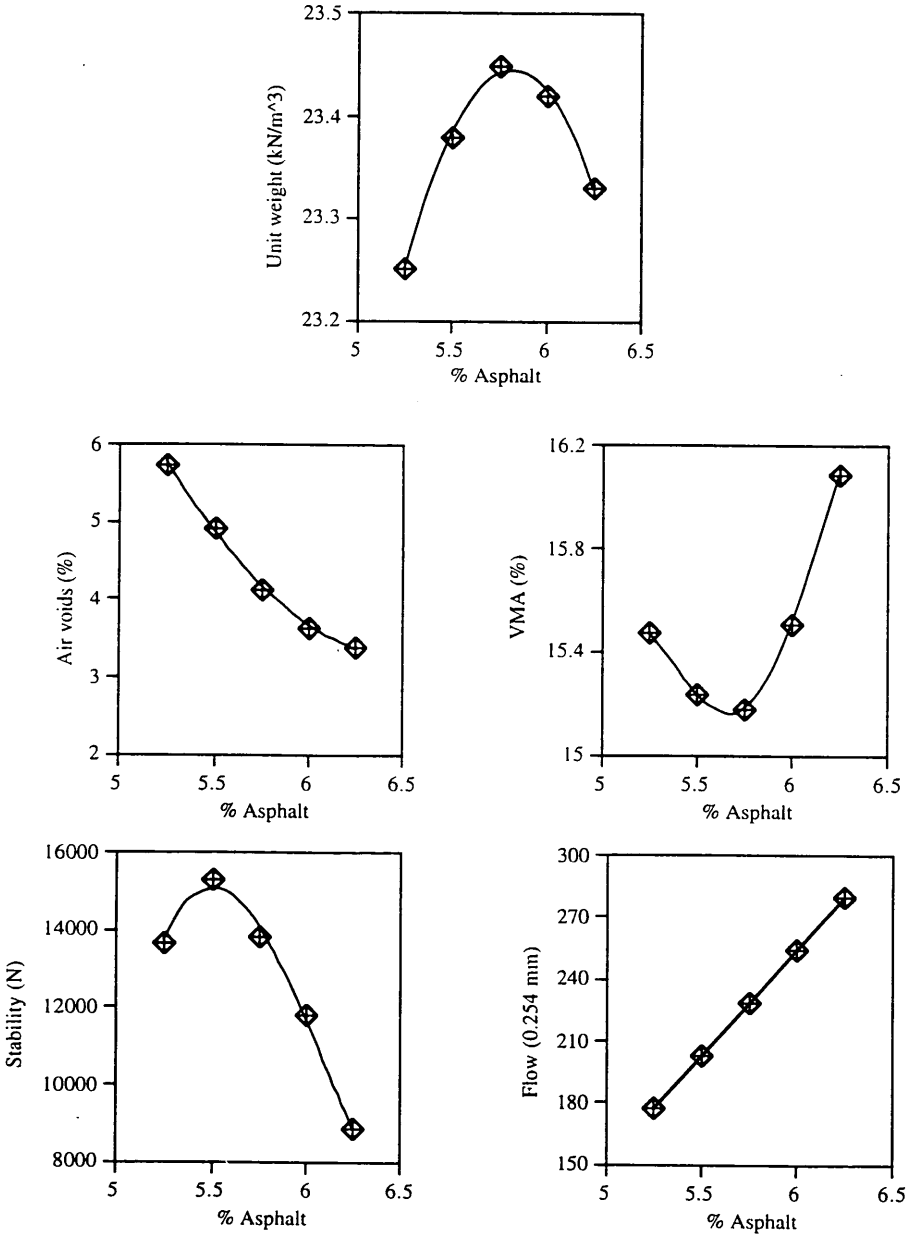

FIGURE 3 Physical and mechanical properties of conventional aggregate mixture at varying asphalt contents.

TABLE 2 Asphalt Institute Criteria

Parameters	Acceptance Range
Marshall Stability, N.	6675 minimum
Flow (0.254 mm)	203-406
Air Voids, %	3-5
VMA, % for 9.53 mm. maximum size	14 minimum

1 lb = 4.45 N

1 inch = 25.4 mm

further densification under traffic or expansion to the asphalt that would occur on a hot summer day is expected. However, if the air void contents are high, there is a possibility that water will get into the mix, penetrate the thin asphalt films within the aggregate and asphalt mass, and lower the resistance of the mix to the action of water.

Marshall stability is defined as the maximum load carried by a compacted specimen tested at 60°C at a loading rate of 5 cm/min (2 in./min). This stability is generally a measure of the mass viscosity of the aggregate-asphalt cement mixture and is affected significantly by the angle of internal friction of the aggregate and the viscosity of the asphalt cement at 60°C. Stability values are also influenced by the aggregate gradation. The aggregate that has

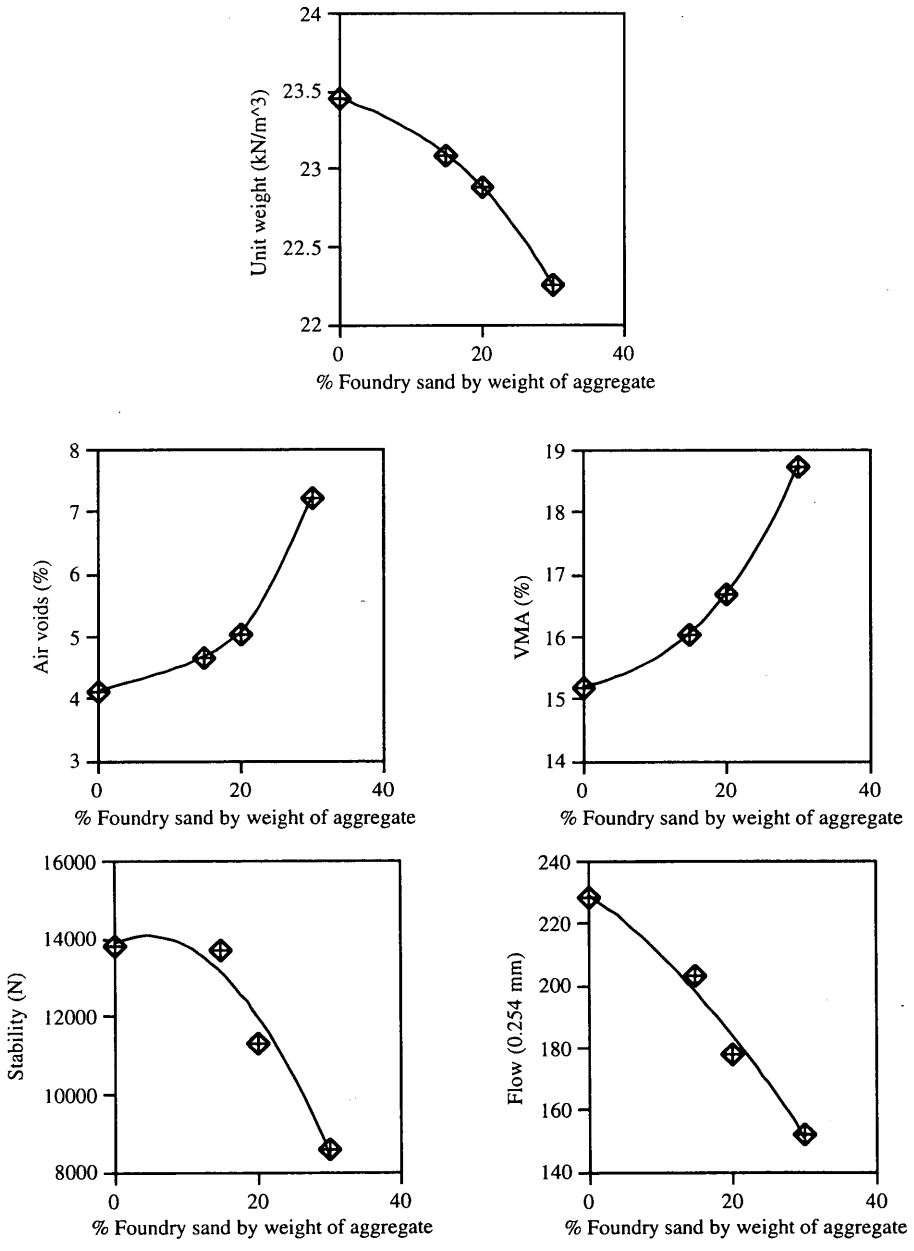

FIGURE 4 Physical and mechanical properties using different percentages of WFS at 5.75 percent asphalt content.

TABLE 3 Results of Indirect Tension Before and After Immersion

Before Immersion

Sample #	CF0	CF15	CF30
Foundry sand, %	0	15	30
Bulk specific gravity	2.393	2.341	2.281
Tensile strength, kPa	1424.58	1341.28	814.33

After immersion

Sample #	CF0	CF15	CF30
Foundry sand, %	0	15	30
Bulk specific gravity	2.395	2.345	2.280
Tensile strength, kPa	1504.64	1451.86	682.59

1 psi = 6.89 kPa

TABLE 4 Weighted Uncompacted Void Content with Blending of Increased Quantities of WFS

Type of Sample	Weighted Uncompacted Void Content[1]
Control mix	47.7
Control mix + 15% WFS	47.8
Control mix + 20% WFS	47.9
Control mix + 30% WFS	47.9

[1] Weighted UVC = (W1 × U1 + W2 × U2 + W3 × U3)/W

W1 = Weight of limestone aggregates

U1 = UVC of limestone aggregates

W2 = Weight of natural sand used in the control mix

U2 = UVC of natural sand

W3 = Weight of WFS

U3 = UVC of WFS

W = Total weight of aggregates

maximum density provides increased stability through increased interparticle contacts and reduced VMA (*6*). Stability values obtained by blending 15 percent WFS were found to be essentially the same as those of the control mix. However by blending more WFS, stability was found to decrease as compared with the control mix. The increase in roughness due to increased blending of WFS was very insignificant as compared with deviation from dense gradation, which ultimately resulted in decrease of stability.

The flow is equal to the vertical deformation of the sample (measured from the start of loading to the point at which stability begins to decrease) in 0.254 mm (0.01 in.). High flow values generally indicate a plastic mix that will experience permanent deformation under traffic, whereas low flow values may indicate a mix with higher-than-normal voids and insufficient asphalt for durability. Such a mix may experience premature cracking due to mixture brittleness during the life of the pavement (*6*). It was found that flow values decreased with increased amounts of WFS. The low flow values were associated with increasing air voids caused mainly by increase in uniformly graded WFS.

The indirect tensile strength also decreased with blending of increased amounts of WFS. Both the control sample and the sample containing 15 percent WFS showed an increase in strength after immersion in water (Table 3). This might have occurred because of asphalt hardening. However, the sample containing 30 percent WFS showed a decrease in strength after immersion. This was due to a significant increase in the percentage of air voids. High air voids resulted in stripping caused by the introduction of water between the asphalt and the aggregate particles.

CONCLUSIONS

A number of conclusions may be drawn from the testing program reported here:

1. When as much as 15 percent of this particular WFS is blended with conventional aggregates, the performance of the asphalt concrete mixture is not very different from that using conventional materials. However, using more than 15 percent WFS in the conventional aggregates resulted in low flow values and high air voids, which may lead to mixture brittleness and consequently premature cracking.
2. The increase in roughness with blending of increased quantities of WFS was very insignificant as compared with deviation from dense gradation.
3. With a few exceptions, WFSs of different Indiana foundries are very similar in gradation (Figure 2) and shape and texture (Table 1). Thus, conclusion 1 may be generally applicable.
4. Lumps in the WFS may be a problem, requiring some cleaning or washing before use.
5. Even with the washing requirements, WFS will be viable for limited blending with conventional aggregates in asphaltic concrete mixtures.

ACKNOWLEDGMENTS

The authors wish to extend their appreciation to the Indiana Cast Metals Association, which provided funding for this research. In addition, Shabbir Alam deserves thanks for his assistance in the laboratory work.

REFERENCES

1. Javed, S. *Use of Waste Foundry Sand in Highway Construction—Interim Report.* Report JHRP-92/12. School of Civil Engineering, Purdue University, West Lafayette, Ind., May 1992.
2. Javed, S., and C. W. Lovell. Use of Waste Foundry Sand in Highway Construction. In *Proc., 44th Highway Geology Symposium*, Tampa, Florida, May 1993.
3. Wendt, R. E. *Foundry Work.* McGraw-Hill, New York, 1942.
4. Hayes, R. A. Reclaiming Chemically Bonded Sands: A Technology Review. *Modern Casting*, May 1993, p. 37.
5. Cannon, W. A. *How to Cast Small Metal and Rubber Parts*, 2nd ed. TAB Books, Inc., Blue Summit, Pa., 1986, p. 10.
6. Roberts, F. L., P. S. Kandhal, E. R. Brown, D. Y. Lee, and T. W. Kennedy. *Hot Mix Asphalt Materials, Mixture, Design, and Construction.* NAPA Education Foundation, Lanham, Md., 1991.
7. Indiana Department of Highways. *Standard Specifications.* Indianapolis, 1988.
8. Herrin, M., and W. H. Goetz. Effect of Aggregate Shape on Stability of Bituminous Mixes. *HRB Proc.*, Vol. 33, 1954.
9. Meininger, R. C. *Proposed Method of Test for Particle Shape and Texture of Fine Aggregate Using Uncompacted Void Content.* National Aggregates Association, Md., March 1989.
10. Asphalt Institute. *Mix Design Methods for Asphalt Concrete and Other Hot Mix Types.* Manual Series No. 2, MS-2. College Park, Md., 1988.

Toward Automating Size-Gradation Analysis of Mineral Aggregate

AHMAD ALJASSAR AND RALPH HAAS

One of the most important properties of an aggregate blend is its size gradation, which defines the percentages (by weight or volume) of different particle sizes that are present in the blend. Since aggregate represents more than 90 percent of a hot asphalt mix, aggregate gradation profoundly influences the properties of the hot mix (such as air voids, workability, and asphalt binder required) and the properties of the pavement (such as stiffness, stability, and durability). Aggregate gradation is determined by the well-known and widely used sieve analysis method. One major drawback of this method is the consumption of time and effort. The time factor is a major barrier to implementing sieve analysis as an aggregate gradation control measure in asphalt plants where production rates are high and interruptions to the production process are very undesirable. There has been some progress in the automation of gradation analysis of the coarse portion of an aggregate blend. The gradation of the fine portion, however, has major effects on the properties of an aggregate blend. A simple and low-cost approach to automate the gradation analysis of fine aggregate is presented in this paper. The approach is based on the concept of differential settling of aggregate particles in a fluid medium because of differences in particle sizes. It is essentially a fractionating-column methodology. A prototype system was fabricated to test particles passing the No. 8 sieve (or <2.38 mm in size). The system is described in the paper, along with some example results.

Modern asphalt plants are almost fully automated. Execution of different activities in an asphalt concrete (AC) production process is fast, resulting in high production rates. These activities are associated mainly with aggregate handling and include the following: aggregate cold feeding, heating, proportioning, and mixing with asphalt cement to produce AC (*1*). The order of these activities may differ depending on whether the plant is one in which there is batch mixing or drum mixing. One additional activity that would be very desirable in an asphalt plant is monitoring of aggregate gradation. The aggregate is the main component of an AC structure, occupying more than 90 percent of the structure mass. Hence, properties of the AC are highly affected by the properties of the aggregate, one of the most important of which is aggregate size gradation. Size gradation can be defined as the distribution of particle sizes expressed as a percent of the total weight (or volume). Aggregate size gradation affects almost all the important properties of an AC, including stiffness, stability, durability, permeability, workability, fatigue resistance, resistance to moisture damage, air voids, and asphalt binder required (*2*).

The only well-established method of determining the size gradation of an aggregate sample is sieve analysis, which is performed by passing the aggregate through a series of sieves stacked with progressively smaller openings from top to bottom and weighing the material retained on each sieve (ASTM C136). This method is well known for being time-consuming and difficult. In fact, the use of sieves to separate grains according to size is not less than 3,000 years old (*3*). The relatively long time required to perform sieve analysis is probably the reason for not using it as a measure for aggregate gradation control in asphalt plants. Moreover, because sieve analysis is the only established method for determining aggregate size gradation, monitoring of such an important property of aggregates simply does not exist in asphalt plants. This deficiency in the current AC production process was recognized during the Strategic Highway Research Program, in which the development of an on-line aggregate gradation monitoring and control system applicable to asphalt plants was suggested (*4*).

Some research studies have been carried out to automate the analysis of aggregate gradations (*5–8*). These studies resulted in systems that all use a two-dimensional image analysis approach; that is, an aggregate sample is scanned by a camera that generates an image that is then digitized and analyzed by custom-designed software, and the three-dimensional information (volumes of particles) is extracted. The lower bound of the particle size-discerning capabilities of these systems apparently ranges from 1 to 0.3 mm (material passing the No. 50 sieve), but this range is open to question. It may be that the fine particles are hidden by larger particles, that the camera's resolution is limited, or simply that it is impractical to deal with a very large range of particle sizes (400:1 is a typical particle size ratio for an AC aggregate blend). The fine portion of an aggregate sample has a profound effect on many of the AC mix properties, one of the most important of which is the required asphalt cement content. This is because the fine particles contribute the most to the surface area of an aggregate blend, which needs to be coated with asphalt cement in order to obtain the required adhesion, durability, and so on.

The purpose of this paper is to describe a prototype automated system developed at the University of Waterloo, Canada, to deal with the fine portion of an aggregate blend. In its current configuration, the system analyzes aggregate samples with the size range of 2.38 to 0.074 mm, but a hybrid approach in which the entire aggregate size range can be analyzed is also described.

SIGNIFICANCE OF FINES IN AC MIX

The size-gradation specification envelope for the aggregate blend contained in an AC mix must be satisfied. This holds for fine and coarse portions of an aggregate gradation curve. The portion representing the fine particles, however, is of major importance with respect to total surface area of the blend. The surface area is a major factor in defining the optimum asphalt content in a hot mix, and finer particles have more specific surface area (surface area per unit weight) than coarser particles.

A. Aljassar, Department of Civil Engineering, Kuwait University, P.O. Box 5969, Safat 13060, Kuwait. R. Haas, Department of Civil Engineering, University of Waterloo, Waterloo, Ontario N2L 3G1, Canada.

The surface area (a_s) of a particle, depending on the assumed particle shape, can be calculated by

$$a_s = Cd^2 \tag{1}$$

where $C = 6$ for a cubical particle where d is the cube dimension, and $C = \pi$ for a rounded particle where d is the particle's diameter.

To quantify the effect of particle size on the total surface area, assume that particles are rounded with diameter d. Therefore, the volume of one particle is

$$v = \frac{\pi}{6} d^3 \tag{2}$$

The volume (V) of a given weight (W) of aggregate particles having a certain specific gravity (G_s) can be calculated as

$$V = \frac{W}{G_s \rho_w} \tag{3}$$

where ρ_w is the density of water. The number of aggregate particles (N) is therefore

$$N = \frac{V}{v} = \frac{6}{\pi} \frac{W}{G_s \rho_w d^3} \tag{4}$$

The total surface area of all particles (A_s) can be calculated using

$$A_s = a_s * N = \frac{6W}{G_s \rho_w} \frac{1}{d} \tag{5}$$

which shows that the surface area of a given number of particles is inversely proportional to the particle size. For example, assuming that $G_s = 2.67$ and $\rho_w = 1000$ kg/m^3, a 1-kg sample of 74-μm particles has a total surface area of 30 m^2, whereas a 1-kg sample of 10-mm particles has a total surface area of only 0.2 m^2.

Aggregate gradations can be used to calculate the total surface area per unit weight of an aggregate blend. For example, to calculate the total surface area of an aggregate blend (in square meters per kilogram), the following table is used by multiplying the factor by the percentage passing for each sieve size and totaling for all sieve sizes (all noted sieves must be used in the analysis) (*2*) (1 ft^2/lb = 0.205 m^2/kg):

Sieve Size (mm)	*Surface Area Factor*
Maximum sieve size	0.41
4.76 (No. 4)	0.41
2.38 (No. 8)	0.82
1.19 (No. 16)	1.64
0.590 (No. 30)	2.87
0.297 (No. 50)	6.15
0.149 (No. 100)	12.30
0.074 (No. 200)	32.80

The foregoing factors show that smaller particles contribute substantially more to the total surface area of an aggregate blend than do coarser ones. Consequently, they have more effect on the asphalt content required for an AC mix.

In a study on binder mixes by Kandhal and Cross (*9*), direct relationships were established between asphalt content and percentage passing sieves No. 4 (P_4) and 8 (P_8). These relationships are

$$AC = 2.186 + 0.060P_4 \qquad R^3 = 0.64 \tag{6}$$

$$AC = 2.025 + 0.084P_8 \qquad R^2 = 0.63 \tag{7}$$

where R^2 is the statistical coefficient of determination for the two regression equations.

Equations 6 and 7 show that material passing the respective sieve size influences the asphalt content of the hot mix.

GENERIC REQUIREMENTS FOR ON-LINE AGGREGATE GRADATION MONITORING SYSTEM

Part of an early stage of the research that led to publication of this paper was the identification of the requirements for an on-line system to monitor the aggregate gradation in the AC production process. In the early stages of the research, video-imaging was assumed to be the best available and applicable technology for solving the problem, and hence the requirements developed may be a little skewed toward video-imaging. However, learning about the developed imaging systems and their limitations led to a search for other approaches to address the fine-particle-size portions of an aggregate blend.

Location in Asphalt Plant

Asphalt plants are generally of two types, batch mixing and drum mixing. They differ in several ways, including gradation control of the aggregate used in the AC mix. In batch-mixing plants, the primary control of aggregate gradation is at the cold feed bins, where proportions of aggregate are controlled before the aggregate is fed into the dryer. The secondary or final gradation control is at the hot bins, where the aggregate is screened according to size and the amounts from different bins are controlled by the gates at the bottom of the hot bins. In drum-mixing plants, gradation control at the cold feed bins is critical because after that point, aggregate is fed into the dryer, where it is dried, heated, and mixed with the asphalt cement (*1*).

Although ideally it would be desirable to check the aggregate gradation of the final mix, it is apparent that this check is more difficult in a drum-mixing operation than in a batch-mixing operation, simply because in the former, the aggregate is dried, blended, and mixed with the asphalt cement in one phase (in the drying drum), and hence access to the dried aggregate (before the asphalt cement is added) is more challenging than in batch-mixing plants.

In a batch-mixing operation, the monitoring system needs to be near the pugmill, where the final aggregate blend is ready to be mixed with the asphalt cement. Sampling of aggregate in the final blend is the current practice in batch-mixing plants where aggregates in the hot bins are analyzed for gradation, and the results of the analysis are used to proportion the hot bins at the beginning of a plant operation.

System-Specific Requirements

System requirements are summarized in Figure 1 and are based on the current configuration of asphalt plants and the nature of

the material to be analyzed. They are categorized as performance/operating requirements and output requirements. In addition to the accuracy of the output results, the most important requirement is the processing time, which prohibited implementation of sieve analysis as a measure to monitor aggregate gradation in asphalt plants.

In a modern batch-mixing plant, the time needed to produce one batch of AC mix is approximately 10 min; that is, a particle takes 10 min to travel from the cold feed bin to the pugmill and be mixed with asphalt cement. It is apparent that to check every batch of AC produced, the processing time of a monitoring system must be less than 10 min to allow for adjustments at the cold bins or at the hot bins, or both, and to reduce the amount of out-of-specification batches. However, if such processing time was found to be unrealistic, it could be increased to less than 20 min and every other batch would be checked, in which case 50 percent of the batches would be checked. For a continuous operation, 50 percent is a very good representation of the population.

WHAT APPROACH BEST MEETS THE REQUIREMENTS?

A number of potential approaches were considered to meet the requirements identified in the previous section. The first was the image analysis approach because of its apparent applicability and because it has found use in many industrial, scientific, engineering, medical, and other areas. Included was careful consideration of the work carried out by other investigators or agencies (*5–8*).

It appeared, however, that in addition to the limitations with this approach for fine-particle-size gradation analysis, it also did not meet some of the other requirements of Figure 1, such as processing time. Moreover, the cost could be quite prohibitive.

Consequently, other approaches were considered and some were further evaluated in pilot experiments. The one that seemed the most promising, the simplest, and with a low cost was the fractionating water column approach, described in the next section.

PERFORMANCE/OPERATING REQUIREMENTS

- High resolution: must be able to distinguish and measure particles as small as 0.074 mm and preferably smaller.
- Must be capable of discerning particles in the size range of 30 mm to 0.074 mm.
- Should not require extensive sample pre-processing prior to testing.
- Should require a minimum of skilled operator intervention.
- Must be resistant to high temperatures from heated aggregate.
- Must be compatible with asphalt plant rough environment (e.g., the exposed parts must be wear and dust proof).

OUTPUT REQUIREMENTS

- Must provide results quickly (processing time < 10 minutes).
- Results must closely approximate the results attained with standard sieve analysis (tolerances may be based on specification gradation envelopes).
- Results from the same sample must be repeatable.
- Output must be compatible with a personal computer (i.e., digitized output).

FIGURE 1 Generic system requirements for on-line aggregate size-gradation analysis.

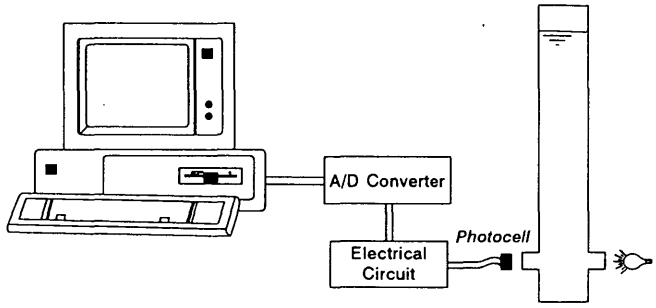

FIGURE 2 Schematic of main system components.

FRACTIONATING WATER COLUMN

The fractionating water column approach utilizes the difference in effect of drag force on particles of different sizes when they settle under gravity in a water column. This phenomenon was modeled (in a more general form) by Sir George Stokes and has become known as Stokes' law (*10*).

This phenomenon was exploited to develop a system to analyze aggregate particles in the fine size range (<2.38 mm). It uses a water column to separate particles according to size. A schematic of the main system components is shown in Figure 2. The system consists mainly of a Plexiglass tube 1.5 m long and 77 mm in (inner) diameter with a "window" near the bottom of the column through which a constant-power light is transmitted, which is received on the other side by a serial array of light-sensitive photocells. The resistance of the photocells changes with changing received light intensity. The electrical circuit consists of a DC power supply that applies a constant voltage across the photocells. When the photocells change their resistance (as a result of a change in light intensity), the current through the circuit changes proportionally and a voltage measured across a constant resistance in the circuit is recorded. The recording of the voltage reading is automated by the use of an analog-to-digital (A/D) converter board, which sends the digitized voltage signals to a computer run by software that reads the signals from the A/D board and stores the results for analysis.

Basic Concept

The basis for the system is Stokes' modeling of the drag force that a solid spherical particle is subjected to when traveling in a fluid medium.

The aim was to maintain some separation among particles in a fine aggregate blend and to develop a way of measuring the amount (weight or volume) of particles in each size range. To sort particles according to size, a water column is used and a sample of mixed fine aggregate is introduced at the water surface. The particles travel downward at different speeds; according to Stokes (*10*), the terminal velocity v of a spherical solid particle falling freely in a fluid is given by

$$v = \frac{d^2 g(\rho_s - \rho_f)}{18\eta} \tag{8}$$

where

d = particle diameter,
g = gravitational acceleration,
ρ_s = mass density of solid particle,
ρ_f = mass density of fluid, and
η = dynamic viscosity of fluid.

Assuming that the particles in the tested size range (<2.38 mm) reach their terminal velocity in a very short time, their mean velocity h/t (where h is the distance travelled in time t from the water surface to the photocell detection level) could be used in Equation 8, which can be rewritten as

$$t = \frac{18\eta h}{d^2 g(\rho_s - \rho_w)} \tag{9}$$

when water is used as the fluid medium ($\rho_f = \rho_w$). For a given water temperature and assuming the same density for all solid particles, the term $18\eta h/g(\rho_s - \rho_w)$ has a constant value. Therefore, Equation 9 can be rewritten as

$$t = \frac{C}{d^2} \tag{10}$$

where, assuming a room temperature of 24°C and using parameter values given elsewhere (*11*),

$$C = \frac{18\eta h}{g(\rho_s - \rho_w)}$$

$$= \frac{18\ (8 \times 10^{-3}\ \text{N} \cdot \text{sec/m}^2)\ (1.5\ \text{m})}{(9.907\ \text{m/sec}^2)\ (2670 - 996)\ \text{kg/m}^3}$$

$$= 13.2 \times 10^{-6}\ \text{m}^2 \cdot \text{sec}$$

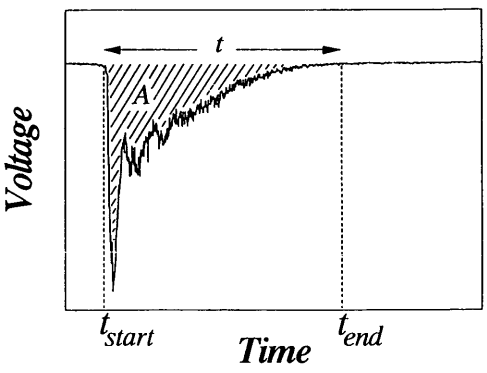

FIGURE 3 Typical voltage-time profile of aggregate sample run through system shown in Figure 2.

Taking the logarithm of both sides of Equation 10 yields

$$\text{Log } t = a - b \text{ Log } d \tag{11}$$

where a = Log C −4.9 (theoretically), and b = 2 (theoretically). It should be noted that the tested sample size (50 g) is very small compared with the body of water contained in the column of Figure 2. Therefore, when heated aggregate is tested, it is not expected to change the water temperature significantly or the viscosity of the water.

To determine the experimental values of a and b in Equation 11, five size ranges of fine aggregate were considered. These size ranges, along with their corresponding sieve numbers, are as follows:

Size Range (mm)	*Corresponding Sieve No.*
2.38–1.19	8–16
1.19–0.595	16–30
0.595–0.300	30–50
0.300–0.149	50–100
0.149–0.074	100–200

To calibrate the system, washed samples were used to eliminate the effects of the presence of "dust" (material less than 0.074 mm in size or passing the No. 200 sieve). To cover the range of expected weights found in real samples, five to six weights were considered in each size range. From each weight group, 10 samples were analyzed. This resulted in 50 to 60 samples per size range for a total of approximately 280 samples. These samples were run through the system (shown schematically in Figure 2) and a voltage-time profile (similar to that in Figure 3) was produced for each.

Figure 3 shows the two pieces of information extracted from each voltage-time profile: scan time, t (in seconds), required by all particles in the sample to cross the photocell sensing zone, and the area, A (in volt-seconds), bound by the initial voltage level and the voltage profile during time t.

Assuming no interference (the presence of one particle does not affect the settling time of another particle), time t is assumed to be the same for all samples in one size range. Therefore, for each size range, an average time, t_{av}, is calculated by averaging the scan times of all samples in that size range. It should be noted that the column's diameter (77 mm) may cause some boundary drag, which could affect the settling mechanism of particles depending on their position with respect to the column boundaries. The column's diameter, therefore, is one of the system variables that should be tested at a subsequent stage for sensitivity.

After a regression analysis was performed between t_{av} and the mean particle size in each of the size ranges shown earlier, the experimental values of parameters a and b in Equation 11 were determined to be −3.16648 and 1.38584, respectively.

The deviations (≈33 percent between respective absolute values) of the experimental values obtained for constants a and b from the theoretical values (obtained from Stokes' law) are assumed to account for simplifying assumptions, such as lack of particle interference and spherical particles.

Using the experimental values for a and b in Equation 11 and solving for d yields

$$d = \frac{f_1}{10^{f_2 \log t}} \tag{12}$$

where d is in millimeters and t in seconds, and $f_1 = 5.189434$, and $f_2 = 0.721584$. From each group of samples representing a certain weight in a size range, an average area, A_{av}, is calculated by averaging the areas produced by the samples in that group. As expected, A_{av} increases, for a given size range, with increasing weight. This is because more weight means more particles, and hence more light blockage (less registered voltage) in a given instant. A relationship between the weight of a sample (in grams) and the produced area (in volt-seconds) is established for each size range.

The actual area-weight relationships for the five size ranges considered are shown in Figure 4, in which they exhibited linear correlations. Therefore regression analyses were performed and the regression lines were passed through the origin point on the basis of the logic that when no particles were introduced (weight of 0 g), there would be no drop in voltage (area of 0 v · sec). Note also that the slope of the line representing the area-weight relationship increases with decreasing mean size. This proportionality is modeled by the curve shown in Figure 5, which relates the slope of the regression line (area/weight ratio) and mean size of each size range. The equation represented by the curve in Figure 5 is

$$S = 0.124188 + \frac{0.120318}{d^2} \tag{13}$$

where S is the slope of the regression line (from Figure 4) in volt-seconds per gram, and d is the particle size in millimeters.

The two relationships represented by Equations 12 and 13 are used to determine the size gradation of an aggregate sample using the system shown in Figure 2. After some sensitivity analyses were performed on the results of different mixed samples, it was found that the calculated gradation is closest to the actual one when a value of 0.82 is used for the parameter f_2 in Equation 12. The values of the parameters in Equations 12 and 13 may have to be adjusted for samples retrieved from a different type of aggregate. This could be done by testing samples with known gradations. The calculation procedure is summarized in Figure 6. After a mixed sample is introduced at the surface of the water

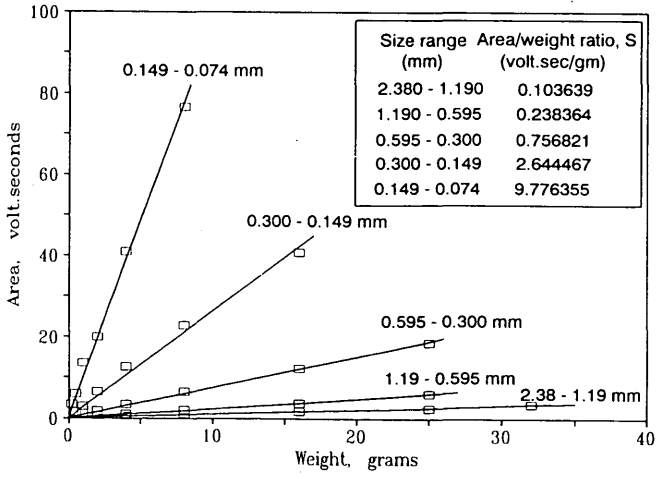

FIGURE 4 Area-weight relationships for five particle size ranges.

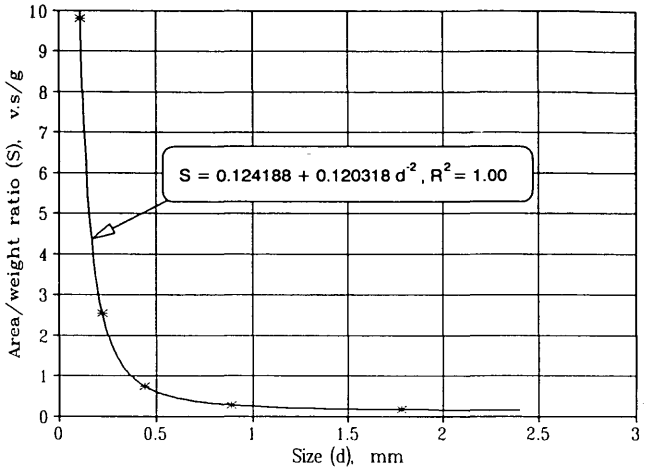

FIGURE 5 Area/weight ratio versus particle size.

column, the particles separate (as they travel downward) according to their sizes and produce a voltage-time profile similar to the one shown in the middle of Figure 6. The area bound by the profile and the initial voltage horizontal line is divided into small slices. Each slice a_i represents a small number of particles crossing the photocell sensing level at time t_i. The size d_i of the particles producing the area a_i is determined by substituting the value of t_i in Equation 12. The weight w_i of these particles is obtained by dividing the area a_i by the ratio S from Equation 13 corresponding to size d_i. The result of performing this process on all the area slices produced by the voltage-time profile is a set of d_i, w_i pairs, which are similar to the results obtained by conventional sieve analysis. These pairs are then used to construct the size gradation curve of the tested mixed sample as shown at the right side of Figure 6. A scan time of about 200 sec is required to run a mixed sample through the system.

DISCUSSION OF EXAMPLE GRADATIONS CALCULATED BY FRACTIONATING WATER COLUMN

The fractionating water column prototype was tested with a set of aggregate blends with particle sizes ranging from 0.074 mm (No. 200 sieve size) to 2.38 mm (No. 8 sieve size), the actual gradations of which were predetermined. These blends represent washed material passing the 2.38-mm sieve and retained on the 0.074-mm sieve. The calculated gradations of these blends are shown in Figures 7 and 8 along with their actual gradations for comparison. Figures 7 and 8 show that the calculated gradation curves suggest an underestimation of the coarser portion of the blend and an overestimation of the finer portion. These deviations of the calculated gradation curve from the actual one seem to represent a trend. The amount of deviation, however, varies for different tests.

Showing the gradations of two different samples on the same graph (Figures 7 and 8) adds to the credibility of the approach in that the calculated gradation curves follow their actual counterparts and do not deviate randomly. The tested aggregate blends represent the fine portions of aggregate blends whose gradations

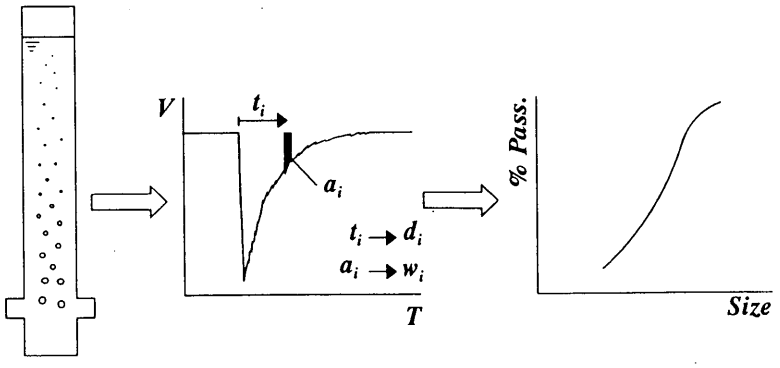

FIGURE 6 Schematic summary of analysis process.

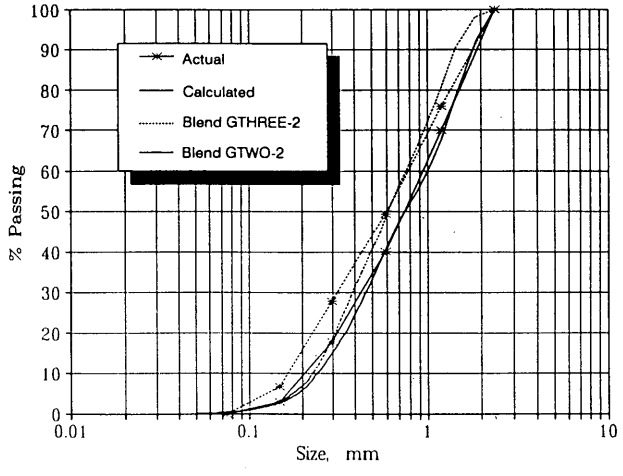

FIGURE 7 Examples of system output: Blends GTHREE-2 and GTWO-2.

fall in the specification envelope for a densely graded aggregate of an asphalt hot mix that is normally used for leveling or as a binder or surface course (*12*).

Figure 9 shows the gradation of an aggregate blend containing particles of 26.5 mm maximum size. This blend is typical for a hot-mix asphalt used as a binder (*12*). The calculated gradation of the fine portion (<2.38 mm) of the blend is superimposed on the respective part of the curve to show how the calculated gradation would look in the context of a total blend gradation. It is clear that the "absolute" deviations would be reduced when the calculated gradation of the fine particles is shown as part of a total gradation curve. The absolute deviation of percent passing at any particle size will be reduced by the value of the percent passing the 2.38-mm sieve in the total aggregate blend.

In the sieving process, the fine particles require longer sieving times than coarser particles. If an aggregate sample was sieved down to the 2.38-mm sieve, the passing material could be analyzed using the developed system. This hybrid approach is illustrated schematically in Figure 10. To further automate the analysis

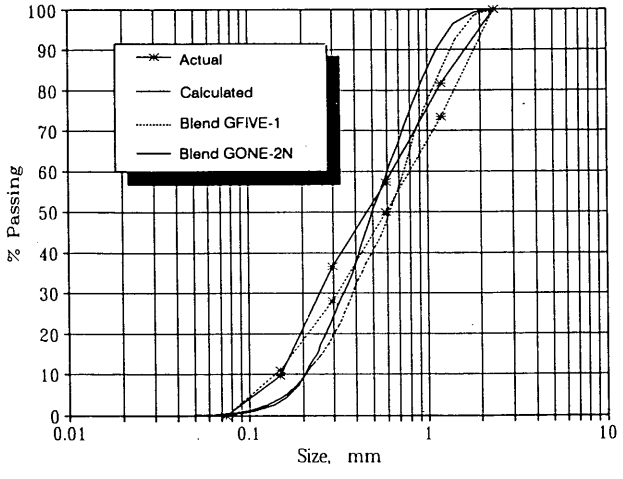

FIGURE 8 Examples of the system output: Blends GFIVE-1 and GONE-2N.

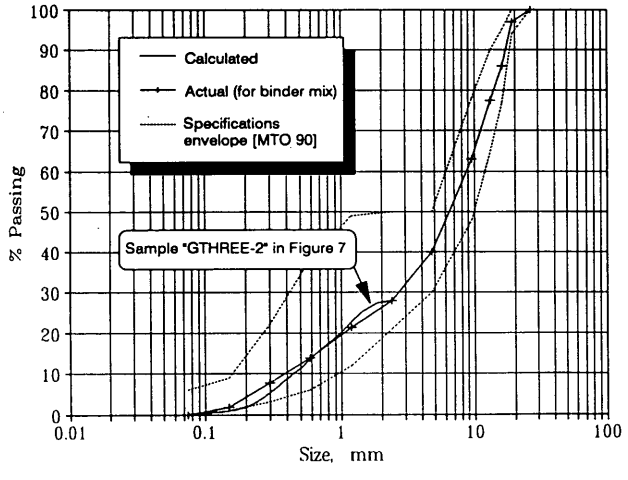

FIGURE 9 Gradation of fine portion (tested by fractionating water column) in context of total gradation curve of aggregate blend.

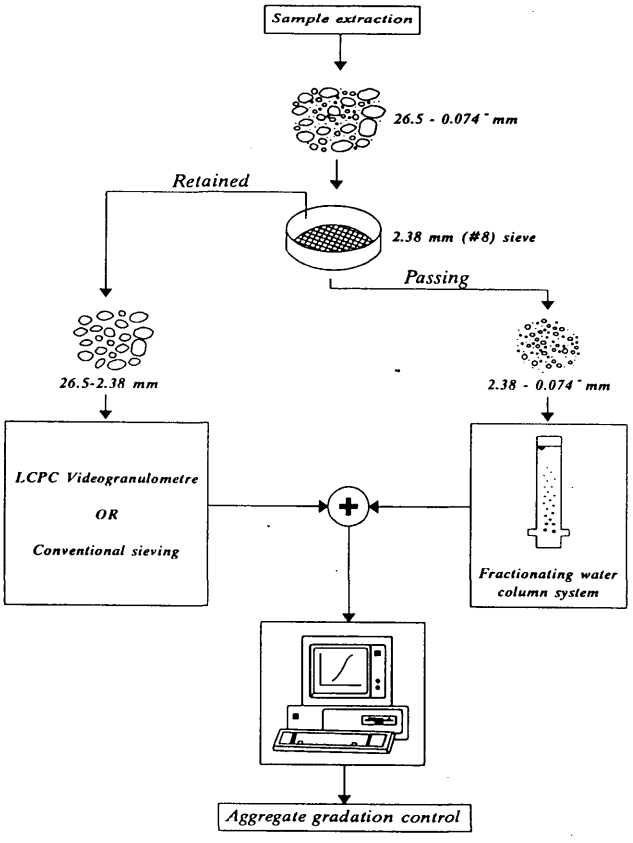

FIGURE 10 Conceptual illustration of hybrid system.

of the coarser portion of an aggregate blend (>2.38 mm), a system such as the French Videogranulometre (*8*) could be employed, and the full process would then be nearly fully automated. The gradations of the coarse and fine portions of the blend could easily be combined to produce the total gradation curve.

One aspect of the developed system that should be addressed is the capability of handling samples with dust (material finer than 74 m or passing the No. 200 sieve). This could be accomplished by adding another photocell near the top of the water column (Figure 2). The dust material is composed of very small particles

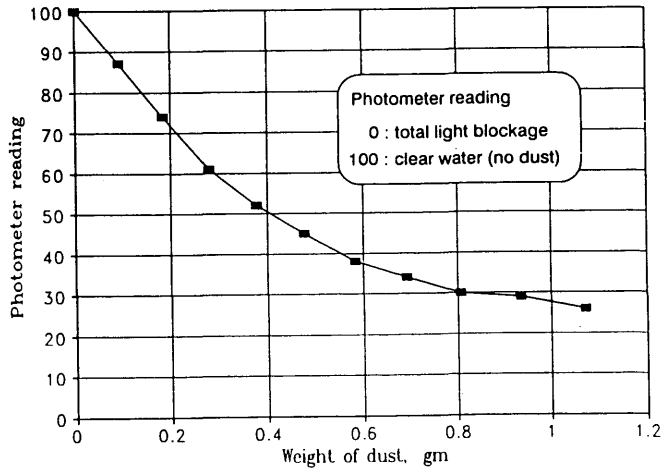

FIGURE 11 Results of pilot study on dust using photometer.

that will not have enough time to settle during the test period (200 sec). A voltage reading (at the end of a test) by the top photocell could be related to the amount of dust present in the tested sample. If necessary, the voltage reading of the bottom photocell could also be used to help in accurately determining the amount of particles finer than 74 m remaining in the water column.

Relating the light intensity to the amount of dust was proved to be possible by a simple experiment that was performed during the early stages of the research using a simple photometer and a jar filled with water. The jar was placed between a light source and the photometer's light sensor. Different amounts of dust were added to the water in the jar and the corresponding photometer readings were recorded. The weight of dust versus the photometer reading exhibited the relationship shown in Figure 11. A similar relationship could be established for the fractionating water column system.

CONCLUSION

For a very long time, sieve analysis was (and still is) the only established method for determining the size gradation of an aggregate blend. One major drawback associated with sieving is the relatively long processing time. Some research investigations resulted in working systems for automating the size gradation analysis of the coarse portion (>1 mm) of an aggregate blend. The fractionating water column methodology presented in this paper was developed to automate the analysis of the fine portion (<2.38 mm). The time required to run a sample of fine aggregate through the water column is approximately 200 sec (3.3 min). The voltage-time readings produced are already in digital format, and hence all the calculations (currently performed using electronic spreadsheets) could be performed in a negligible amount of time by a computer program that can be coded to replace the spreadsheets.

Some modifications to the fractionating water column system are required to make it adaptable to a full-scale environment. These modifications include the hardware (and consequently the software) to handle dust in a tested aggregate blend and the tube setup to automate the flushing and replacement of water after a test is performed. If the time needed to set the system for another test was found to be inconveniently long, two (or more) tubes could be used, each with a photocell and a light source. The A/D converter can very easily be instructed to read the voltage from the photocell of the tube that is being used. After these modifications are implemented, the system can be used as part of a hybrid system to automate the analysis of an aggregate blend. The other part of such a hybrid system would be to analyze the coarse portion (>2.38 mm) of the blend.

ACKNOWLEDGMENT

The authors would like to acknowledge financial support from Kuwait University in the form of a scholarship to the first author.

REFERENCES

1. Asphalt Institute. *Asphalt Plant Manual.* Manual Series No. 3 (MS-3). College Park, Md., 1986.
2. Roberts, F. L., P. S. Kandhal, E. R. Brown, D. Y. Lee, and T. W. Kennedy. *Hot Mix Asphalt Materials, Mixture Design, and Construction.* NAPA Education Foundation, Lanham, Md., 1991.
3. Heywood, H. The Origins and Development of Particle Size Analysis. *Proceedings of the Society of Analytical Chemistry,* 1970, pp. 1–18.

4. *Innovations Deserving Exploratory Analysis (IDEA) and Testing and Evaluation of IDEA Products.* Strategic Highway Research Program, National Research Council, Washington, D.C., 1990.
5. Alba, J. F. *Development of a Prototype for On-line Real-Time Measurement and Control of Aggregate Gradation in Asphalt Plants.* Phase I Final SHRP-IDEA Report. Felix ALBA Consultants, Inc., Murray, Utah, May 1992.
6. Gao, Q. *A Hybrid Approach to Rock Image Segmentation.* Master's thesis. University of Waterloo, Ontario, 1988.
7. Maerz, N. H. *Photoanalysis of Rock Fabric.* Ph.D. thesis. University of Waterloo, Ontario, 1990.
8. *Yernaux Pesage: Videogranulometre.* Emaco (Canada) Ltd., Montreal, Quebec, 1991.
9. Kandhal, P. S., and S. A. Cross. Effect of Aggregate Gradation on Measured Asphalt Content. Presented at the 72nd Annual Meeting, Transportation Research Board, Washington, D.C., 1993.
10. Head, K. H. *Manual of Soil Laboratory Testing.* Vol. 1. Pentech Press, London, England, 1984.
11. Fox, R. W., and A. T. McDonald. *Introduction to Fluid Mechanics.* John Wiley & Sons, New York, 1985.
12. *Ontario Provincial Standard Specifications.* OPSS 1149. Ministry of Transportation of Ontario, Downsview, Ontario, 1990.

Evaluation of Fine Aggregate Angularity Using National Aggregate Association Flow Test

STEPHEN A. CROSS, BARBARA J. SMITH, AND KAREN A. CLOWERS

The state of Kansas currently requires a minimum percentage of crushed aggregate in their high-stability hot-mix asphalt mixtures. The current test methods rely on visual and microscopic examination of aggregate samples to determine percent crushed material. The test method for fine aggregates requires the use of a microscope and is time consuming, subjective in nature, and operator dependent. Therefore, it was desirable to develop a simple test that could be utilized in the field to determine aggregate acceptability. The National Aggregate Association (NAA) flow test was modified to replace the use of microscopic evaluation of fine aggregate to determine percent crushed material. The results of the modified flow test were compared with those of the NAA flow test, and the effects of natural sands on the void content were determined. The results from the modified flow test were related to the gyratory elastoplastic index, a measurement of mixture performance. As a result of this study, a new specification was developed utilizing the modified flow test to replace microscopic examination in the determination of percent crushed material. A void content of 46 percent or greater was found to provide satisfactory performance.

The Kansas Department of Transportation (KDOT) currently requires a minimum percentage of crushed aggregate in their high-stability hot-mix asphalt mixtures. The percentage crushed material varies from a high of 85 percent to a low of 50 percent, allowing the use of between 15 and 50 percent natural sands and uncrushed gravel. The eastern one-third of the state of Kansas has abundant deposits of stone that produce adequate amounts of high-quality crushed coarse aggregates and manufactured sands. The western two-thirds of the state relies mainly on deposits of sands and gravels for construction aggregates. Crushed gravels are generally utilized to meet the specification requirements for crushed material. Current KDOT specifications (*1*) for crushed gravel limit the minimum size before crushing, to ensure that all material is crushed, and the amount of material passing the No. 200 sieve after crushing. Historically, the major problem in meeting the specification requirements for crushed gravel occurs from contamination of the material with silts, clays, limestone fragments, and friable materials.

The current test methods employed by KDOT to determine whether aggregates meet the requirements for crushed gravel rely on visual and microscopic examination of aggregate samples submitted by contractors. The aggregates are tested to determine whether the material is crushed or uncrushed, not to determine the extent of crushing or the number of crushed faces. The current test method is easy to perform for coarse aggregates, requiring a visual check; however, for fine aggregates the test requires the use of a microscope. The test for fine aggregate is time consuming and subjective in nature, and has proved to be very operator dependent. Therefore, it was desirable to develop a simple test that could be utilized in the field to determine aggregate acceptability. Ideally, the test developed would relate to mixture performance.

A review of the literature indicated that the National Aggregate Association (NAA) flow test (*2*) might meet the requirements of the department. Several recent studies (*3–5*) indicate that the NAA flow test, a measure of aggregate angularity and surface texture, is related to flexible pavement performance. In addition, the use of the NAA flow test would allow the measurement of the angularity and texture of the aggregate, which is related to performance rather than percent crushed material.

OBJECTIVES

The objectives of this study were threefold: first, to develop a test method to replace the use of microscopic evaluation of fine aggregate in determining percent crushed material; second, to differentiate between blends of crushed and uncrushed samples and samples of crushed material with slight contamination; and third, to develop justifiable specification limits that are related to performance.

SCOPE

Samples of crushed gravel from four pits that supply aggregates to western Kansas were selected for testing. The aggregates from these four pits are typical of the aggregates utilized in western Kansas for production of crushed gravel. The aggregates were tested for percent crushed material using the current KDOT test method (microscopic examination), and the uncompacted void content was determined utilizing the NAA flow test and a proposed modification to the NAA flow test. Samples of the aggregates were combined, and the effects of differing amounts of natural sand in the blend on uncompacted void content were investigated. Aggregate blends were mixed with asphalt cement and compacted on the U.S. Army Corps of Engineers gyratory testing machine (GTM) and the gyratory elastoplastic index (GEPI) was determined.

TEST RESULTS AND DATA ANALYSIS

The entire project encompassed four phases. The original investigation was an exploratory process in which one phase of the plan was completed, and the following phases were determined on the basis of the results and findings from the previous phases.

S. A. Cross, Department of Civil Engineering, 2006 Learned Hall, University of Kansas, Lawrence, Kans. 66045-2225. B. J. Smith and K. A. Clowers, Kansas Department of Transportation, Docking State Office Building, 915 Harrison, Topeka, Kans. 66612.

The experimental plan was developed and all testing was carried out by the Geology and Bituminous Sections of the Research Unit of the Bureau of Materials and Research, KDOT.

Phase 1

Phase 1 consisted of determining whether the NAA flow test could be utilized to determine the percent crushed material in a sample of fine aggregate, thereby replacing the current KDOT method of evaluating material under a microscope. In all, 54 samples from 4 different pits were evaluated.

The percent crushed material in each sample was determined utilizing microscopic examination, and the uncompacted void content was determined from NAA flow test Methods A, B, and C (2). Method A consists of testing 190 g of a standard sand grading.

TABLE 1 Results from Aggregate Testing: Phases 1 and 2

			UNCOMPACTED VOID CONTENT (%)						
LAB No.	SOURCE	PERCENT CRUSHED*	KDOT METHOD A	NAA METHOD A	NAA METHOD B	NAA METHOD C	BULK SPECIFIC GRAVITY	APPARENT SPECIFIC GRAVITY	PERCENT ABSORPTION
134	Fullmer Pit	99.6	50.2	49.1	53.5	39.1	2.62	2.67	0.7
247	Fullmer Pit	99.1	N/T	48.3	52.5	40.0	2.59	2.62	0.4
248	Fullmer Pit	98.8	47.7	48.5	52.6	40.4	2.61	2.65	0.6
249	Fullmer Pit	99.2	47.3	47.9	52.1	39.3	2.58	2.65	1.0
383	Fullmer Pit	98.8	46.9	48.1	52.3	37.9	2.57	2.63	0.9
384	Fullmer Pit	99.0	46.3	48.2	52.2	38.4	2.58	2.63	0.7
385	Fullmer Pit	99.5	47.9	48.9	52.6	39.3	2.60	2.65	0.7
386	Fullmer Pit	99.3	47.4	48.2	52.4	40.4	2.58	2.65	1.0
387	Fullmer Pit	99.2	47.0	49.4	53.0	39.7	2.61	2.66	0.7
413	Fullmer Pit	N/T	46.8	47.3	51.3	37.9	2.56	2.65	1.3
414	Fullmer Pit	99.2	47.5	47.9	51.7	38.3	2.58	2.65	1.0
415	Fullmer Pit	N/T	46.7	47.9	52.5	39.2	2.60	2.67	1.0
416	Fullmer Pit	99.5	47.6	47.6	51.5	37.3	2.57	2.65	1.2
417	Fullmer Pit	N/T	47.0	47.7	51.4	38.3	2.55	2.64	1.3
418	Fullmer Pit	99.1	46.9	41.2	50.4	38.7	2.56	2.65	1.3
419	Fullmer Pit	N/T	47.0	47.1	51.0	36.1	2.55	2.62	1.0
420	Fullmer Pit	99.6	46.9	46.9	51.0	36.8	2.55	2.59	0.6
421	Fullmer Pit	N/T	46.5	48.3	52.7	39.6	2.64	2.67	0.4
1242	TSG-Potter	99.4	47.4	48.5	53.2	42.1	2.61	2.68	1.0
497	JoDee Pit #1	98.8	48.5	48.6	52.4	39.3	2.62	2.65	0.4
3133	Trap Rock	N/T	N/T	50.1	54.5	N/T	2.66	2.77	1.5
388	TSG-Oldham	96.7	47.7	48.0	52.1	37.3	2.52	2.66	2.1
442	TSG-Oldham	97.0	48.3	47.8	52.2	37.8	2.49	2.62	2.0
443	TSG-Oldham	98.7	47.3	49.6	52.8	38.8	2.54	2.68	2.1
444	TSG-Oldham	98.6	48.4	49.2	53.2	39.5	2.57	2.67	1.5
445	TSG-Oldham	97.4	47.4	48.0	51.9	38.5	2.53	2.65	1.8
446	TSG-Oldham	98.6	47.4	48.7	52.8	41.0	2.58	2.66	1.2
447	TSG-Oldham	96.5	47.9	48.9	53.2	41.0	2.56	2.71	2.2
479	TSG-Oldham	97.3	48.2	47.8	52.2	39.0	2.55	2.67	1.8
480	TSG-Oldham	95.7	48.0	48.8	53.0	39.6	2.56	2.66	1.5
481	TSG-Oldham	97.6	48.0	46.4	52.4	39.2	2.53	2.63	1.5
482	TSG-Oldham	96.6	48.3	49.8	53.8	40.0	2.57	2.62	0.7
600	TSG-Oldham	96.1	47.6	48.6	52.9	39.7	2.56	2.71	2.2
601	TSG-Oldham	96.1	48.3	48.2	52.2	38.8	2.55	2.69	2.0
602	TSG-Oldham	97.9	47.5	52.6	53.3	39.7	2.60	2.68	1.1
603	TSG-Oldham	98.0	47.6	49.3	53.1	40.6	2.61	2.67	0.9
981	TSG-Oldham	97.2	41.4	46.9	N/T	N/T	2.59	2.69	1.4
982	TSG-Oldham	98.3	46.9	44.1	49.3	40.6	2.48	2.57	1.4
1055	TSG-Oldham	98.9	46.6	46.8	51.6	43.4	2.58	2.68	1.4
1056	TSG-Oldham	99.0	47.1	47.4	N/T	42.7	2.59	2.69	1.4
1057	TSG-Oldham	99.5	46.0	47.9	52.5	43.4	2.63	2.68	0.7
1137	TSG-Oldham	99.5	46.7	48.1	N/T	40.3	2.60	2.67	1.0
1138	TSG-Oldham	99.6	46.8	46.8	N/T	41.0	2.54	2.65	1.6
1191	TSG-Oldham	N/T	47.2	45.4	50.3	40.2	2.51	2.64	2.0
1192	TSG-Oldham	99.5	47.5	48.1	N/T	42.2	2.63	2.68	0.7
1193	TSG-Oldham	N/T	47.6	46.6	51.8	41.1	2.58	2.67	1.3
1282	TSG-Oldham	N/T	47.6	46.3	51.2	40.7	2.53	2.67	2.1
1356	TSG-Oldham	99.3	42.1	46.0	51.2	42.8	2.59	2.70	1.6
1357	TSG-Oldham	99.2	N/T	47.3	N/T	40.6	2.61	2.68	1.0
1358	TSG-Oldham	N/T	46.0	42.6	47.8	38.0	2.43	2.52	1.5
1447	TSG-Oldham	99.3	46.4	46.6	51.8	42.7	2.59	2.70	1.6
1448	TSG-Oldham	N/T	47.0	44.3	49.1	38.8	2.45	2.51	1.0
1449	TSG-Oldham	99.0	52.1	49.5	53.6	43.1	2.59	2.68	1.3
1450	TSG-Oldham	99.2	47.6	50.3	54.6	44.1	2.66	2.77	1.5

N/T = Not Tested
* Microscopically determined.

TABLE 2 Summary Statistics: Phases 1 and 2

SOURCE	TEST STATISTIC	PERCENT CRUSHED*	UNCOMPACTED VOID CONTENT (%) KDOT METHOD A	NAA METHOD A	NAA METHOD B	NAA METHOD C	BULK SPECIFIC GRAVITY	APPARENT SPECIFIC GRAVITY	PERCENT ABSORPTION
ALL	n	43	51	54	48	52	54	54	54
	Mean	98.47	47.25	47.74	52.13	39.89	2.58	2.67	1.26
	Std Dev	1.13	1.49	1.84	1.28	1.81	0.05	0.06	0.50
	Maximum	99.6	52.1	52.6	54.6	44.1	2.70	2.80	2.20
	Minimum	95.7	41.4	41.2	47.8	36.1	2.50	2.50	0.40
Fullmer	n	13	17	18	18	18	18	18	18
	Mean	99.22	47.27	47.69	52.03	38.71	2.60	2.66	0.88
	Std Dev	0.27	0.87	1.75	0.80	1.19	0.00	0.05	0.29
	Maximum	99.6	50.2	49.4	53.5	40.4	2.60	2.70	1.30
	Minimum	98.8	46.3	41.2	50.4	36.1	2.60	2.60	0.40
Oldham	n	28	32	33	27	32	33	33	33.0
	Mean	98.08	47.20	47.65	52.06	40.51	2.57	2.68	1.49
	Std Dev	1.22	1.77	1.93	1.51	1.79	0.06	0.06	0.45
	Maximum	99.6	52.1	52.6	54.6	44.1	2.70	2.80	2.20
	Minimum	95.7	41.4	42.6	47.8	37.3	2.40	2.50	0.70

* Microscopically determined.

Method B consists of testing three fine aggregate size fractions: the Nos. 8 to 16, Nos. 16 to 30, and Nos. 30 to 50. Method C consists of testing 190 g of the as-received gradation.

The bulk and apparent specific gravity and the percent absorption of the samples were determined in accordance with Kansas Test Method KT-6 (*3*). The results are shown in Table 1, and Table 2 shows the statistics of mean, range, and standard deviation. The bulk specific gravity, excluding the trap rock sample, ranged from a low of 2.50 to a high of 2.70 and the absorption from a low of 0.4 percent to a high of 2.2 percent. The range of specific gravities and absorptions of the materials tested are similar to those of the sands and gravel utilized in western Kansas.

The relationship between uncompacted void content and the percent crushed material is shown in Figure 1. The results show no correlation and indicate that the NAA flow test is not discrete enough to detect slight changes in percent crushed material for the samples evaluated. The results also indicate that the three methods, A,B, and C, give different results. The results of the correlation between percent crushed material and void content were as expected, because the NAA flow test is a measure of aggregate angularity and surface texture, not percent crushed material.

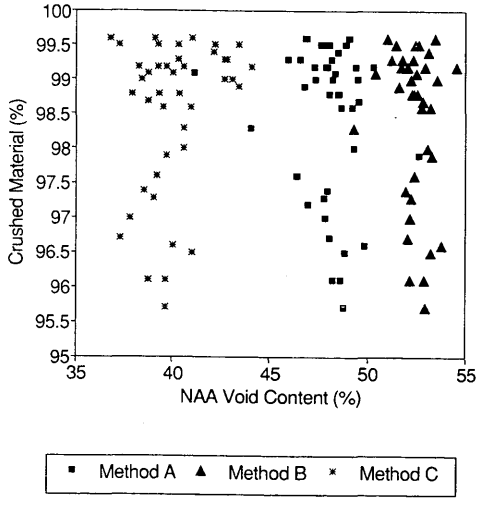

FIGURE 1 Percent crushed material versus NAA void content.

Phase 2

The NAA flow test requires the determination of the bulk specific gravity of the sample, which requires a 24-hr soak of the aggregate, making the test undesirable to KDOT for field testing for acceptance of material as crushed gravel. The aggregates typically utilized in western Kansas have low absorptions and similar specific gravities. Therefore, it was believed that apparent specific gravity could be determined instead of bulk specific gravity without significantly affecting the results. Eliminating the need to determine the bulk specific gravity of the aggregate would reduce the time required to complete the test, making it adaptable for field use. The proposed KDOT flow test involved a modification to the NAA test in which the aggregate in the calibrated cylinder is transferred to a volumetric flask and both are weighed. The volume of the sample is determined by adding water and reweighing. The substitution of the apparent specific gravity for the bulk specific gravity changed the original calculations and simplified the formula for void content to

$$\text{Percent void content} = \{[B - A - (200 - V)]/V\} * 100 \quad (1)$$

where

A = weight of 200-ml flask and sample,
B = weight of 200-ml flask full of water and sample, and
V = volume of calibrated cylinder.

Each sample from Phase 1 was tested using the KDOT Method A flow test and the results are shown in Table 1. The statistics of mean, range, and standard deviation are shown in Table 2. The results indicate that the KDOT Method A flow test and the NAA Method A flow test have similar means, 47.2 percent and 47.7 percent, respectively. The standard deviations for the two Method A tests show less variation for the KDOT method, 1.49 percent compared with 1.84 percent, indicating better repeatability.

To determine whether the similarity in means was significant, a one-way analysis of variance (ANOVA) was performed on the uncompacted void contents. The analysis indicates a significant difference between the means at a confidence limit of 95 percent ($\alpha = 0.05$). Duncan's multiple range test was performed on the means to determine which were significantly different at a confidence limit of 95 percent. The results show that the NAA Method A and KDOT Method A tests give similar results but are significantly different from the NAA Methods B and C. Therefore, the KDOT Method A flow test could be used in lieu of the NAA Method A flow test and be expected to give the same results with less testing time for aggregates typically utilized in western Kansas for crushed gravel.

The above tests were performed on aggregates typical to western Kansas. The aggregates are silicious, with less than 15 percent carbonates, and have similar specific gravities and low absorptions. Differing results would probably be obtained for materials with greatly differing specific gravities and absorptions.

Phase 3

The results from Phase 2 showed that the KDOT Method A and NAA Method A flow tests gave similar results. The similarity of test results would allow the use of the KDOT flow test for evaluation of aggregates for acceptance as crushed gravel if an acceptance level for void content could be established and if undesirable amounts of contamination could be detected. The third phase of the study consisted of determining whether (*a*) the results from the KDOT flow test were related to percent angular and rounded material in a mixture; (*b*) the KDOT flow test could detect contamination of a sample with natural sands, silts, or clays; and (*c*) the KDOT flow test would relate to GEPI, a measure of a mixture performance. Adoption of the KDOT flow test would be a move away from a measure of crushed material toward a measure of aggregate angularity and surface texture, which was deemed desirable by KDOT.

Aggregate Angularity

The relationship between percent angular and rounded material in a mixture and the uncompacted void content from the KDOT flow test was determined by mixing samples of a very angular material, blast furnace slag, with differing amounts of very rounded material, Ottawa sand and glass beads, and determining the uncompacted void content. A series of samples were made to the Method A gradation (*2*) with various percentages of rounded material. Samples were prepared with 100 percent slag and with slag replaced by rounded material in 5 percent increments, keeping the gradation of the sample constant. The void content was determined using the KDOT flow test and the above experiment was repeated using crushed gravel as the angular material and Kansas River sand as the rounded material.

The results of the above testing are shown in Table 3 and presented in Figure 2. The relationships were found to be linear, with an R^2 of 0.98 for the slag and 0.99 for the gravel. However, the slopes of the regression lines appear to be dependent upon the material.

Effect of Contaminants

To determine the effect of sample contamination on uncompacted void content, a crushed gravel was mixed to the Method A gradation and material was substituted using the same procedure as that described earlier to replace a series of percentages of each sieve. Many different blends of crushed and rounded material and various sizes of contaminants were evaluated with similar results. Only three trials are reported here—No. 8 material, a 50/50 blend of plus and minus No. 200, and plus No. 200 as the contaminant. The uncompacted void content of the samples was determined using the KDOT flow test to determine the effect of contamination on uncompacted void content, and the results are shown in Table 4 and in Figures 3–5.

The results indicate that the uncompacted void content falls off from a high of approximately 45 percent for 100 percent crushed material to a point where the fines bulk the sample at approximately 50 to 75 percent contaminants. This corresponds to a void content of 38 to 42 percent. The void content either increased or stayed constant with a further increase in contamination. However, in only one instance, the 100 percent crushed sample, did the void content rise above the initial one. Therefore, if the void content is set at an appropriately high level, indicating 100 percent crushed material, the test could be used to differentiate between crushed material and crushed material with varying amounts of contamination.

GEPI Testing

There is no good, direct measure of aggregate performance in an asphalt mix; however, several researchers (*4–6*) have stated the importance of angular, rough-textured aggregates in asphalt mixtures. Samples of aggregates with known KDOT Method A flow test values were prepared and mixed with 5 percent asphalt cement by weight of the aggregate to give the mixtures cohesion. The samples were tested for GEPI in accordance with ASTM D3387 at 827.4 kPa (120 psi), 1 degree gyration angle, for 60 revolutions. The GEPI is a measure of the shear strain experienced by a sample and is an index of the angle of internal friction of the aggregate. Mixtures with low GEPI are typical of angular, rough-textured aggregates and high GEPI of rounded, smooth-textured aggregates.

Samples of 100 percent crushed limestone and 100 percent Kansas River sand and three samples of crushed gravel with the highest, mean, and lowest KDOT Method A void contents of the gravels tested in Phase 1 were tested for GEPI. In addition, samples of the highest void content crushed gravel were blended with 25, 50, and 75 percent river sand were also tested. The results are shown in Table 5 and Figure 6. For the 100 percent crushed gravels, the GEPI was constant at a level of 1.48, with uncompacted void contents ranging from 44.4 to 51.5 percent. For the remaining

TABLE 3 Results of Angular and Rounded Uncompacted Void Testing

PERCENT ANGULAR MATERIAL	KDOT METHOD A VOID CONTENT (%) SLAG	CRUSHED GRAVEL
100	54.0	43.61
95	54.5	
90	52.4	42.5
85	52.4	
80	50.6	42.52
75	47.2	
70	49.0	41.59
65	48.3	
60	47.3	41.39
55	46.3	
50	45.4	40.56
45	44.3	
40	43.9	39.87
35	42.3	
30	41.1	39.36
25	39.5	
20	N/T	38.48
15	N/T	
10	N/T	37.65
5	N/T	
0	35.1	37.07

N/T = Not Tested.

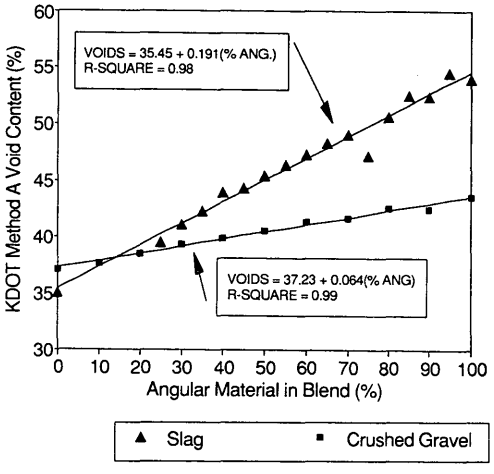

FIGURE 2 KDOT modified flow test versus aggregate angularity.

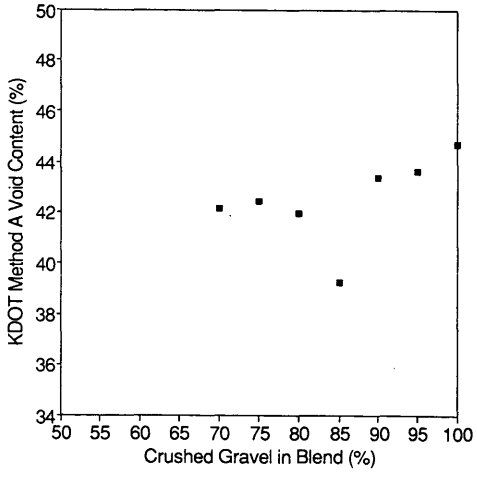

FIGURE 4 KDOT modified flow test versus plus No. 200 contamination.

TABLE 4 Results of Contamination on KDOT Method A Voids

PERCENT CRUSHED GRAVEL	KDOT METHOD A VOID CONTENT (%) PLUS No. 8	PLUS No. 200	50/50 BLEND +No. 200 -No. 200
100	43.66	44.73	44.51
95	N/T	43.67	43.39
90	42.68	43.39	42.6
85	N/T	39.26	41.44
80	40.83	41.96	40.75
75	N/T	42.46	40.21
70	39.88	42.16	40.89
65	N/T	N/T	40.53
60	38.32	N/T	40.69
55	N/T	N/T	40.68
50	37.9	N/T	40.76
45	N/T	N/T	42.75
40	40.18	N/T	N/T
30	40.93	N/T	N/T
20	42.98	N/T	N/T
25	N/T	N/T	47.72

N/T = Not Tested.

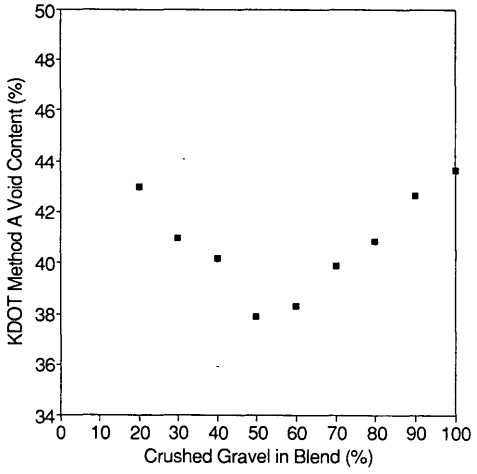

FIGURE 3 KDOT modified flow test versus plus No. 8 contamination.

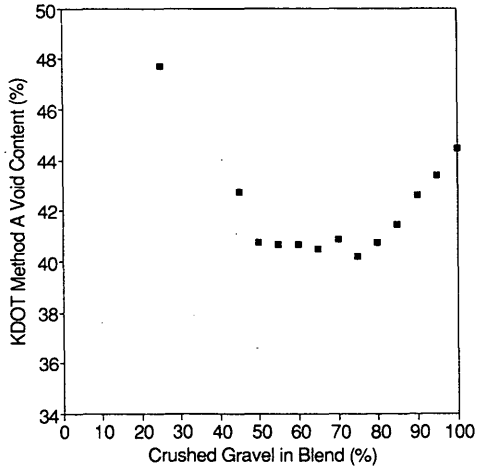

FIGURE 5 KDOT modified flow test versus 50/50 blend of plus and minus No. 200 contamination.

TABLE 5 Results of GEPI Testing

SAMPLE	KDOT METHOD A VOIDS (%)	GEPI
100% Crushed Limestone	49.0	1.4
100% Crushed Gravel High Quality	51.5	1.5
100% Crushed Gravel Medium Quality	47.0	1.5
100% Crushed Gravel Low Quality	44.5	1.5
75% Crushed Gravel 25% Natural Sand	45.0	1.6
50% Crushed Gravel 50% Natural Sand	42.5	1.7
25% Crushed Gravel 75% Natural Sand	39.5	1.7
100 % Natural Sand	37.0	1.9

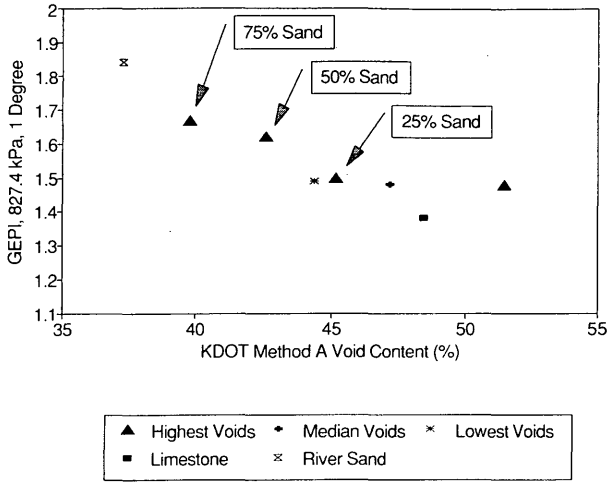

FIGURE 6 GEPI versus KDOT modified flow test.

crushed gravel and 100 percent natural sand mixtures, the GEPI increased with an increase in natural sand, indicating a less stable, more rounded, smooth-textured mixture. The results show that mixtures with an uncompacted void content of 46 percent or higher would have a GEPI, or an index of internal friction, as low as a sample of 100 percent crushed gravel.

From the results of the above testing it was believed that for the aggregates utilized in this study, a void content of 46 percent or higher would be indicative of a fine aggregate with a rough angular surface texture, which would give the same performance as a mixture utilizing 100 percent crushed gravel. The uncompacted void content of 46 percent is slightly higher than the value of 44.5 percent reported by Kandhal et al. (*7*) as separating natural from manufactured sands. The void content reported by Kandhal et al. (*7*) is based on the bulk specific gravity, and this study utilized the apparent specific gravity, which would give a higher void content.

TABLE 6 Results of KDOT Flow Tests for Phase 4

LAB #	SOURCE	% GRAVEL	KDOT METHOD A	KDOT METHOD C WITH - No. 100 MATERIAL REMOVED	KDOT METHOD C WITH - No. 200 MATERIAL REMOVED	KDOT METHOD C
A1	A	100	48.1	45.3	43.9	42.7
A3	A	100	48.6	46.3	44.6	42.7
A5	A	100	48.3	45.7	43.9	43.1
A7	A	100	48.4	45.1	43.9	42.2
A9	A	100	48.4	43.3	44.1	42.5
A11	A	100	48.1	45.8	44.5	42.6
A13	A	100	48.1	45.8	44.4	42.9
A15	A	100	48.5	43.9	44.7	38.2
B1	B	100	45.8	43.3	43.0	40.4
B3	B	100	46.1	43.3	43.3	40.4
B5	B	100	47.0	43.9	43.0	40.9
B7	B	100	46.6	43.9	42.2	40.8
B9	B	100	46.0	43.6	42.0	40.6
B11	B	100	46.0	45.6	41.9	41.4
B13	B	100	46.2	45.0	41.7	40.5
B15	B	100	46.4	43.7	42.7	41.5
A31	A	95	48.0	45.4	44.0	42.4
A32	A	95	47.3	45.5	44.1	42.0
A33	A	95	47.1	45.6	44.3	42.4
A34	A	95	47.6	46.0	44.5	42.4
A35	A	95	47.3	45.0	43.9	42.0
A36	A	95	48.0	45.7	44.5	41.9
A37	A	95	47.5	45.3	44.3	42.3
B31	B	95	45.7	43.4	41.9	40.3
B32	B	95	45.9	43.3	42.0	41.2
B33	B	95	N/T	43.0	41.9	39.6
B34	B	95	N/T	43.5	41.8	40.4
B35	B	95	N/T	43.8	41.6	40.8
B36	B	95	N/T	43.9	41.8	41.3
B37	B	95	N/T	43.3	42.6	41.2
B38	B	95	N/T	43.0	41.7	40.3

N/T = Not Tested.

Phase 4

The fourth phase of the study consisted of (*a*) verifying the proposed specification limit of 46 percent KDOT Method A void content, (*b*) determining the repeatability of the test method, and (*c*) determining whether Method C (2), the as-received aggregate gradation, could be utilized, thereby saving test preparation time. Two new aggregate sources were selected for Phase 4, one a high-quality crushed gravel (Source A) and the other a crushed gravel with a prior history of failing to pass the current KDOT crushed gravel specification (Source B).

Samples were prepared with 100 and 95 percent crushed gravel and 0 and 5 percent Kansas River sand. The samples were prepared to the Method A gradation, the as-received gradation (Method C), and to Method C with the percent passing the No. 100 and the No. 200 sieves removed. The results from the previous phases indicated that the variability occurring in Method C might be caused by the addition of the No. 8 and No. 200 material. By removing the percent passing the No. 100 and No. 200 sieves, it was thought that the variability might be reduced to an acceptable level.

The uncompacted void contents for Phase 4 are shown in Table 6. An ANOVA was performed on the data to determine whether there was a statistically significant difference between the means of the treatments. The analysis confirms that each flow test was statistically significantly different from the other and could differentiate between sources at a confidence limit of 95 percent ($\alpha = 0.05$). The means and standard deviations from Phase 4 are shown in Table 7. Duncan's multiple range test showed that none of the test methods could consistently differentiate between the samples with and without natural sand by source. This indicates that none of the test methods are discrete enough to detect slight amounts of natural sand. The means of the void contents shown in Table 7 indicate that Source B, a marginal gravel, would fail the proposed specification limit of 46 percent voids at 95 percent crushed gravel but not at 100 percent gravel. Source A, a high-quality gravel, has enough angularity and surface texture to pass the test with 5 percent natural sand.

The results indicate that either Method A or C could be utilized to replace the current specification for crushed gravel. However, the proposed specification limit of 46 percent would need to be lowered approximately 5.5 to 6.0 percent if Method C were utilized. The standard deviation for Method A was less than that for Method C, 1.00 percent to 1.12 percent, indicating that Method A would be more repeatable and therefore more desirable to use.

TABLE 7 Simple Statistics from Phase 4 Flow Test

TEST STATISTIC	KDOT FLOW TEST	SOURCE A 95% GRAVEL	SOURCE A 100% GRAVEL	SOURCE B 95% GRAVEL	SOURCE B 100% GRAVEL
MEAN	Method A	47.55	48.31	45.78	46.26
STD DEV	Method A	0.351	0.201	0.191	0.400
MEAN	- No. 100	45.50	45.14	43.39	44.02
STD DEV	- No. 100	0.307	1.022	0.320	0.823
MEAN	- No. 200	44.22	44.24	41.90	42.45
STD DEV	- No. 200	0.234	0.334	0.287	0.610
MEAN	Method C	42.19	42.11	40.64	40.80
STD DEV	Method C	0.209	1.608	0.568	0.440

CONCLUSIONS

On the basis of the data obtained in this study and for the materials investigated, the following conclusions are warranted:

1. The NAA flow test, Methods A, B, or C, did not correlate with percent crushed material, determined by microscopic evaluation, for the gravel mixtures evaluated.
2. The KDOT Method A flow test and the NAA Method A flow test gave statistically similar results at a confidence limit of 95 percent for the samples utilized.
3. The relationship between the KDOT Method A void content and sample angularity and surface texture was found to be linear.
4. A GEPI of 1.48 was found to differentiate between 100 percent crushed gravel and natural sand and crushed gravel samples. This corresponded to a minimum KDOT Method A flow test void content of 46 percent.

RECOMMENDATIONS

On the basis of the results of this study, KDOT developed a special provision to the standard specifications for crushed gravel. The requirements for determining the percent crushed material on that portion of the material passing the No. 4 sieve was changed from a microscopic evaluation to a minimum uncompacted void content of 46 percent as measured by the KDOT Method A flow test. The requirements for initial gradation before crushing and percent passing the No. 200 sieve after crushing were left unchanged.

ACKNOWLEDGMENTS

The research documented was conducted and coordinated by KDOT. Credit is due to Glenn Fager, Bituminous Research Engineer, and Engineering Technicians Dick Hoch, Chuck Espinosa, Ray Brownell, and Ken Mathewson for their assistance in sampling and testing and interpretation of test results.

REFERENCES

1. *Standard Specifications for State Road and Bridge Construction.* Kansas Department of Transportation, Topeka, 1990.
2. Meininger, R. C. *Proposed Method for Test for Particle Shape and Texture of Fine Aggregate Using Uncompacted Void Content.* National Aggregate Association, Silver Spring, Md., March 1989.
3. *Construction Manual, Part 5.* Kansas Department of Transportation, Topeka, 1991.
4. Cross, S. A., and E. R. Brown. Selection of Aggregate Properties to Minimize Rutting of Heavy Duty Pavements. In *Effects of Aggregates and Mineral Fillers on Asphalt Mixture Performance*, Special Technical Publication 1147 (R. C. Meininger, ed.), ASTM, Philadelphia, Pa., 1992.

5. Brown, E. R., and S. A. Cross. A National Study of Rutting in Hot Mixed Asphalt (HMA) Pavements. *Journal of the Association of Asphalt Paving Technologists,* Vol. 61, 1992.
6. Parker, F., and E. R. Brown. Effects of Aggregate Properties on Flexible Pavement Rutting in Alabama. In *Effects of Aggregates and Mineral Fillers on Asphalt Mixture Performance*, Special Technical Publication 1147 (R. C. Meininger, ed.), ASTM, Philadelphia, Pa., 1992.
7. Kandhal, P. S., M. A. Khatri, and J. B. Motter. Evaluation of Particle Shape and Texture of Mineral Aggregates and Their Blends. *Journal of the Association of Asphalt Paving Technologists,* Vol. 61, 1992.

The opinions, findings, and conclusions are those of the authors and not necessarily those of the University of Kansas or KDOT.

Siliceous Content Determination of Sands Using Automatic Image Analysis

TODD W. THOMAS, THOMAS D. WHITE, AND THOMAS KUCZEK

The characteristics of fine aggregate have a significant influence on the field performance of hot asphalt concrete mixtures. Siliceous and rounded particles, which make up a significant percentage of natural sand, are generally related to rutting and possibly stripping of asphalt mixtures. This study was conducted to develop and verify manual counting and automatic image analysis techniques to evaluate aggregate blends for amount of siliceous sand-size particles. Verification involved preparation of samples with known proportions of siliceous (translucent) and calcareous (opaque) particles. The samples prepared were analyzed manually with the aid of a microscope and automatically with an image analyzer. It was found that automatic image analysis can be used with a higher degree of confidence and accuracy than manual counting techniques in determining percent translucent particles. After the image analysis techniques were developed, extracted fine aggregates from field cores of various highway pavements in Indiana were examined with the image analyzer to determine amounts of translucent particles. The percentages of translucent sand particles, assumed to be natural sand, were evaluated for the effect on the gradation, and it was found that as the siliceous sand content on the field cores increased, humps on the 0.45 power gradation curve were likely to increase. Image analysis was found to be up to four times faster than manual counting techniques.

Rutting is a major type of distress associated with asphalt pavements, resulting in pavement roughness and vehicle hydroplaning and steering control difficulties. Factors that affect tendency for rutting include materials, construction, temperature, and traffic loading. Materials include both the binder and mineral aggregate, and the mineral aggregate consists of blends of coarse and sand sizes. Within the sand size, material may be crushed or uncrushed particles. Uncrushed sand is referred to as natural sand, which, with some exceptions, tends to be rounded and can consist of siliceous sand. The amount and type of natural sand in an asphalt mixture has been shown to influence asphalt mixture stability because of its shape and texture. As a result, specifying agencies have placed limits on the amount of natural sand allowed in asphalt mixtures. The ability to determine the amount of natural sand or siliceous sand in a sand blend is important for specifications and research. Since siliceous sand particles often are translucent in appearance, this study focuses on the ability to detect translucent particles in a sand blend with image analysis.

REVIEW OF LITERATURE

Effects of Natural Sand on Rutting

A combined laboratory and field study by Button et al. (*1*) addressed the effects of natural aggregate on plastic deformation in asphalt concrete pavements. Creep tests were used to determine that 20 percent natural sand resulted in large deformations during long-term loading for low and high air void contents. As a result of observations and tests on in situ pavements, excessive sand-size particles and the rounded shape and smooth texture of natural (uncrushed) aggregate particles were factors associated with rutting. It was recommended that the natural (uncrushed) particle content of asphalt mixes in pavements subjected to a high traffic volume be limited to about 10 to 15 percent.

Ahlrich (*2*) investigated the effects of natural sands on the engineering properties of asphalt concrete mixtures. Compacted specimens were prepared using crushed limestone and 0, 10, 20, and 30 percent natural sand. At the No. 30 sieve size, the gradation, when plotted on a 0.45 power gradation chart, exhibited a slight hump at 20 percent natural sand and a noticeable hump at 30 percent natural sand. In general, as the percent of natural sand increased, a hump at the No. 30 sieve size developed. All laboratory tests indicated that asphalt concrete mixtures containing all crushed aggregates had lower rutting potential than mixtures containing natural sand. Ahlrich recommended a maximum of 15 percent natural sand content for pavements carrying high-pressure-tire traffic.

Classification of Fine Aggregate

Classification methods of fine aggregate particles found in the literature have mostly been by means of particle shape and texture. One method for examining aggregate particle shape is the Corps of Engineers' Method CRD-C120-55, Method of Test for Flat and Elongated Particles in Fine Aggregate. Particle shape is evaluated by observing individual sand particles with a microscope and reporting the percentage of particles in the sample with a length-to-width ratio of more than 3.

Another method of measuring particle shape is ASTM D 3398, which provides an index of relative particle shape to a specified volume of fine aggregate by determining the voids in a standard volume after application of different compactive efforts. This method, however, is long and tedious.

Kandhal et al. (*3*) evaluated the National Aggregate Association's Proposed Method of Test for Particle Shape and Texture of Fine Aggregate Using Uncompacted Void Content. In this test, fine aggregate of a specified gradation flows through a funnel into a calibrated cylinder. The particle index value is computed from the voids in the resulting uncompacted specimen. The particle index is a quantitative way of defining the sand characteristics.

Image Analysis Studies on Mineral Aggregates

Perdomo and Button (*4*) conducted a study of coarse and fine crushed limestone and river gravel using grey-level image analysis

T. W. Thomas, Koch Materials Company, 400 N. 10th Street, P.O. Box 1507, Terre Haute, Ind. 47808. T. D. White and T. Kuczek, Purdue University, West Lafayette, Ind. 47907.

of digitized photographic images. They hypothesized that images of crushed limestone could be distinguished from images of river gravel by the fractal dimension, or "roughness," of the images. They found that the coarse crushed limestone and river gravel had statistically different fractal dimensions, thus distinguishing the two different types of aggregate. However, the two different types of fine aggregate could not be distinguished from one another using the same technique that was used for the coarse aggregate. They suggested that an aggregate classification system could be developed using fractal dimension analysis.

A detailed study by Barksdale et al. (*5*) investigated particle shape characteristics of fine and coarse aggregate particles. The particles were classified by computer programs into different shape categories, thus quantitatively describing the aggregate particles. This method was very labor intensive. However, three dimensions of the aggregate particles were measured, and the study also presented a method for measuring surface roughness.

IMAGE ANALYSIS

Image analysis is "the quantitative measurement of geometrical features that are exposed on two-dimensional images" (*6*). Methods of measurement are manual and automatic (computerized). A microscope can be used for manual image analysis, in which, for example, particles of interest in a specimen are identified and counted. This procedure is laborious and subject to errors, including operator judgment. One technique of automatic image analysis of mineral particles distinguishes one mineral from another by the optical signal strengths emitted from the minerals. This technique can be used to view the whole specimen surface and quantify the area occupied by each type of mineral. This procedure, once calibrated, is fast and eliminates individual operator judgment. The system used at Purdue University is a fully automated area-measuring system that is capable of measuring image characteristics such as area, number, perimeter, shape, and size distribution of aggregate particles. However, this study focused on distinguishing between opaque and translucent particles.

Automatic image analysis technology can be described as being composed of five distinct but related components: image generation and capture, image coding, image reconstruction, image enhancement, and image analysis. These components are discussed below.

Image Generation and Capture

Image generation and capture refers to the process of creating the image and capturing it in such a way that it may be encoded in a digital format. The key objective is to prepare the specimen and the image so that the level of detail and resolution can be captured without losing important information that cannot be reconstructed later. Methods used for image generation tend to be application specific and may encompass a range of specialized techniques.

Image Coding

Image coding refers to techniques used to store the captured image. Regardless of how the image has been captured, data are stored in such a way that each discrete element of the picture (pixel) is uniquely associated with several parameters (e.g., *x*-coordinate, *y*-coordinate, and brightness) (see Figure 1). Good image analysis systems allow for identification of 256 brightness levels. In this study, brightness levels (also called grey levels) are used to discriminate between different minerals in the image on the basis of the optical brightness of the opaque and translucent particles.

Image Reconstruction

Image reconstruction refers to the process of reconstructing an image that has been captured and coded. During the reconstruction, specific algorithms may be used, for example, to correct the image for the effects of distortions as a result of the capturing technique. In most cases, reconstruction is not necessary.

Image Enhancement

Image enhancement or processing refers to a range of techniques used to improve certain aspects of an image before analysis. These "high-level" image-processing activities are also known as morphological transformations. The aim is to minimize the required amount of enhancement required. Common examples of image enhancement include separating overlapping particles, crispening edges, and removing noise. Image reconstruction and enhancement capabilities are the features that distinguish one image analyzer from another.

Image Analysis

Image analysis refers to the actual determination of preselected parameters in relation to the enhanced image and is often referred to as "low-level" image processing. An example for this study

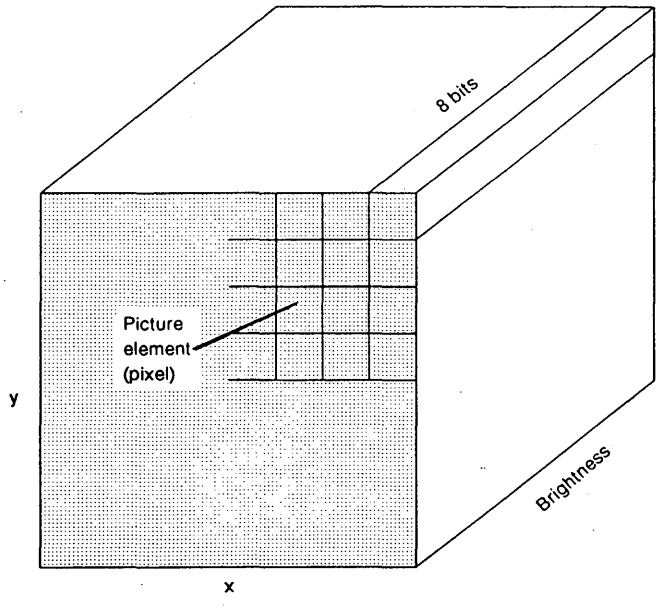

FIGURE 1 Relationship between pixels and brightness.

is calculating the areas of translucent and opaque particles on the basis of brightness level.

TEST METHODS

The laboratory-prepared samples used for the microscope evaluation were also used for the image analysis evaluation. Samples were prepared of known proportions by weight of translucent to opaque sand particles. Ottawa sand was used as the translucent sand in this study. Limestone, obtained from stockpiles at Fauber Construction in Lafayette, Indiana, was crushed in the laboratory and used for the opaque sand. The two types of sand particles were sieved separately into four sizes: passing no. 16, retained on No. 30; passing No. 30, retained on No. 50; passing No. 50, retained on No. 100; and passing No. 100, retained on No. 200. Samples were prepared with three levels (percentages) of translucent sand. These percentages were selected on the basis of minimum and maximum amounts of natural sand expected in highway pavements: 10, 20, and 40 percent. The sand particles were blended in these proportions for each individual size. Because of problems with magnification and focusing of different size particles at one time, it was necessary to view the particles in the separate sizes. The percentages of translucent and opaque particles were determined in each sand blend.

As a basis for evaluation, the first part of the study involved using a microscope to manually count the opaque and translucent particles of these prepared samples. The proportion of each was then determined. In the second part of the study, the image analyzer was used to determine the proportions of the same samples by area. The image analysis results were compared with the results obtained from the manual microscopic examination method. In the third part of the study, fine aggregate extracted from pavement cores was analyzed for the percentage of translucent aggregate. The results were evaluated for effects on gradation, assuming that the translucent sand is natural sand.

Sample Preparation

Samples for viewing were prepared in disposable petri dishes, with a volume of particles dependent on the size of the individual particles. Sample preparation was the same for both image analysis and microscope methods for the same particle size. The petri dishes were clear plastic and had a diameter of 3.5 in. It was desired to have the size of the sample approximately the same for each particle size to be viewed. A single layer was also important to avoid overlapping particles, which might have affected the results. Kitchen measuring spoons were found to provide the easiest way to measure out the sand grains on the petri dish. Multiple samples were prepared and viewed until the entire sample, either for the microscope or image analyzer method, was measured.

Manual Testing Procedure

A binocular microscope was used for counting the translucent and opaque particles by moving the prepared sample under the eyepiece of the microscope from top to bottom and then from left to right and counting sand particles at each location of the eyepiece. Magnification was determined for each particle size by considering a reasonable number of particles to view at one time to avoid eyestrain and to make counting easy. A magnification of 40 was used for sieve sizes No. 100 and No. 200 and 10 for sizes No. 30 and No. 50. The number of particles viewed at one time was normally between 15 and 40. The percentage of each type of particle, translucent or opaque, was determined for each sample. Based on a 95 percent confidence limit and a relative error of plus or minus 2 percent, a minimum of 1,111 total counted particles was required for 90 percent opaque, 2,500 for 80 percent opaque, and 6,667 for 60 percent opaque. If the measured percentage was different from the predetermined proportion, a new minimum value was calculated, and if the actual number counted was less, more particles were counted.

Automatic Image Analysis Testing Procedure

The automatic (image analysis) procedure measures translucent and opaque proportions by the area occupied by each mineral. The image processing and analysis system used for this project includes a microscope, solid-state monochrome camera, hardware, and application software packages. The operator console system includes one color monitor to display menus, results, and programming commands and a second color monitor to display camera output or stored images and graphics overlay, a mouse, a keyboard, and a lamp voltage power supply for specimen illumination. Control of the system is with a 20-MHz 386 personal computer with 2 Mbytes RAM, 40 Mbyte hard drive, and high-density 3.5- and 5.25-in. diskette drives.

Camera settings in the image analysis study were adjusted so that the most the sample could be seen while still obtaining a resolution by which the different type of sand particles could be detected. This was not possible with the camera for the No. 200 particles, so these particles were viewed by the image analyzer through the binocular microscope by means of a special camera hookup. Magnification for the No. 30, 50, and 100 sieve sizes was between 1 and 2. Magnification for sieve size No. 200 was 8.

An optical image from the camera or microscope is converted by the image analysis system into an analog signal, which is digitized into 256 grey levels. A series of successive images are averaged to filter out noise, and the resulting averaged image is stored in temporary computer memory. Stored images are manipulated by a grey-tone image processor, which performs morphological transformations. In this study, a morphological transformation known as delineation was applied to sharpen the edges of aggregate particles. This transformation improved detection of the particles.

Different types of particles are detected by a process called thresholding. Particles emit an optical brightness. Each pixel has a brightness value, or grey level, from 0 to 255. Many pixels are usually required to represent each sand particle. When the grey level of the pixels is plotted on a histogram, different types of particles can be separated by distinct grey levels. This is the thresholding process. A typical histogram is shown in Figure 2. Threshold values used to separate the two different types of minerals were manually selected at the two "valleys" on the chart. In this example, a grey value of 70 was the separation between translucent and opaque particles. A value of 174 separated the background light from the lightest particles. The area occupied under each portion of the histogram is calculated to determine the percentage of each mineral in the viewed sample. Several meas-

urements were made for each sample, and the average and standard deviation were determined for opaque particles. On the basis of a 95 percent confidence limit and the standard deviations obtained, it was determined that seven or eight measurements were adequate in most cases to satisfy statistical requirements.

RESULTS AND DISCUSSION

Statistical analyses were performed on the data collected from the microscope study and image analysis study. Because of the method with which the data were collected, different analyses were performed.

Microscope Study

A null hypothesis (H_o) was tested to determine if the opaque particle proportion was equal to the weight proportion. The chi-square equation (*7*) was used to determine if H_o was true. The chi-square equation, corrected for continuity, is

$$X_c^2 = \sum_{i=1}^{k} \frac{(|f_i - F_i| - 0.5)^2}{F_i} \quad (1)$$

where f_i is the number of counts observed in Class i, F_i is the frequency expected in Class i if H_o is true, and the summation is performed over the k categories of data, opaque and translucent particles. A value of 3.84 for the chi-square test statistic was used based on a risk-level alpha of 0.05 and one degree of freedom. The data obtained by manually counting the sand particles using the microscope are shown in Table 1. The volume proportions of the opaque particles were determined to be 89.80, 79.63, and 59.46 compared with the prepared weight proportions of 90, 80, and 60, respectively. These were determined on the basis of the limestone apparent specific gravity of 2.71 and the Ottawa sand apparent specific gravity of 2.65.

On the basis of the data, H_o was rejected in every case except for retained sieve size No. 50 opaque proportion of 60 percent. Some proportions were relatively close to the expected proportion, but because of the certainty guaranteed with the large number of particles counted, H_o was rejected. There are several possibilities for the rejection. The particles may not have been identified correctly. However, they were clearly distinguishable. It was originally assumed that particle proportion was equal to the volume proportion if the particles were of the same shape. It was found, however, that the particles were not of the same shape. The translucent particles, which were obtained from a natural source, were fairly round. An angular particle passing a certain sieve can be several times larger than a round particle passing the same sieve because of shape characteristics such as elongation. This may have resulted in the rejection of H_o.

In conclusion, the method of counting to determine the percentages of different materials by volume in a sand blend resulted in the rejection of H_o in all but one case. In other words, except for one sand blend, the method of counting was not accurate in determining the relative volumes of opaque and translucent particles using this procedure. This is based on two categories of data. If three or more different types of minerals were being counted, it is expected that the accuracy would be much less. The time required using this procedure was significant—about 1 to 4 hr for each sample. An instrument such as the image analyzer was desired for speed and accuracy.

Image Analysis Study

A different method of analysis was used for evaluating the image analysis data. The image analysis results were compared on an area basis, not by weight as in the microscope study. Results of percent opaque particles determined from image analysis are shown in Table 2. It was found, using the *t*-test and a 95 percent confidence interval, that the percentages of opaque particles measured were not statistically different as the amount present in the

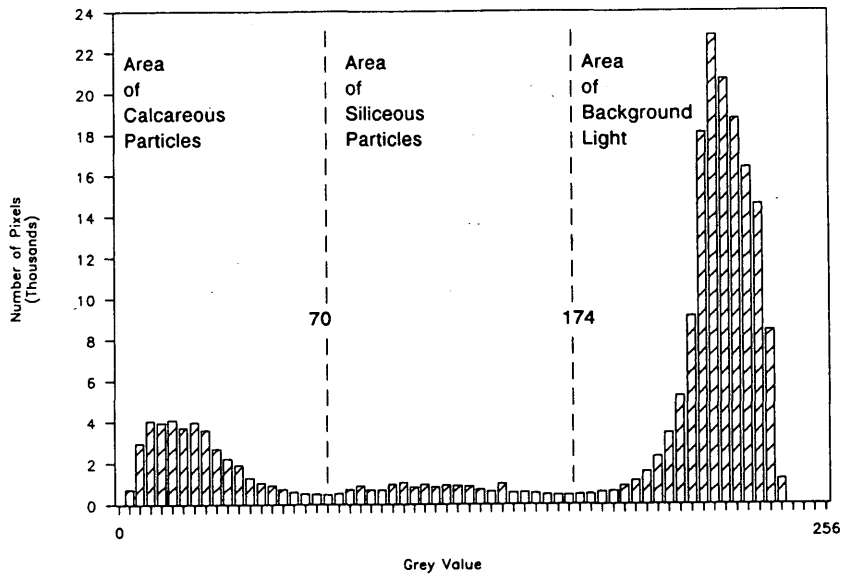

FIGURE 2 Grey level distribution.

TABLE 1 Results of Microscope Study

Sieve Size	Percent Opaque by Weight	Counted Particles Opaque	Counted Particles Transl.	Measured Percent Opaque	Expected Number Opaque	Expected Number Transl.	Chi Square	Decision
30	90	3177	537	85.5	3335	379	72.89	Reject Ho
30	80	3136	1142	73.3	3407	871	105.48	Reject Ho
30	60	5143	4794	51.8	5909	4028	244.6	Reject Ho
50	90	19484	2357	89.2	19613	2228	8.25	Reject Ho
50	80	15808	4474	77.9	16151	4131	35.66	Reject Ho
50	60	13176	8975	59.5	13171	8980	0.0038	Ho
100	90	15512	1574	90.8	15343	1743	18.14	Reject Ho
100	80	15743	2897	84.5	14843	3797	267.6	Reject Ho
100	60	4703	2166	68.5	4084	2785	231	Reject Ho
200	90	2226	193	92.0	2172	247	12.91	Reject Ho
200	80	2677	399	87.0	2449	627	103.68	Reject Ho
200	60	4941	1735	74.0	3970	2706	585.31	Reject Ho

sample for four of the samples, as indicated by a Yes in the last column. A No indicated that the amount measured was statistically different as the amount present in the sample, using a 95 percent confidence interval. Because of problems in producing distinguishable threshold limits for the retained No. 200 particles, no data for this size were collected.

At 95 percent confidence interval, the data from image analysis show that four of the nine specimens displayed measured levels of opaque particles that are not significantly different from levels of particles present in the samples. Overall, the ability of image analysis to determine relative amounts of particles was very good compared with the manual counting techniques. The largest difference from image analysis between measured and actual level was 3.12 percent (for No. 30, 60 percent opaque by weight). The largest difference from manual counting between the measured and actual level was 8.5 percent (for No. 100, 60 percent opaque by weight), not taking into account the No. 200 particles. It should be noted that the standard deviations of the image analysis results are low and resulted in the rejection of H_o in some cases. For example, for No. 100, 90 percent opaque by weight, H_o was rejected, although the difference between measured and actual particle proportion was 0.87 percent. Image analysis resulted in values much closer to actual values than the manual counting technique. The time required for the measurements was 45 min to 1 hr.

Comparisons of Microscope and Image Analysis Methods

The previous statistical analyses compared results with the weight percentages present in the blends. The manual counting and automatic image analysis techniques are also compared. The results are shown in Table 3. The retained No. 50 sizes with opaque proportions of 60 and 80 percent are the only two of the nine in which the microscope method is not significantly different from the automatic image analysis method. This was determined with the standard normal distribution and 95 percent confidence level. In general, the two techniques do not compare well.

TABLE 2 Measured Opaque Particles by Image Analysis

Sieve Size	Percent Opaque By Weight	By Area	Measured	Number of Observations	Standard Deviation	Significant
30	60	59.46	62.58	13	4.15	No
30	80	79.63	79.81	16	3.54	Yes
30	90	89.80	88.03	12	2.10	No
50	60	59.46	60.19	28	5.68	Yes
50	80	79.63	78.24	27	3.65	Yes
50	90	89.80	88.06	28	1.84	No
100	60	59.46	61.44	27	3.54	No
100	80	79.63	78.89	25	3.28	Yes
100	90	89.80	88.93	25	1.60	No

TABLE 3 Microscope and Image Analysis Comparison

Sieve Size	Percent Opaque: Expected (By Area)	Image Analysis	Microscope	Number of Particles	Standard Deviation	Significant
30	59.46	62.58	51.8	9937	0.0025	No
30	79.63	79.81	73.3	4278	0.00299	No
30	89.80	88.03	85.5	3714	0.00203	No
50	59.46	60.19	59.5	22151	0.00162	Yes
50	79.63	78.24	77.9	20282	0.00121	Yes
50	89.80	88.06	89.2	21841	0.00065	No
100	59.46	61.44	68.5	6869	0.0026	No
100	79.63	78.89	84.5	18640	0.00096	No
100	89.80	88.93	90.8	17086	0.00064	No

Field Specimens

Image analysis tests were performed on samples taken from Indiana highway pavements using the same procedure as that for the laboratory-prepared samples. The percentage of translucent particles was then compared with the 0.45 power gradations determined after extraction. Percent translucent contents for the field samples are shown in Table 4. Percent translucent sand for each sieve size by weight is shown. Total translucent content of the material retained on the No. 30, 50, and 100 sieves by weight of the entire sample is also shown, assuming zero percent siliceous content of coarse aggregate. The data are listed in order of increasing translucent sand content (by weight) of the entire sample. Table 4 also summarizes humps observed around the No. 16, 30, and 50 sieves by these categories: no hump, very slight hump, slight hump, hump, large hump, and severe hump. Gradation examples are shown in Figures 3, 4, and 5. The field measurements show that as the percent of translucent material or natural sand increases, a hump is more likely to occur. The reason why translucent contents were lower for the field samples than for the laboratory-prepared samples is that natural sand used in construction is not entirely siliceous. However, it is expected that a relationship exists between translucent content measured and the amount of natural sand placed in the mixtures.

CONCLUSIONS

On the basis of the results and statistical analysis of the data, the following conclusions were drawn:

1. Manual counting techniques to determine relative particle proportions do not produce accurate results. The procedure is time consuming and subject to errors.

TABLE 4 Translucent Contents and Humps on Gradation Curves

Designation	Route	Percent Translucent by Individual Sieve: No. 30	No. 50	No. 100	Total Translucent Content (%)	Comments
218B	SR-8	21.1	44.7	44.4	2.659	Very slight hump at 50
711B	I-65	13.2	39.6	39.3	3.479	Very slight hump at 50
821B	SR-37	14.8	32.6	42.0	4.51	Hump at 16
118B	US-24	8.8	33.4	23.4	4.898	No hump
821C	SR-37	15.0	32.0	36.7	5.316	No hump
721C	I-74	17.7	55.7	67.8	5.62	No hump
412B	SR-14	22.7	56.6	74.6	5.993	Severe humps at 30 and 50
721B	I-74	19.7	50.3	65.0	6.458	No hump
318B	I-69	16.0	48.1	56.4	7.176	Very slight hump at 50
321B	US-31	18.0	47.5	53.1	7.341	Severe humps at 30 and 50
128B	US-31	19.0	52.7	63.3	7.68	Slight hump at 50
811B	US-421	27.6	48.4	52.7	7.972	Large humps at 30 and 50
421C	SR-8	16.4	45.4	56.5	9.588	Large humps at 30 and 50
123C	US-31	14.9	49.4	55.4	10.124	No hump
621B	SR-245	29.2	60.0	56.4	10.322	Large humps at 30 and 50
623C	SR-245	26.8	57.9	62.1	10.666	Large humps at 30 and 50
521C	I-64	38.6	66.9	49.7	11.201	Max line at 16, 30, and 50
611B	SR-446	25.2	47.8	48.1	11.202	Large humps at 30 and 50
424B	SR-8	15.4	52.1	68.4	13.603	Severe humps at 30 and 50
521B	I-64	42.7	73.1	60.1	14.335	Large humps at 30 and 50
511B	I-64	29.8	59.3	62.8	14.761	No hump

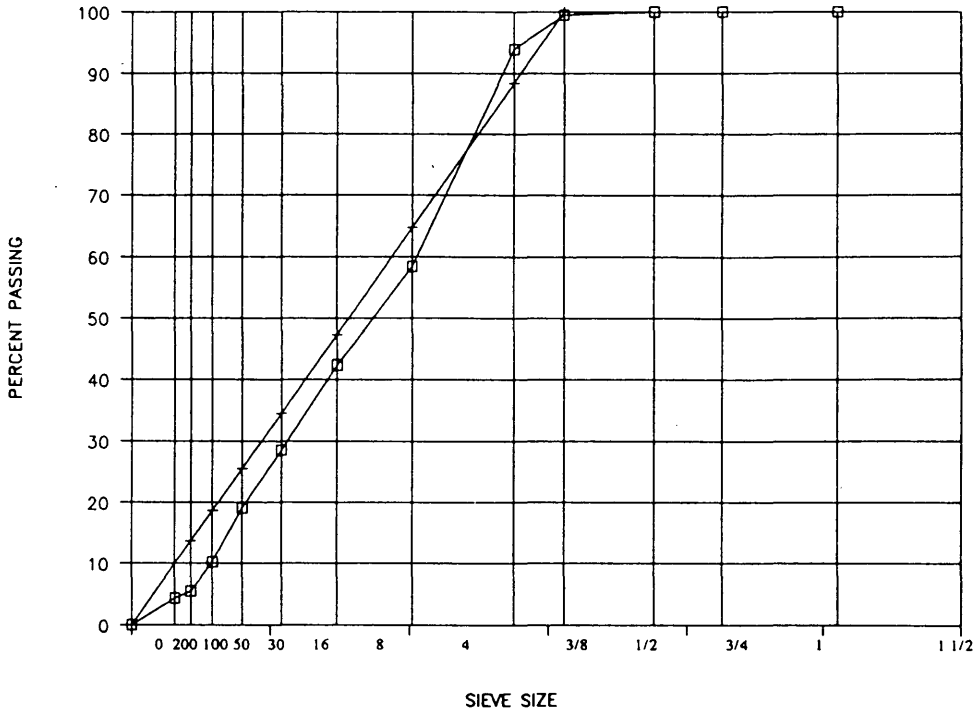

FIGURE 3 Sieve sizes raised to 0.45 power: no hump gradation (118B).

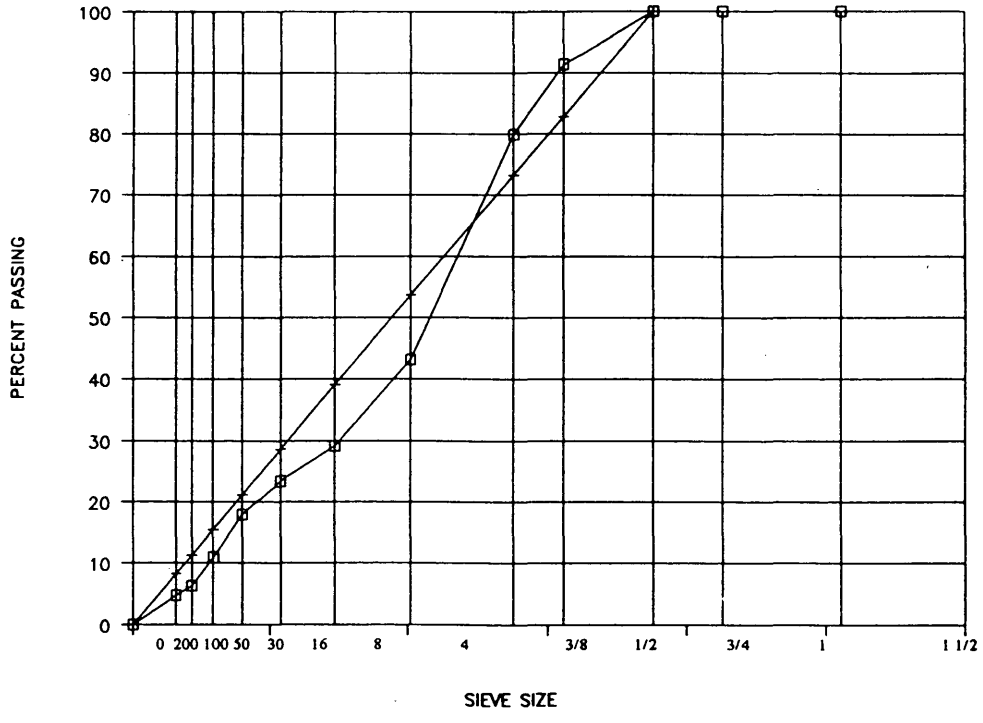

FIGURE 4 Sieve sizes raised to 0.45 power: slight hump gradation (128B).

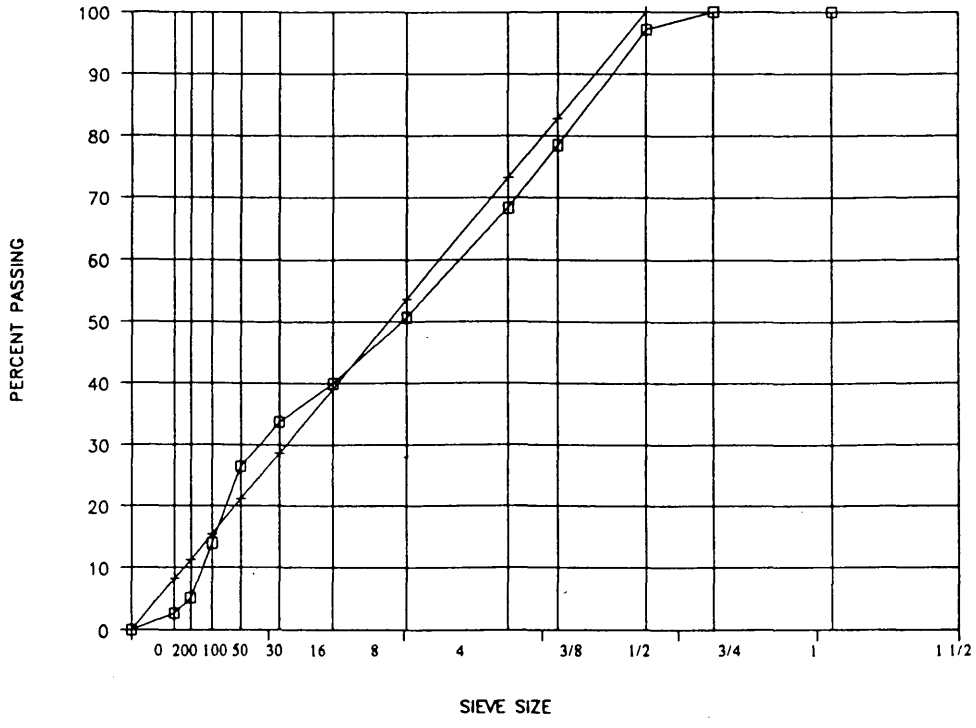

FIGURE 5 Sieve sizes raised to 0.45 power: severe hump gradation (424B).

2. Image analysis techniques to determine relative particle proportions produce results closer to actual proportions than manual counting techniques. Standard deviations are small. Image analysis is faster and subject to less errors than manual counting techniques.

3. The field measurements show that as the percent translucent material increases, it is more likely for a hump to occur. This hump has been found by other researchers to result in a tender mix.

ACKNOWLEDGMENTS

The research was funded by the Indiana Department of Transportation (INDOT) and FHWA. The image analysis system was purchased with an equipment grant from the National Science Foundation. David Frost contributed much information on the image analysis section.

REFERENCES

1. Button, J. W., D. Perdomo, and R. L. Lytton. Influence of Aggregate on Rutting in Asphalt Concrete Pavements. In *Transportation Research Record 1259*, TRB, National Research Council, Washington, D.C., 1990.
2. Ahlrich, R. C. *The Effects of Natural Sands on Asphalt Concrete Engineering Properties.* Technical Report GL-91-3. U.S. Army Engineer Waterways Experiment Station, Vicksburg, Miss., 1991.
3. Kandhal, P. S., J. B. Motter, and M. A. Khatri. Evaluation of Particle Shape and Texture: Manufactured Versus Natural Sands. In *Transportation Research Record 1301*, TRB, National Research Council, Washington, D.C., 1991.
4. Perdomo, D., and J. W. Button. *Identifying and Correcting Rut-Susceptible Asphalt Mixtures.* Research Report 1121-2F. Texas Transportation Institute, College Station, Tex., 1991.
5. Barksdale, R. D., M. A. Kemp, W. J. Sheffield, and J. L. Hubbard. Measurement of Aggregate Shape, Surface Area, and Roughness. In *Transportation Research Record 1301*, TRB, National Research Council, Washington, D.C., 1991.
6. Oosthuyzen, E. J. The Application of Automatic Image Analysis to Mineralogy and Extractive Metallurgy. In *ICAM 81, Proceedings of the First International Congress on Applied Mineralogy*, Geological Society of South Africa, Johannesburg, 1983.
7. Zar, J. H. *Biostatistical Analysis.* Prentice-Hall, Inc., Englewood Cliffs, N.J., 1974.

Methodology for Improvement of Oxide Residue Models for Estimation of Aggregate Performance Using Stoichiometric Analysis

TERRY DOSSEY, JESSICA V. SALINAS, AND B. FRANK MCCULLOUGH

A methodology is presented for improving the predictive ability of oxide-based chemical models that predict aggregate material properties using the chemical composition of the coarse aggregate. Because portland cement concrete is composed of 70 to 85 percent coarse and fine aggregates (by weight), the aggregate material properties have a profound effect on the material properties of the finished concrete and ultimately on pavement performance. An existing computer program, CHEM1, has been used to estimate these concrete properties (compressive and tensile strength, elastic modulus, and drying shrinkage) through stochastic models based on user-input oxide residues. This approach, although adequate for some applications, suffers from the fact that concrete properties are influenced more by the mineralogy of the aggregate than by the oxides formed from their decomposition. Using stoichiometric analysis, the CHEM2 program backcalculates the original mineral composition from the oxides and thereby improves the accuracy of the models. The CHEM2 program also adds the ability to predict for aggregate blends and a model for thermal coefficient of expansion, both of which were lacking in CHEM1.

In Texas Department of Transportation Project 422/1244, concrete specimens were cast from eight coarse aggregate sources commonly used in Texas rigid pavements. Water-cement ratio, other mix design elements, and curing conditions were held as constant as possible so that any variation in concrete properties would be due to the influence of coarse aggregate. The specimens were then tested for tensile strength (f_t), compressive strength (f_c), elastic modulus (E), drying shrinkage (Z), and thermal coefficient (a) after various lengths of curing. Subsequent analysis based on this testing developed descriptive models (based on curing time and aggregate type) and predictive models (based on curing time and chemical composition) (*1*). This effort was termed the Phase II experiment. Complete mix designs can be found elsewhere (*1*).

In order to easily apply the chemical models, a computer program, CHEM1, was developed for the IBM personal computer (*1*). Earlier testing focused only on limestone and river gravel aggregates was termed Phase I (*2*). This program requires as input the percentage by weight of certain oxide residues produced by standard fusion testing. It then predicts f_t, f_c, E, and Z for curing times ranging from 1 to 28 (256 for Z) days. The object of the program was to give a rough prediction of material properties for concrete made with a new aggregate source before actual laboratory testing.

The overall purpose of predicting concrete material properties for various aggregates is to determine design parameters (steel percent, bar size, etc.) needed to attain a desired level of pavement performance. Using design tools such as the continuously reinforced concrete pavement programs (*3*), these factors can be estimated. In this way, it is hoped that equal and adequate performance from very different aggregates can be obtained.

Center for Transportation Research, University of Texas at Austin, 3208 Red River, Suite 200, Austin, Tex. 78705.

CHEM2 OBJECTIVES

Improved Models for Limestones and River Gravels

CHEM1 currently uses one model to predict for all types of aggregates. CHEM2 obtains better results by first identifying the type of aggregate and then making a prediction using a model specifically developed for that aggregate class. This is especially important for aggregate types that produce similar oxide residues [e.g., siliceous river gravel (SRG) and granite, both high in SiO_2] but differ in mineral composition and therefore exhibit characteristic differences when cast in concrete. The program can either identify the class of aggregate by direct user input or determine it through a simple set of IF statements based on the oxide test results. Once the class is determined, the original mineral content is first backcalculated from the oxide residue stoichiometrically (*4*).

Since limestones and river gravels are the focus of the overall study, special attention has been given to these aggregates. Two new limestones and two new river gravels are currently being tested (Phase II experiment), which will add enough additional data to make more type-specific models possible. These models would estimate differences in strength, modulus, shrinkage, and expansion based on small differences in the characteristic minerals composing the aggregates, presumably calcium carbonate (Ca_2CO_3) and dolomite ($CaMg(CO_3)_2$) for limestone and quartz (SiO_2) for river gravel.

At this time, CHEM2 predictions for aggregates other than limestone or river gravel consist simply of identifying the aggregate (e.g., granite) and producing the absolute or normalized curing curves determined in Phase II.

Prediction of Thermal Coefficient

CHEM1 does not predict thermal coefficient of expansion. This is a vitally important property, particularly for pavements placed in the summer season when temperature extremes are great and

peak ambient temperature may coincide with peak heat of hydration (as in morning placements). Under such conditions, for a given steel design, a high thermal coefficient tends to produce more closely spaced early-age cracking compared with an aggregate that has a lower coefficient.

Despite the desirability of such a model, problems with using the oxide residues directly prevented the development of a definitive model. This difficulty has been overcome by first backcalculating the original mineral content. Additional thermal coefficient testing in the Phase III experiment will provide additional data to further improve the thermal coefficient model. CHEM2 currently predicts thermal coefficient based on the Phase II data.

Predictions for Aggregate Blends

CHEM2 also adds a facility for predicting the performance of blended aggregates. Phase III testing included an experiment to determine the effect of blending limestone with river gravel at various proportions. This experiment was designed to reveal the shape of the blending curves (Figure 1), which could then be normalized for each material property and used to predict the performance of blends. Initially, it was not known whether the properties of a blended aggregate could be described by the weighted average for the two aggregates (Figure 1, Curve A, linear) or by a nonlinear combination (Figure 1, Curves B and C). Initial results from Phase III testing support Curve A, the simple linear combination. CHEM2 will determine properties for blended aggregates by estimating for each individual aggregate and then taking a weighted average according to the blending ratio.

PROGRAM FLOW

The CHEM2 program operates as follows:

1. User input of chemical composition data is obtained;
2. Prediction models for the five material properties are produced;

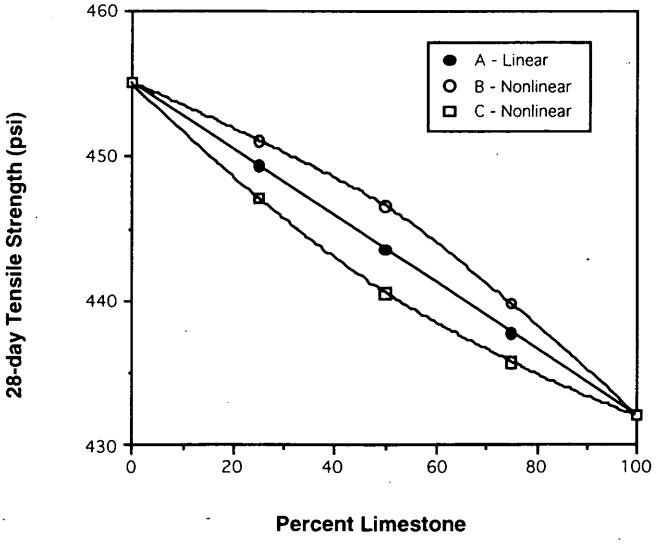

FIGURE 1 Possible performance shapes for blended river gravel.

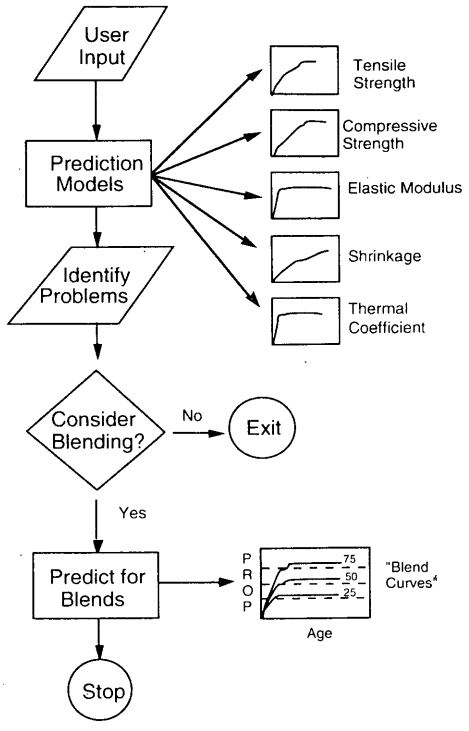

FIGURE 2 CHEM2 program flow.

3. Potential problem areas are highlighted (e.g., excessively high thermal coefficient); and
4. At the user's option, a parametric series of curves is produced predicting the performance of the original aggregate blended 75/25, 50/50, and 25/75 with a standard or user-input limestone (Figure 2). These graphs (Figure 3) have grid lines so that the user can screen print them and determine the approximate blending level needed to produce the material properties that result in the desired level of performance.

STOICHIOMETRIC ANALYSIS

One of the problems encountered in the development of the CHEM1 models was that only the oxide residues were considered as predictors. Since different minerals may break down to different oxides of the same compound (e.g., dolomite and calcite both contribute to the calcium oxide residue), direct empirical modeling based on oxide residue is problematic. Therefore, a methodology was developed for backcalculating the percentage by weight of the various minerals that compose the aggregates used in the Phase II study. Mineral composition determined in this way can then be used to develop more robust predictive models for such aggregate-dependent concrete properties as tensile strength, compressive strength, elastic modulus, drying shrinkage, and thermal coefficient of expansion.

Problems with Existing Chemical Models

Phase II testing under this project collected aggregate chemical composition data for eight aggregates commonly used in Texas

pavements and for a number of additional aggregates (*1*). Several analytical procedures were performed, including determination of principal mineral composition by x-ray diffraction and oxide residue analysis after fusion.

Dossey and McCullough (*1*) document an effort to predict aggregate performance based solely on oxide residues. Although some useful models were developed, some of the models were later determined to have weak predictive ability outside the inference space of the eight tested aggregates. The problem with oxide-based models is that few of the oxides measured actually existed in the aggregate before chemical testing; in fact, most of the oxides were formed by the breakdown of more complex minerals in the sample. For example, little if any calcium oxide (CaO) was present in the aggregate before fusion; most was produced by the oxidation of calcite (limestone, $CaCO_3$), and an additional amount came from dolomite ($CaMg(CO_3)_2$).

This situation gives rise to a fundamental problem: since the amount of each oxide is proportional not to a single mineral but to several, no strong direct correlation is observed between oxide percentage and concrete material properties. The models developed by Dossey and McCullough (*1*) attempt to compensate by considering interactions. These interactions serve as surrogate variables or indirect indicators for the original mineral content of the sample.

Methodology

A much better method is to develop models based directly on the original mineral composition of the aggregates. Fortunately, stoichiometric analysis can be used to backcalculate these percentages (*3*).

Using the results from x-ray crystallography (Table 1), the principal minerals in each sample were determined. Most are composed primarily of any or all of the following: calcite ($CaCO_3$), quartz (SiO_2), or dolomite ($CaMg(CO_3)_2$). A notable exception is Scotland Granite, which contains a substantial amount of the sodium feldspar albite ($Na_2O \cdot Al_2O_3 \cdot 6SiO_2$). It is the albite (and other feldspars) in granite that cause it to be an outlying point in much of the previous analysis. For instance, the granite (GR) and Vega (VG) aggregates tested had thermal coefficients of 10.3 and 11.7 microstrains/°C (5.7 and 6.5 microstrains/°F), respectively, yet GR has an SiO_2 residue of 71.3 percent versus 66.9 percent for VG. Since quartz is so thermally expansive, this is counterintuitive. Because the breakdown of albite yields additional SiO_2, granite appears to have had the second highest mineral quartz content of the tested aggregates; however, this is not the case. Much of the SiO_2 residue came from albite, not quartz. Albite and quartz have very different physical properties (such as thermal coefficient of expansion). The technique presented here will eliminate this type of problem.

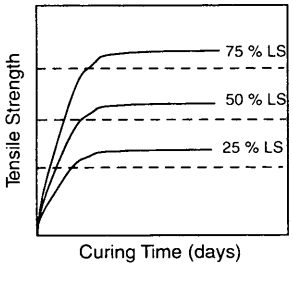

FIGURE 3 Parametric curves for blend design (example).

TABLE 1 Mineral Composition of Phase II Aggregates

Source	Aggregate Type	Most Abundant	Second	Third
McCelligan # 1	DL	Dolomite	Calcite	Quartz
Western-Tascosa	WT	Quartz	Calcite	
Tin-Top # 1	BTT	Calcite	Quartz	
Bridgeport	BTT	Calcite	Dolomite	Quartz
Feld (TCS)	LS	Calcite	Dolomite	Quartz
Fordyce	SRG	Quartz	Calcite	
Vega	VG	Quartz	Calcite	
Ferris # 1	FR	Calcite	Quartz	
Scotland Granite	GR	Quartz	Albite	

Assumptions

Mined aggregate is a complex blend of many minerals; it would be impossible from the rudimentary information given in Table 1 to determine the exact mineral composition of the aggregates. Fortunately, a methodology to backcalculate the principal minerals should be all that is needed to develop more robust models.

Accordingly, the following imprecise but essentially correct assumptions were made:

1. All SiO_2 residue in the sample came from quartz or feldspar (granite is composed of quartz and feldspar). Only the two most commonly occurring types of feldspars, albite (the sodic plagioclase feldspar) and orthoclase and microcline potassium feldspars, chemically ($K_2O \cdot Al_2O_3 \cdot 6SiO_2$), were considered in this analysis. Orthoclase and microcline have the same chemical composition but differ in crystalline structure.
2. All CaO residue in the sample came from calcite or dolomite.

Reactions

The two foregoing assumptions imply the following decompositions:

Calcite:

$$CaCO_3 \rightarrow CaO + CO_2 \quad (1)$$

Dolomite:

$$CaMg(CO_3)_2 \rightarrow MgO + CaO + 2CO_2 \quad (2)$$

Albite:

$$Na_2OAl_2O_3 \cdot 6SiO_2 \rightarrow 6SiO_2 + Al_2O_3 + Na_2O \quad (3)$$

Potassium feldspars:

$$K_2OAl_2O_3 \cdot 6SiO_2 \cdot 6SiO_2 + Al_2O_3 + K_2O \quad (4)$$

Computational Method: Carbonates

Using the molecular weights for the compounds (Table 2) and the balanced equations above, it is a simple matter to determine the weight ratios relating the oxides to the original mineral content. For instance, from Equation 2 it can be seen that dolomite breaks down to MgO in a one-to-one ratio. That is, each mole of dolomite produces one mole of magnesium oxide.

Since the molecular weight of dolomite is 184.407 and the molecular weight of MgO is 40.305, 184.407/40.305 = 4.575 g of dolomite must have existed for each gram of MgO in the original sample.

$$\text{Dolomite (g)} = \text{MgO (g)} \cdot 4.5752 \quad (5)$$

In order to estimate the original calcite in the sample, it is first necessary to subtract the amount of CaO produced from dolomite (CaO_{dol}). The decomposition of dolomite yields CaO in a 1:1 molar ratio, or 56.08 g CaO/184.407 g dolomite = 0.3041.

$$CaO_{dol}\ (g) = \text{dolomite (g)} \cdot 0.3041 \quad (6)$$

Then, CaO from the decomposition of calcite (CaO_{cal}) equals the total CaO (CaO_{tot}) less the amount released from dolomite:

$$CaO_{cal}\ (g) = CaO_{tot}\ (g) - CaO_{dol}\ (g) \quad (7)$$

Now that CaO_{cal} is known, the original percent calcite (limestone) can be calculated. In a 1:1 ratio, 1 mole (100.091 g) of calcite produces 1 mole (56.08) of CaO, giving a molecular weight ratio of 100.091/56.08 = 1.785.

$$\text{Calcite (g)} = CaO_{cal}\ (g) \cdot 1.785 \quad (8)$$

Computational Method: Silicates

A similar process can be employed to determine the original silicate content. First, assuming most or all Na_2O was produced by the breakdown of albite (see Table 1), the following formula is given:

$$\text{Albite (g)} = Na_2O\ (g) \cdot 8.46 \quad (9)$$

Assuming most or all K_2O was produced by the breakdown of potassium feldspars (PF) such as orthoclase and microcline,

$$\text{PF (g)} = K_2O\ (g) \cdot 5.8 \quad (10)$$

Calculating SiO_2 from albite [$SiO_{2(alb)}$]:

$$SiO_{2(alb)}\ (g) = \text{albite (g)} \cdot 0.6874 \quad (11)$$

Calculating SiO_2 from potassium feldspars [$SiO_{2(PF)}$]:

$$SiO_{2(PF)}\ (g) = \text{PF (g)} \cdot 0.6595 \quad (12)$$

Then the remaining SiO_2 must have been quartz before testing:

$$\text{Quartz (g)} = SiO_{2(tot)}\ (g) - SiO_{2(alb)}\ (g) - SiO_{2(PF)}\ (g) \quad (13)$$

TABLE 2 Molecular Weights for Selected Compounds

Compound	Molecular Weight (g)
Calcite	100.091
Dolomite	184.407
Quartz	60.0855
Albite	524.48
PF	546.674
CaO	56.08
MgO	40.305
SiO_2	60.086

TABLE 3 Calculated Percent Mineral Composition

Aggregate	Calcite	Dolomite	Quartz	Albite	PF	Unexplained
BTT	73.98	3.245	15.51	1.269	1.77	4.23
DL	29.87	59.42	5.01	0.76	1.54	4.3
FR	73.87	1.97	12.22	1.44	1.54	8.96
GR	1.11	2.88	31.05	37.23	22.63	5.1
LS	66.53	27.29	0.94	1.18	1.24	2.82
SRG	3.70	0.50	91.53	1.52	1.89	0.86
VG	19.68	1.78	56.93	8.04	6.86	6.71
WT	19.42	1.60	59.35	7.19	6.50	5.94

Results

Percentages after decomposition for the eight aggregates are given in Table 3. A computer program written in the SAS language was developed to calculate mineral content according to Equations 5–13. The results of running this program on the oxide residue data are given in Table 3. As a check of the methodology, the remaining unexplained mineral content is given in the last column.

DISCUSSION OF RESULTS

In general, the procedure performs very well in describing the mineral content of the original sample. No conflict was found with the original crystallography analysis (Table 1). Most of the oxide residue was accounted for, with a maximum of 8.96 percent unexplained for aggregate (FR). This is probably due to the large

amount of ferric minerals found in this aggregate, which were not addressed in the analysis.

THERMAL COEFFICIENT MODEL

Using the estimated mineral content from the stoichiometric procedure (Table 4), regression was used to model thermal coefficient of expansion (α_c) as a function of mineral content in the sample:

$$\alpha_c = e^{1.098} \cdot (\text{quartz})^{0.486} \cdot (\text{calcite})^{-0.106} \cdot (\text{dolomite})^{0.415} \cdot (\text{PF})^{-2.37} \cdot (\text{albite})^{1.635} \quad (14)$$

where

quartz = percent quartz by weight,
calcite = percent calcite by weight,
dolomite = percent dolomite by weight,
PF = percent potassium feldspars by weight,
albite = percent albite by weight, and
FS = albite + PF, all feldspars by weight.

α_c is in microstrains per degree Fahrenheit and can be converted to degrees Celcius by multiplying by 1.8.

Figure 4 shows the fit for the thermal coefficient model. This model has been tested on several additional aggregates and provides reasonable predictions in most cases. Additional models for tensile strength, compressive strength, and elastic modulus were also fit by a similar method:

$$f_c \text{ (psi)} = e^{8.943} \cdot (\text{calcite})^{-0.086} \cdot (\text{quartz})^{-0.072} \cdot (\text{dolomite})^{-0.021} \cdot (\text{FS})^{-0.033} \quad (15)$$

$$f_t \text{ (psi)} = 1298 - 8.87 \cdot (\text{calcite})^{-8.089} \cdot (\text{quartz})^{-7.45} \cdot (\text{dolomite})^{-49.8} \cdot (\text{PF}) + 16.6 \cdot (\text{albite}) \quad (16)$$

$$E \text{ (psi, millions)} = e^{1.115} \cdot (\text{calcite})^{-0.0087} \cdot (\text{quartz})^{0.121} \cdot (\text{dolomite})^{0.088} \cdot (\text{FS})^{-0.101} \quad (17)$$

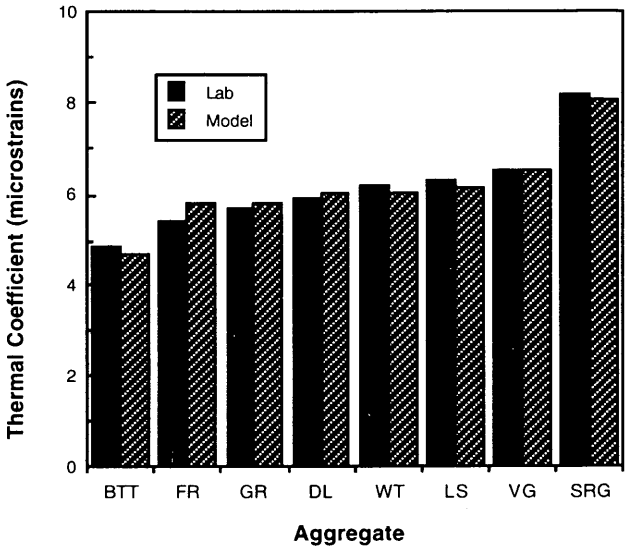

FIGURE 4 Fit for thermal coefficient model (Equation 14).

The terms f_c, f_t, and E can be converted from pounds per square inch to kilopascals by multiplying by 6.9.

It must be stressed that the models were developed using only the Phase II laboratory data (eight Texas aggregates) and thus are very restricted in terms of inference space. It is expected that additional laboratory and field data being collected at this time (Phase III testing) will allow improvement of the model. In particular, as suggested earlier, separate models will be developed for siliceous and calcareous aggregates, which should greatly strengthen their predictive ability.

CONCLUSIONS AND RECOMMENDATIONS

The models given here for thermal coefficient, compressive strength, tensile strength, and elastic modulus are preliminary and

TABLE 4 Phase II Chemical Analysis Results

Source	Aggregate Type	Type	SiO_2	CaO	MgO	CO_2	MnO	Fe_2O_3	Al_2O_3	Na_2O	K_2O	TiO_2	Other
McKelligan	Dolomite	(DL)	6.53[a]	34.9	13.0	42.9	.02	0.21	0.38	0.09	0.26	0.02	1.69
Western-T	S/L	(WT)	68.5	11.4	0.35	8.98	.05	2.64	3.97	0.85	1.1	0.17	1.99
Bridpt+TinTop	L+S/L	(BTT[b])	17.53	42.55	0.71	35.65	0.04	0.57	0.56	0.15	0.30	0.04	1.91
Feld (TCS)	Limestone	(LS)	2.56	45.7	5.97	43.3	.01	0.06	0.21	0.14	0.21	0.02	1.82
Fordyce	SRG	(SRG)	93.8	2.23	0.11	1.77	.01	0.76	0.63	0.18	0.32	0.1	0.09
Vega	SRG	(VG)	66.9	11.6	0.39	9.07	.07	2.33	4.22	0.95	1.16	0.19	3.12
Ferris	L/S	(FR)	14.2	42.1	0.43	34.4	.10	3.70	0.87	0.17	0.26	0.06	3.71
Scotland	Granite	(GR)	71.3	1.5	0.63	0.59	.03	1.52	14.3	4.4	3.83	0.29	1.61

[a]All values are percent by weight.

[b]These aggregates combined in a 50/50 blend when tested in the laboratory for concrete properties.

serve only to demonstrate the two-stage procedure in which mineral content is first backcalculated and then used to estimate concrete material properties. However, the stoichiometric methodology developed (CHEM2) is a significant improvement over direct regression techniques using oxide residue analysis (e.g., CHEM1). As more data become available, the regression models predicting concrete performance from aggregate mineral content will continue to be improved until they are able to predict reliably over a wide range of aggregate types.

CHEM2 offers the pavement designer the opportunity to estimate the performance of new, untried aggregates before undergoing the expense of full concrete testing. At the time of this writing, the oxide residue test needed to run CHEM2 cost less than $100. Of course, CHEM2 is not intended to replace conventional testing procedures.

ACKNOWLEDGMENTS

The authors gratefully acknowledge the sponsorship of the Texas Department of Transportation. This work was done under the auspices of TxDOT Research Study 2/3-8-90/2-1244, entitled "Evaluation of Performance of Texas Pavements Made with Different Coarse Aggregates."

REFERENCES

1. Dossey, T., and B. F. McCullough. *Characterization of Concrete Properties with Age.* Research Report 1244-2. Center for Transportation Research, University of Texas at Austin, March 1992.
2. Aslam, M. F., C. L. Saraf, R. L. Carrasquillo, and B. F. McCullough. *Design Recommendations for Steel Reinforcement of CRCP.* Research Report 422-2. Center for Transportation Research, University of Texas at Austin, Nov. 1987.
3. Won, M., K. Hankins, and B. F. McCullough. *Mechanistic Analysis of Continuously Reinforced Concrete Pavements Considering Material Characteristics, Variability, and Fatigue.* Research Report 1169-2. Center for Transportation Research, University of Texas at Austin, April 1990.
4. Stoker, H. S. *Introduction to Chemical Principles*, 2nd ed. Macmillan Publishing, New York, 1986.